TITLE: **Planck cold load performance degradation at LFI frequency caused by HFI carbon fibre noise source**

DOC. TYPE: TECHNICAL NOTE

PROJECT REF.: PL-LFI-PST-RP-025 **PAGE:** 1 of IV, 84

ISSUE / REV.: 1.0 **DATE:** March 3, 2008

Prepared by	**F. CUTTAIA** **IASF – CNR** **F. VILLA** **IASF – CNR**	**Date:** **Signature:** **Signature:**	March, 2008 
Agreed by	**C. BUTLER** **LFI** **Program Manager**	**Date:** **Signature:**	March, 2008 
Approved by	**N. MANDOLESI** **LFI** **Principal Investigator**	**Date:** **Signature:**	March, 2008 

DISTRIBUTION LIST

Recipient	Company / Institute		Sent
LFI System PCC	IASF – Bologna	lfispcc@bo.iasf.cnr.it	Yes

CHANGE RECORD

Issue	Date	Sheet	Description of Change	Release
0.1	feb, 05, '07	All	First issue of this document	
0.2	Mar, 14th, 2007	All Major changes	Updated analysis: Feeds FM instead of QM; full range in frequency; 3 HFI sources. Missing results in tables TBC.	
0.3	Mar, 16th , 2007	All	filled tables with analytic results from plots. Some new tables added. Analysis not changed.	
0.3.1	Mar, 21th , 2007		Annex 1 added	
0.3.2	Mar, 26th , 2007		Annex 2 added	
0.3.3	May, 29th , 2007		Annex 3 added	
0.3.4	July, 12th , 2007		Annex 4 added	

TABLE OF CONTENTS

1 SCOPE

1.1 Purpose

Purpose of this activity is to investigate the performances degradation of Planck Cold Load emissivity due to the possible mounting of a noise source required by HFI System team .
The load will be used in the Planck Satellite cryo facility to mimic the sky signal.

1.2 Acknowledgments

This document has been issued as a part of the activity performed under the ASI contract for Planck phase E2.

1.3 TERMS and ACRONYMS

4K RL	4K Reference Load
CFS	Carbon Fifer Source
CMB	Cosmic Microwave Background
EBB	Elegant Bread Board
FEM	Front End Module
FM	Flight Model
FPU	Focal Plane Unit
FS	Flight Spare
HFI	High Frequency Instrument
I/F	Interface
IL	Insertion Loss
LFI	Low Frequency Instrument
MS	Mounting Structure
N/A	Not Applicable
PD	Prototype Demonstrator
QM	Qualification Model
RDP	Reference Detector Plane
RH	Reference Horn
RL	Return Loss
RT	Reference Target
SPO	Spillover
SS	Spin-Synchronous
SKL	Sky Load
SW	Software
TBC	To Be Confirmed
TBD	To Be Defined
TBR	To Be Refined
ThL	Thermal Link
WG	Waveguide

2 APPLICABLE AND REFERENCE DOCUMENTS

2.1 Applicable documents

2.2 Reference documents

RD1: PL-LFI-PST-RP-005, "Simulation of RF performance of Planck cold load", F. Cuttaia, November 12th, 2003
RD2: PL-LFI-PST-TN-047 , "RF Comparative Analysis Of Materials And Design For The Planck Cold Load" F. Cuttaia, August 1st, 2003
RD3: SP-PH700916-IAS, "RATIONALE FOR IMPLEMENTING MEASUREMENT OF LOW FREQUENCY EXCESS RESPONSE OF HFI – PART 2"

3 Cold load general configuration

The Planck Cold Load (SKL) is a device placed between the secondary mirror and the FPU of the Planck satellite. It will provide a reference temperature signal at about 4 K (Load temperature is determined by fixing it directly to the bottom of a liquid Helium cryostat) to check the functioning of Planck detectors in about nominal conditions.
It is a large panel (a polygon circumscribing a circle of 630 mm diameter) of pyramids behaving like a perfect black-body.
It is placed in front of the FPU perpendicularly to the RDP z-axis. It is displaced from the 0-RDP in a wise to allow a clearance of 70 mm w.r.t. the nearest feedhorn.
Not disposing of a more updated drawing we refer here to the Alcatel design (Ref drawings: F0278C PLAPLM0S9000 and 1808000009 issue C) to represent the conceptual design.
The absorber was originally drawn according to these constraints.
The absorber dimensions and shape were originally chosen in order to fill a solid angle larger than 45° in front of the nearest feedhorn at the distance of 170 mm. Due to the CSL cryo-chamber mechanical implementation, this distance was reduced to 70 mm.
This change carries two possible consequence:
The solid angle subtended by the absorber is much larger (reducing leakage radiation)
The SKL is placed., especially for lowest frequency (30 GHz), in a region neighboring the very near field region.
This second aspect could in somewhat affect the field modeling on the SKL surface.

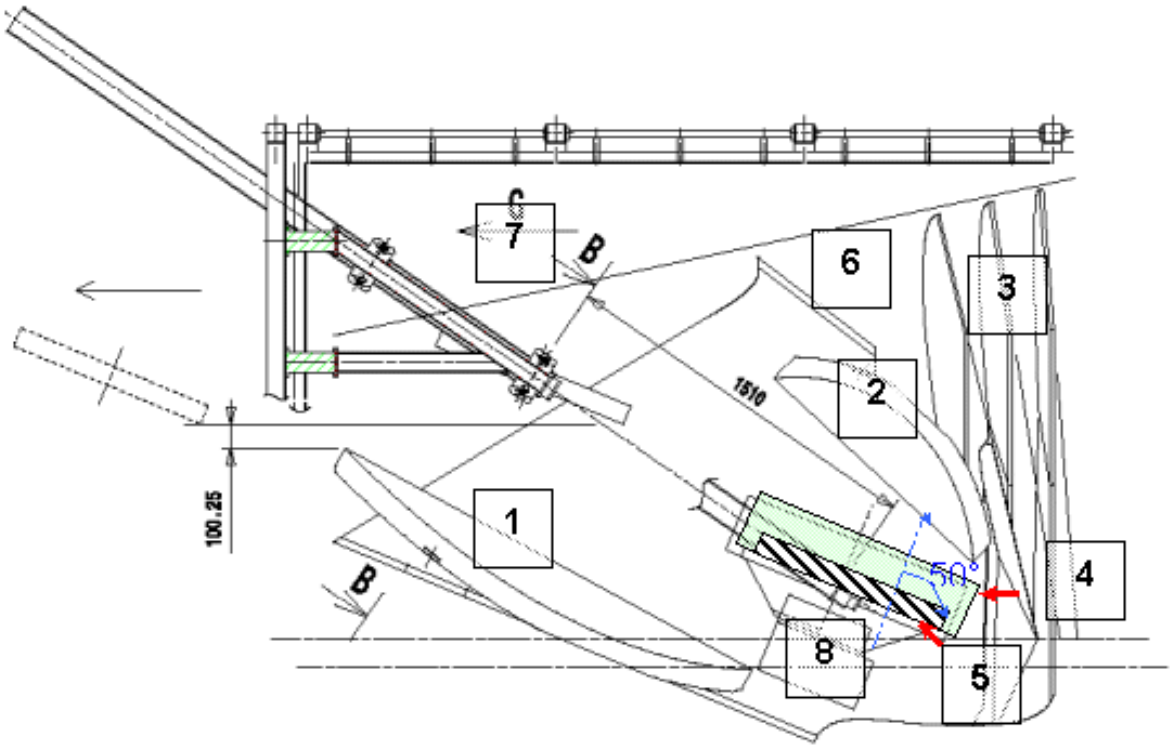

Figure 1: Cold load location (from drawing 1808000009). 1)primary mirror; 2)secondary mirror; 3)V-grooves; 4) volume allocated for the cold screen cryostat (Diameter 960mm, height=240mm); 5) absorber; 6) baffle.

4 Cold Load modelling

The SKL is a panel of absorbing pyramids made of ECCOSORB CR110. Each pyramid has height 40 mm and base 5X5 mm. Pyramids are backed by a 10 mm thick absorbing plate made of the same material. The panel is a modular structure composed of many individual sub-panels (75mmX*130 mm) fixed by custom screws, allowing tightening and differential contraction, to a metal plate.
The SKL was projected basing on mechanical and electromagnetic constrains described in RD1 and RD2.

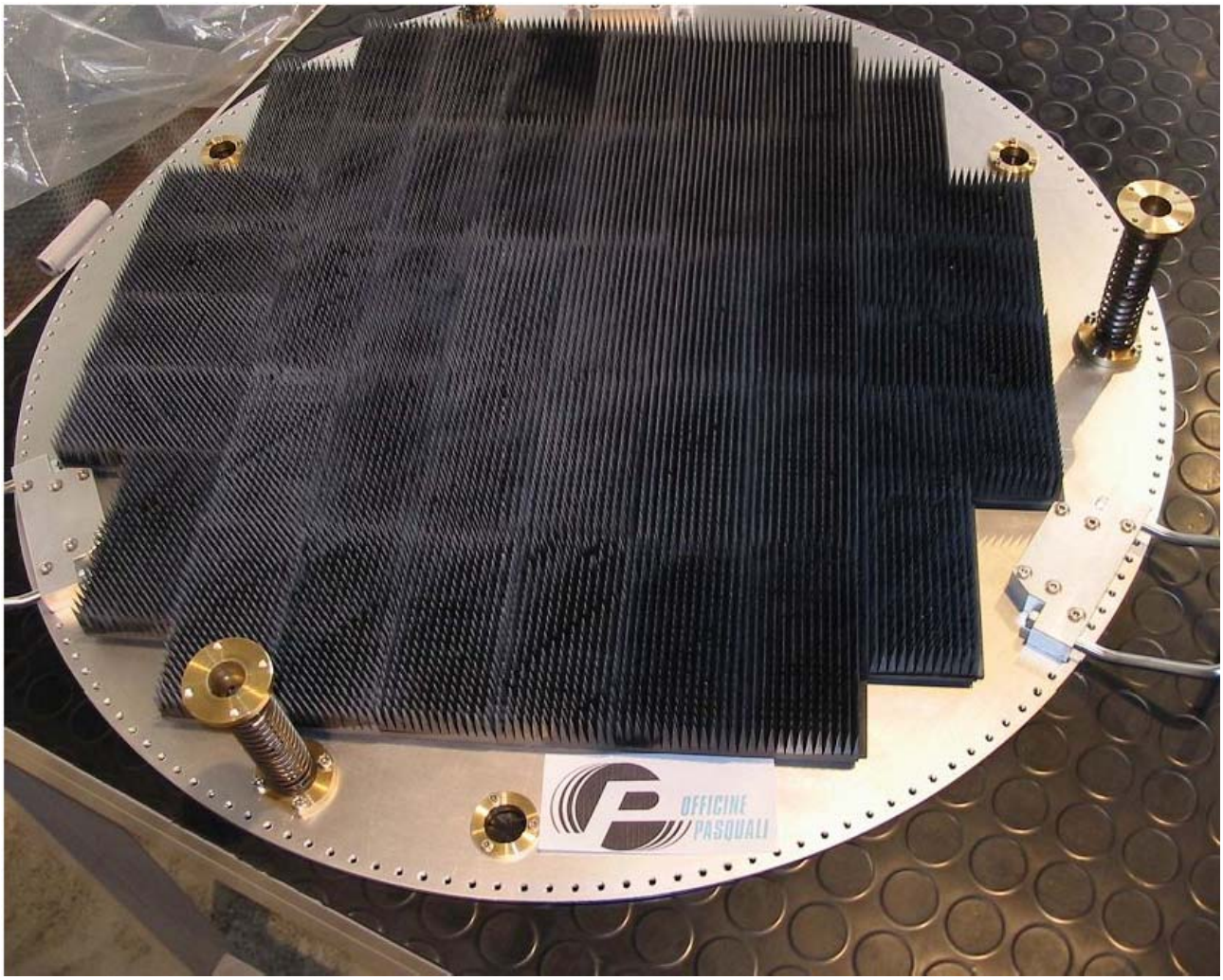

Figure 2

The SKL performances are strictly tied to its emissivity, that is a function of its reflectivity.

The total emissivity can generally be written (REF **) as

$$P_{TOT} = [P_{load} + P_{env}] * (1 - R_H) + P_{inst} \quad (1)$$

Where:

P_{LOAD} = power emitted by the SKL
P_{ENV} = power coming from the environment
R_H = feedhorn mismatching
P_{inst} = power emitted by the instrument back reflected via the SKL

The above formula can be written as:

$$P_{TOT} = \left[T^{A}_{ENV} * SPO + T^{A}_{LOAD} * (1 - \eta)\right] * (1 - R_H) + \left[T_n + kT_{Horn}\,\Delta\nu * \varepsilon_H\right] * S_{11}^{\,2} \quad (2)$$

With:

$$P_{env} = T^{A}_{ENV} * SPO \quad (3)$$

$$P_{load} = T^{A}_{LOAD} * (1 - \eta) \quad (4)$$

$$P_{inst} = P_{broadcast} + P_{Th} \quad (5)$$

The term SPO in (3) is the radiation leaking (directly, SPO_D, or non directly after reflection on the absorbing panel SPO_R) from the environment.

$$SPO_{tot} = SPO_D + SPO_R \quad (6)$$

η is the radiation efficiency:

$$\eta = \frac{P_{radiated}}{P_{emitted}} = \frac{SPO}{1 - S_{11}^{\,2}} = \frac{SPO_D}{1 - S_{11}^{\,2}} + \frac{SPO_R}{1 - S_{11}^{\,2}} \quad (7)$$

The first term in (5) is the noise emitted by radiometers, called broadcast noise. As a first approximation, it is the amplifier noise temperature T_n reflected by the load:

$$P_{broadcast} = T_n * S_{11}^{\,2} \quad (8)$$

Last term in (5) is the thermal emission, due to horn losses, reflected by the load. It can be expressed as:

$$P_{Th} = kT_{Horn}\Delta\nu * \varepsilon_{Horn} * S_{11}^{\,2} \quad (9)$$

In our simulation, the largest contribution is $\left[T^{A}_{LOAD} * (1 - \eta)\right] * (1 - R_H)$, but the term containing the spillover *SPO* contribution is also relevant.

For the purpose of this work we can define the term between brackets in (1) as

$$P_{tot} \propto \int_{\Omega} P(\theta,\phi) T_A(\theta,\phi) d\Omega \quad (10)$$

where P(θ,φ) is the antenna power pattern, $T_A(\theta,\varphi)$ is the observed temperature distribution (expressed in antenna temperature) and the integration is over 4π. Let us assume a symmetry over φ and rewrite the expression as a sum of two contributions:

$$P_{tot} \propto \int_{SKL} P(\theta) T_A^{SKL}(\theta) d\theta + \int_{SL} P(\theta) T_A^{SL}(\theta) d\theta = T_A^{SKL} \int_{SKL} P(\theta) d\theta + T_A^{SL} \int_{SL} P(\theta) d\theta \quad (11)$$

It means that all the power (coming from the SKL or from the sidelobes 'looking' the environment' emitted toward the feed must be convolved times the feed horn pattern.

In our case, given the distance feed-SKL, the pattern must be evaluated in the 'near field' region.
It must be stressed that , in the case of 30 GHz feed, the SKL is placed in the neighbourhood of the 'very near field region', that could in somewhat make the electromagnetic model rough.
Aim of this work is to evaluate the expected degradation of the SKL when any object of given size, supposed for simplicity perfectly reflecting , replace somewhere the SKL absorbing surface. This is a rough representation of the carbon-fibre source required by HFI instrument . No statement is made here about its shape. Due to the original non determination of the carbon fibre source displacement (*d* along z) with respect to the metal plate backing the SKL, in the first issue of this document (0.1) *d* has been parameterized from the maximum (110 mm) to the minimum (70 mm) distance with respect to the 0-RDP, complying with the SKL design. In this new issue, following the new documents provided by HFI (Ref: RD3), d has been fixed at the maximum distance along which some part of the reflecting structure constituting the Carbon Fibre Source is seen from the LFI feeds.
From HFI's preliminary drawings, the cross section of this object (from now on it will be named CFS, carbon fiber source) was supposed to be a square having side 30 mm (considering a little clearance for the mounting structure) : this representation is still in agreement with the last drawings in Ref. RD3.
However, while in the first issue of this document the CFS is supposed to be unique and located in the centre of the SKL, along z [x=0, y=0] of the RDP system, here a different configuration has been analysed, with three CFS sources disposed as a triangle having centre about coincident with the SKL centre. The 3 CFSs location is detailed in last section of Ref. RD3 and is summarized in the following table 1

X	-37	14	14
Y	0	-24	24
Z	168,4	168,4	168,4

Table 1 3 CFS positioning w.r.t. the 0-RDP

Firstly the near field for the 11 LFI's feedhorn is evaluated on a panel distant d=110 mm. d is the clearance between feed LFI_27 and plane where the CFS is placed This is in order to evaluate where the CFS is located w.r.t. the properties of each feed.
Then we can rewrite the (11) as:

$$P_{tot} \propto \int_{SKL-CFS} P(\theta) T_A^{SKL}(\theta) d\theta + \int_{CFS} P(\theta) T_A^{CFS}(\theta) d\theta + \int_{CFS} P(\theta) T_A^{ENV}(\theta) d\theta + \int_{SL} P(\theta) T_A^{SL}(\theta) d\theta \quad (12)$$

The effect of replacing a part of the SKL with a reflecting object (CFS) is double:
It lowers the SKL emissivity depending on the solid angle filled by the CFS in the feed field of view (FOV).
It increases non direct radiation leaking from environment (arrow 1 in Figure) via reflection on the CFS itself.
Both effects are directly proportional to the CFS apparent size, that depends on the distance from each feedhorn.
The electro-magnetic model, taking into account the real geometry of LFI, has been implemented using GRASP-9, in the 'near field ' approximation , using geometric optics.
The CFS was simply represented using as a rectangular surface with side 30 mm.

Results are shown, horn by horn, in the next chapter.

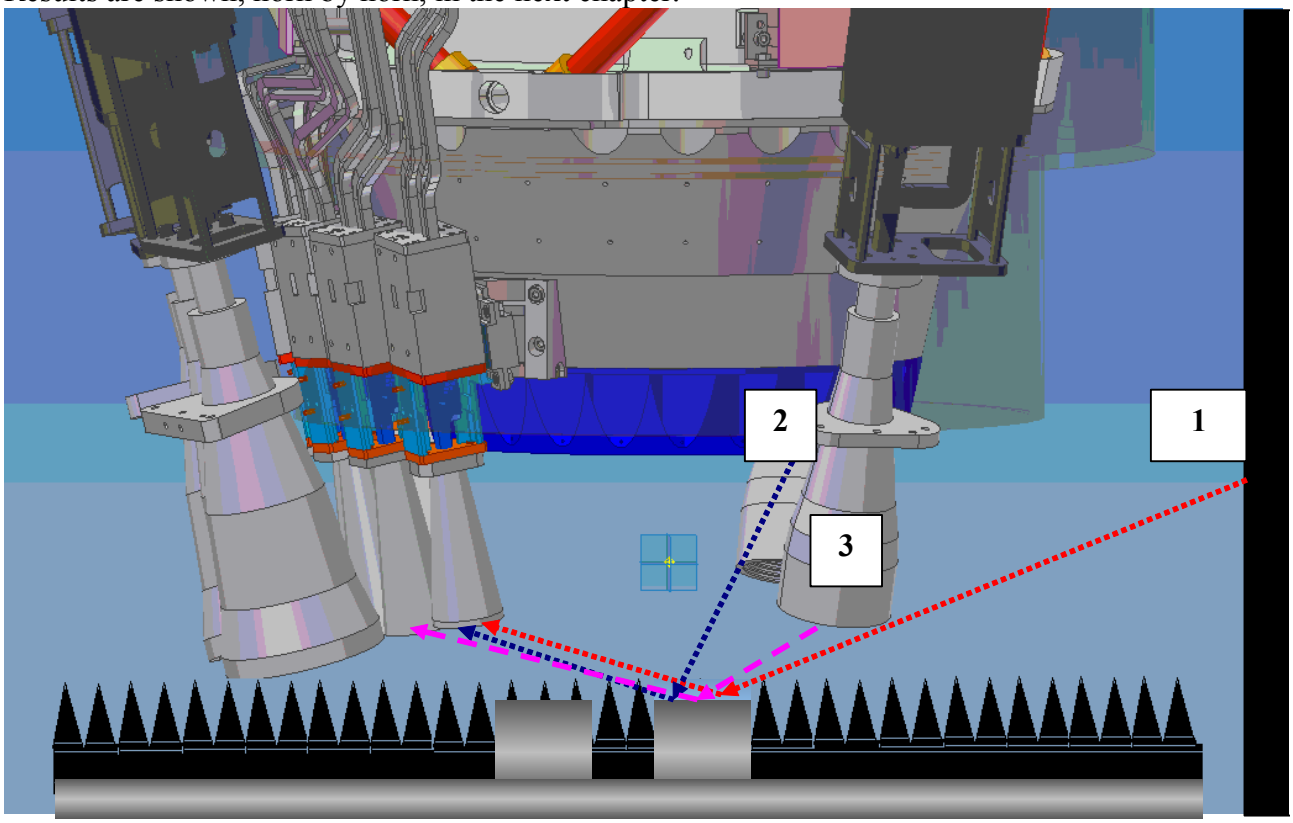

Figure 3 Schematic of the main possible spurious contributions reflected by a metal object replacing the absorbing panel. 1) thermal emission coming from environment or from the internal side of the Baffle (black) ; 2) thermal emission from the FPU (4K) and from HFI feeds (feeds and noise temperature) ; 3) thermal emission form LFI feeds and Noise Temperature emission from LFI radiometers throughout the feeds.

Before to present the detailed results, as a first level of understanding it can be useful to show comparison between two models, considering only geometric ray tracing. It will allow to appreciate the way the solid angle filled by the CFS changes with distance.
In the two next plots the spots projected onto the SKL surface (considered as a squared plane 800mm X 800mm located at the distance of the pyramids tips) are shown. Only rays falling into the solid angle [-45° : +45°] are diaplayed; others are blocked. This corresponds to the original statement put in year 2003 on the SKL drawing: it had to be large to fill a solid angle [-45° : +45°] evaluated from the outermost feedhorn, in order to block or limit radiation from environment.

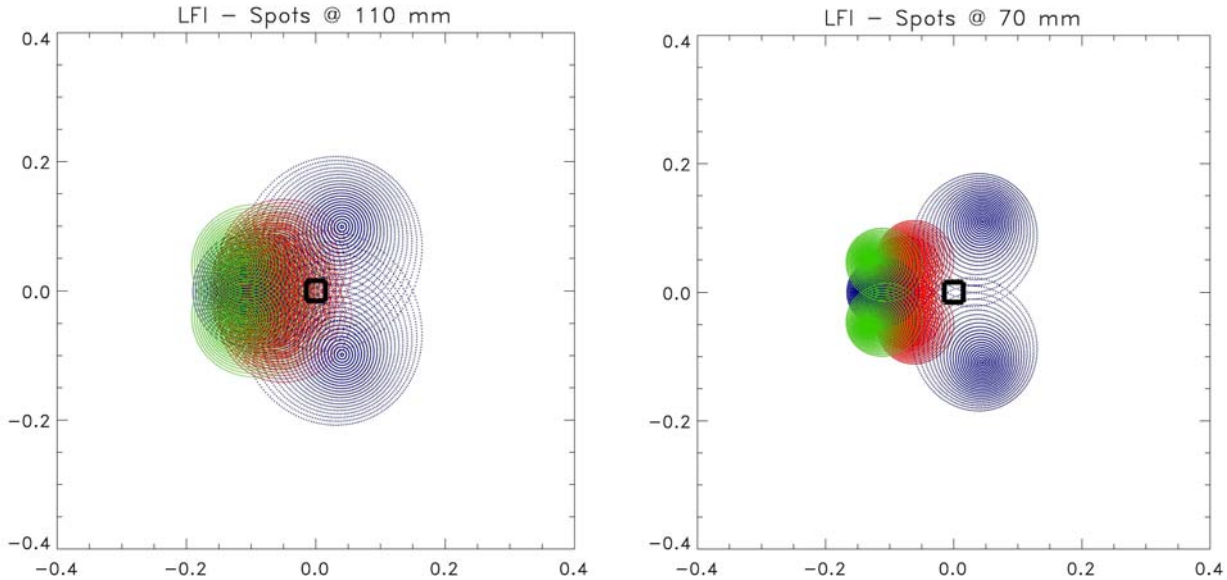

Figure 4 : feed horn spot on panel placed at 110 mm (left) and 70 mm (right) far from the nearest feedhorn (FH_LFI27). 30 GHz spots are displayed in green, 44 GHz spots in blue, 70 GHz spots in red. The CFS is represented by a square 30 mm X 30 mm (black). The spot size reduces considerably reducing the distance. At 70 mm the CFS fills only marginally a few spots . The outermost circle in each spot represents rays inclined by 45 deg w.r.t the feedhorn axis.

5 Main changes w.r.t Issue 0.1

Several changes have been applied in modelling the problem, in order to provide a more realistic description of the feeds.

In the previous issue, a single representation of the feeds was given per frequency: it means, for example, that all the 70 GHz feeds where supposed to be equal. In this Issue each horn has its specific representation in terms of fields in spherical waves.

The horns modelled were the QM feeds. In this new Issue the analysis has been repeated using FM horns. Results presented here supersede the old ones. The most differences are in 70 GHz channels and 44 GHz channels, cause the changes applied in the design of FM feeds w.r.t. QM units: differences practically translate mostly in a larger illumination of the absorbing panel seen by each feed.

In Issue 0.1 the analysis was performed only at the central frequencies (20 GHz, 44 GHz, 70 GHz): here a wide-band (as it is required to LFI detectors) analysis is presented, considering also the case of the response at the lower frequency of the band, (the beam size, in the near field region, scales not negligibly with the wavelength).

Grasp-9 Code was used in Issue 0.2 (Grasp-8 in Issue 0.1)

In Issue 0.1 only one CFS was considered: here three sources are supposed to be observed by LFI's feeds. Their positioning, as described in the previous paragraph, is that proposed by HFI.

6 Results (d=110 mm)

The field distribution on the absorbing panel has been calculated for each feed. Results are presented as contour plots in a logarithmic colour scale. The three sources are represented as squares with thick lines. The possible positioning of only one source is also displayed with dashed lines: its optimised location comes out as result of this work. The frequency is the lower side of each nominal bandwidth, that , as seen before, is the most unfavoured.

6.1.1 70GHZ channels

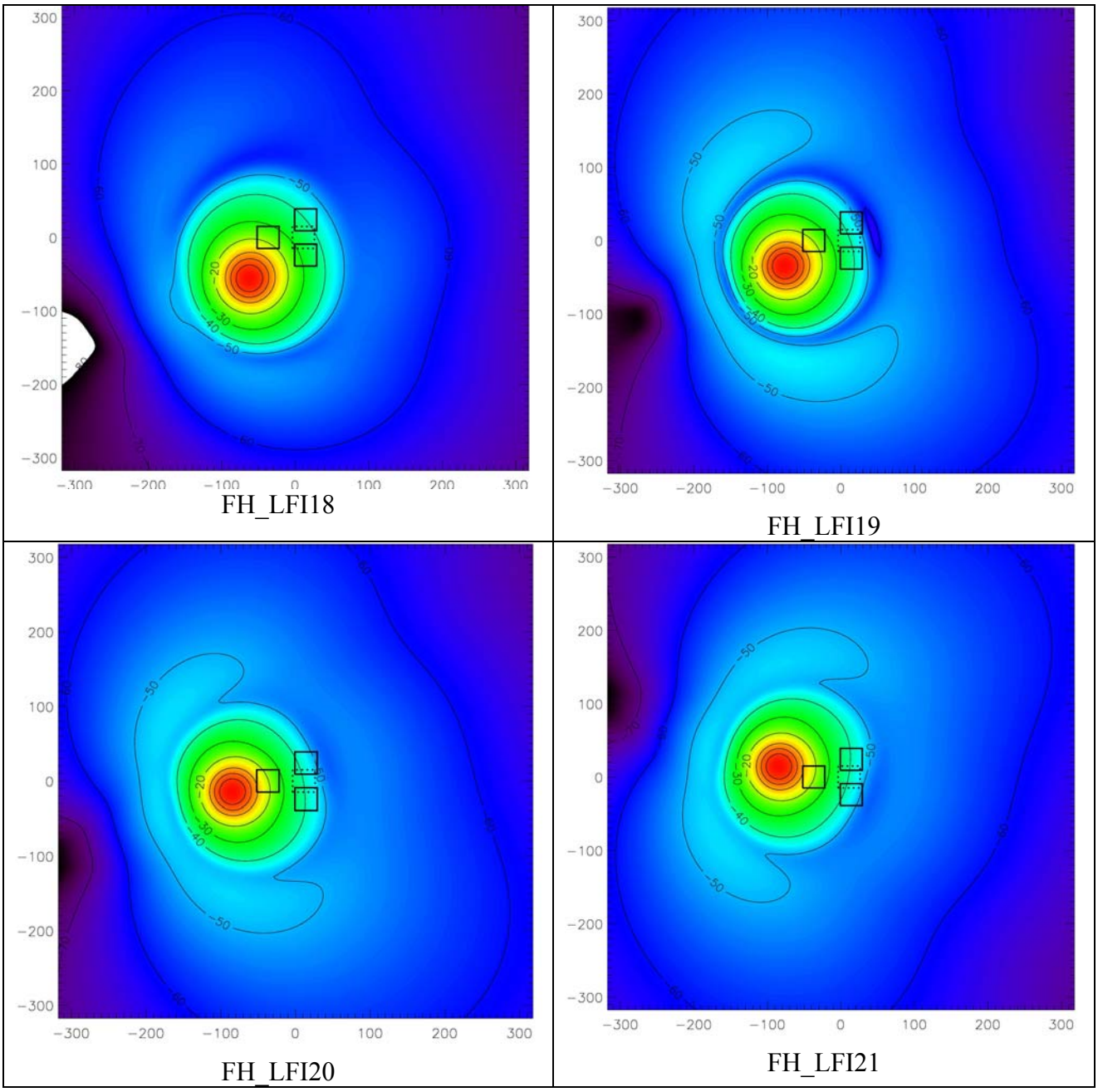

Figure 5

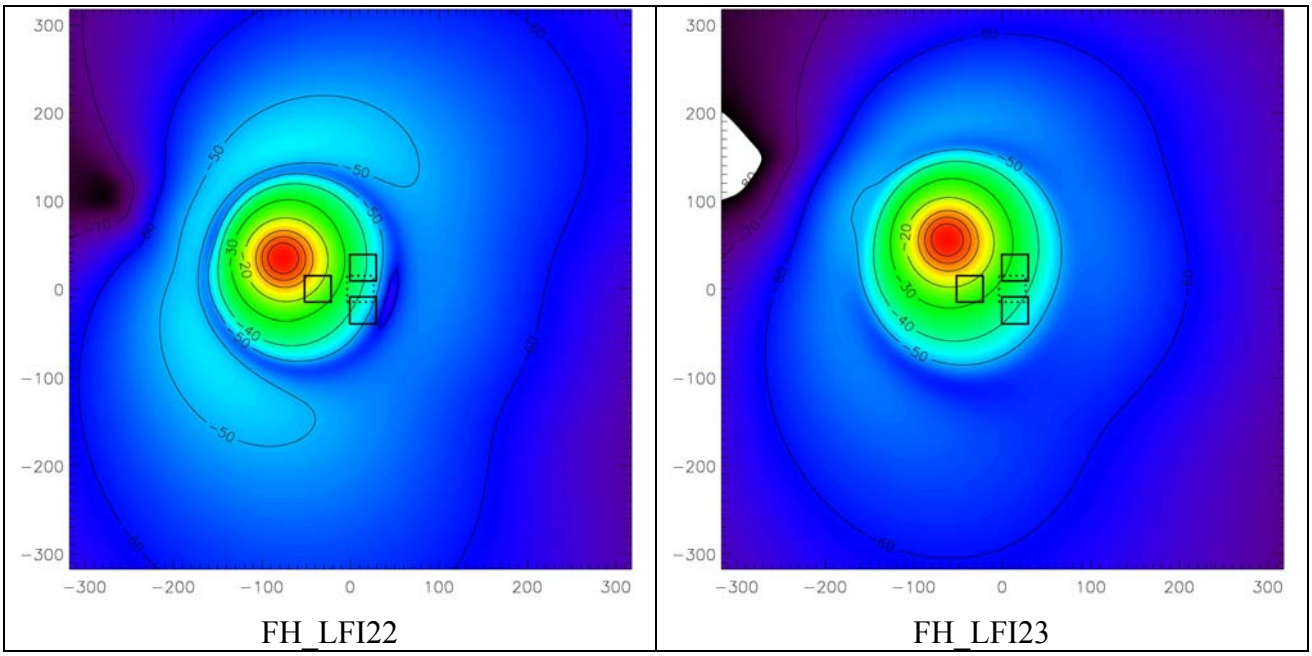

FH_LFI22 FH_LFI23

Figure 6

6.1.2 44GHZ channels

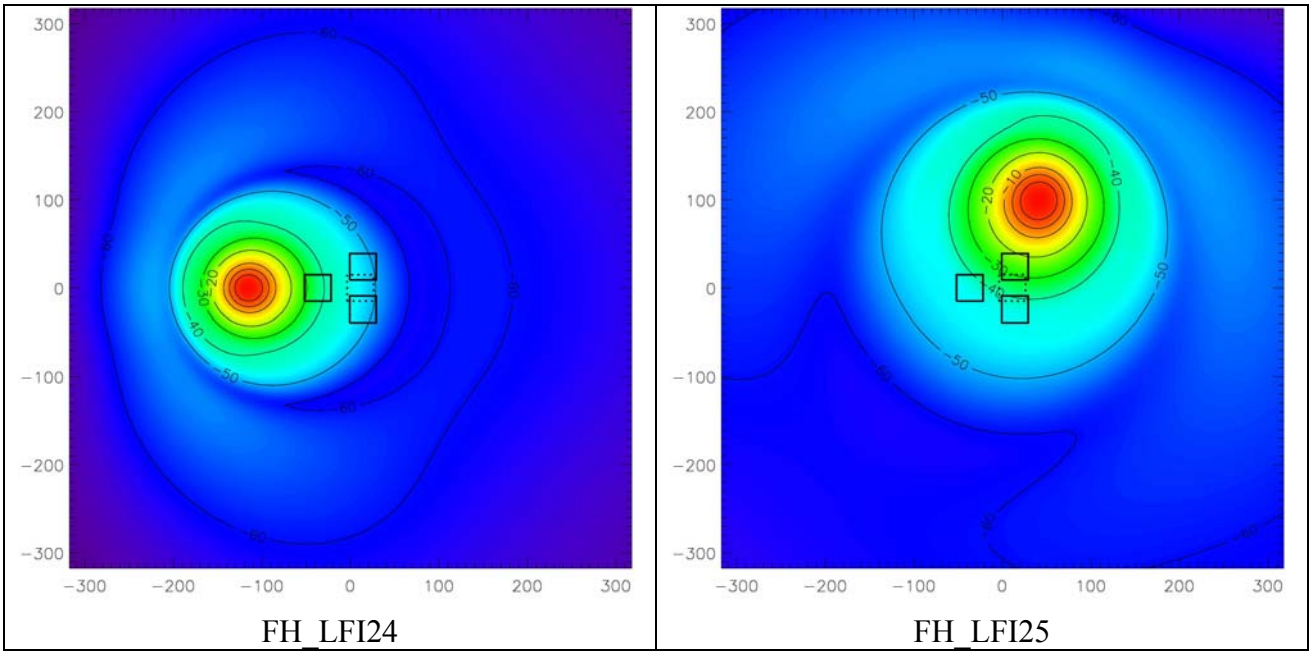

FH_LFI24 FH_LFI25

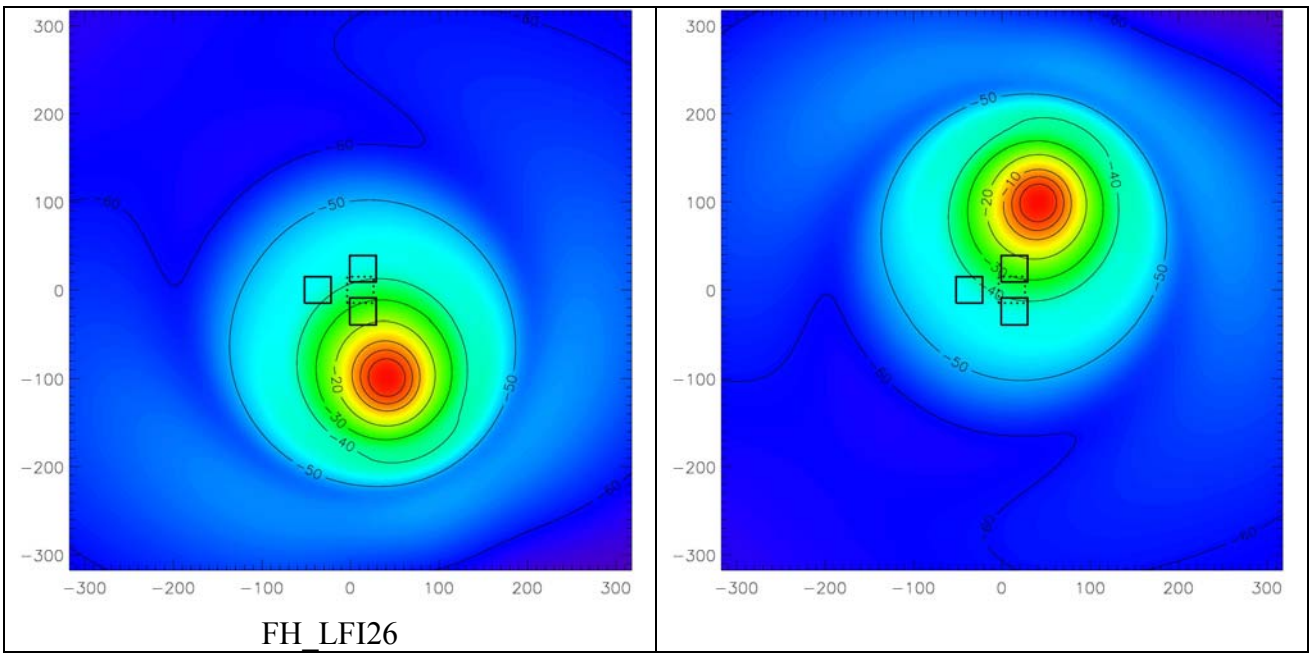

FH_LFI26

Figure 7

6.1.3 30 GHz channels

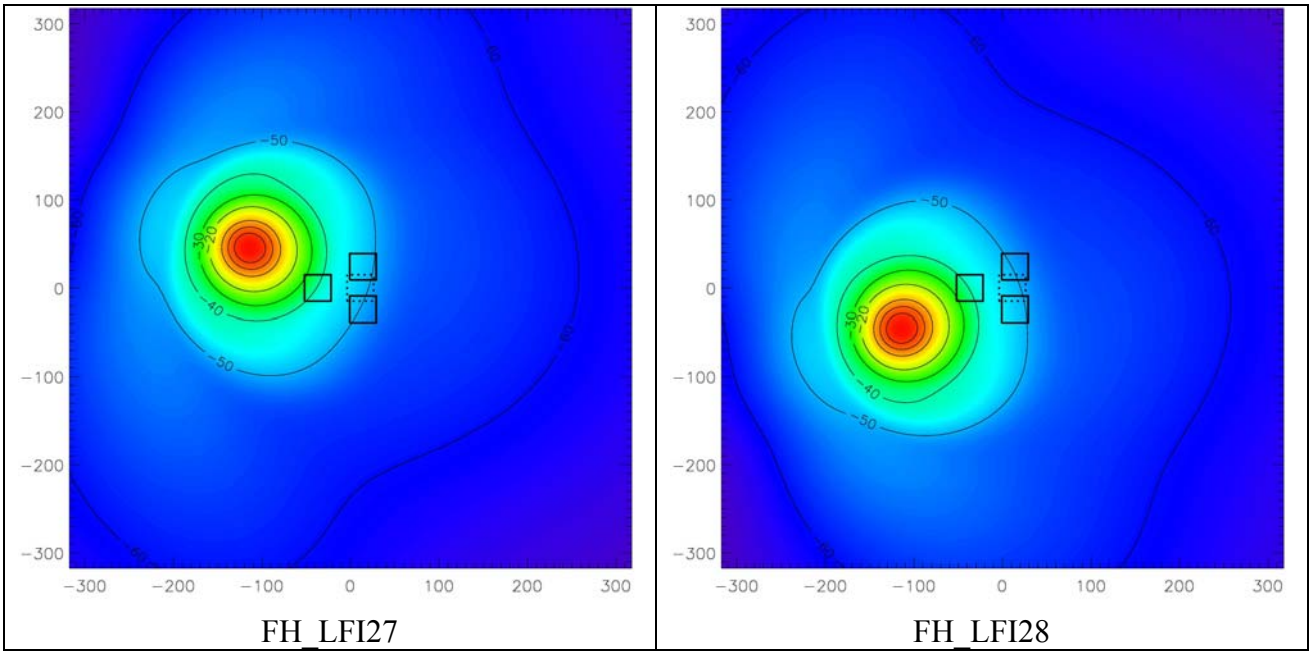

FH_LFI27 FH_LFI28

Figure 8

In order to have a simultaneous comparable representation of all the fields, it was necessary normalize each beam to its maximum. In the next two plots, the maximum (calculated comparing all the 11 beams) normalized power falling in each cell in which the SKL is ideally decomposed (it is here constituted of 128X128 pixels) is displayed: it allows to understand, in an unique plot , how largely the presence of any CFS may impact on feeds performances.
The analysis is presented both at the central frequency and at the lower frequency.
As it can be easily seen, in both cases the 3 CFSs interfere with the beams in regions where the power is considerably high (also higher than -20 dB w.r.t. the maximum in the boresight direction.)

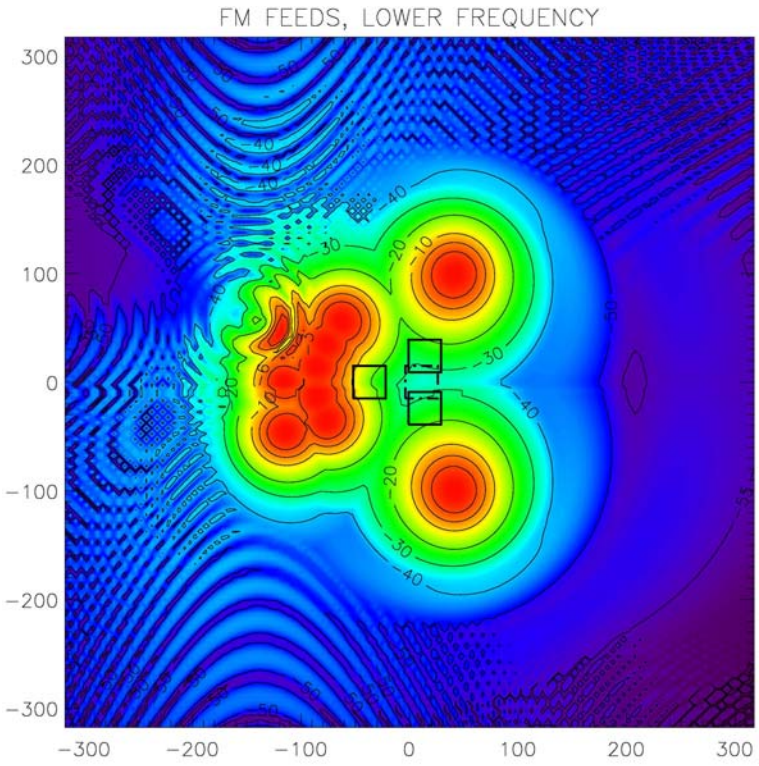

Figure 9 maximum contour plot level for the 11 feeds at the lowest frequencies.

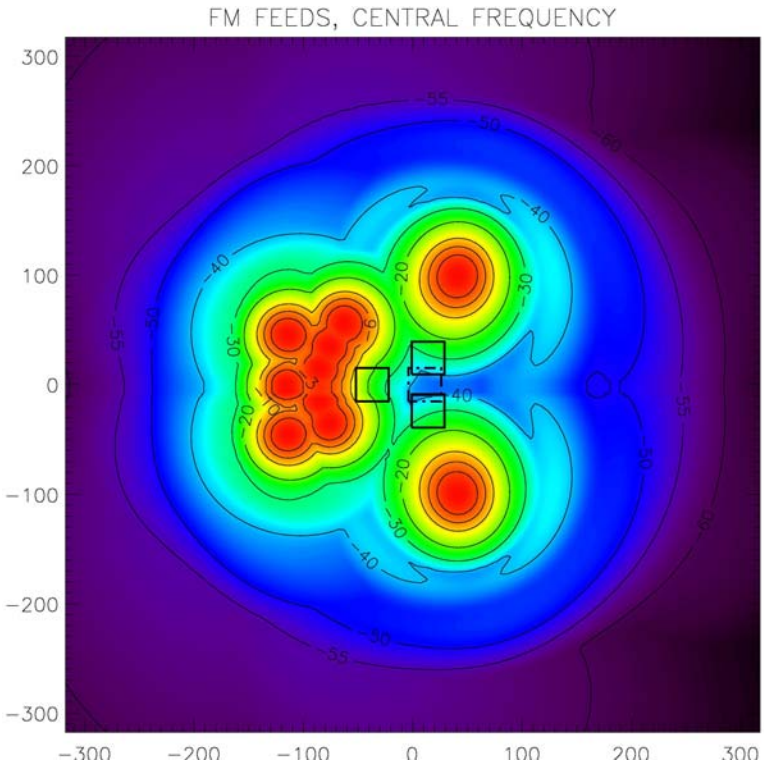

Figure 10 maximum contour plot level for the 11 feeds at the central frequencies.

6.1.4 Analysis

The net power falling on each source (individuated as S1, S2, S3) has been evaluated form the above contour plots. For each feed, the total power is mostly dominated by only one source while the logarithmic sum of the remaining twos generally counts for less than 0.5 dB. Results are shown in Table 2 divided per feeds and sources. It comes out that the 70 GHz channels are the mostly influenced by the CFS (especially by S1); among 44 GHz channels are disturbed RCA 25 (S3) and RCA 26 (S2) , while RCA 24 seems to be in a privileged position; channels at 30 GHz are undisturbed, as already known from ISSUE 0.1 , since the design of 30 GHz QM units and FM units is the same. Numbers reported in Table 2 are obtained as:

$$P_{\mathrm{Re}\,fl} = \frac{\int_{CFSi} P(\theta))d\theta}{\int_{SKL} P(\theta))d\theta} \qquad (13)$$

Together with the numbers coming from modelling, also the uncertainty bars are reported.
A diagram displaying results (Plot 1) and the matrix (Table 3) displaying sources impact on feeds (the >-30 dB is coloured in red) follow**. It is to be noted that the term P_{refl} is roughly similar to the contour level passing through the barycentre of each source**: it can be assumed as simple rule to get rough estimation from a quick look of the individual contour plots.

	S1	S2	S3	TOT (dB)	MAX	MIN
18	-22.4	-30.2	-38.5	-21.6	-18.6	-24.6
19	-19.9	-35.0	-41.1	-19.7	-16.7	-22.7
20	-19.6	-37.2	-40.1	-19.5	-16.5	-22.5
21	-20.3	-40.4	-37.5	-20.2	-17.2	-23.2
22	-21.2	-40.9	-35.1	-20.9	-17.9	-23.9
23	-24.3	-38.3	-30.1	-23.1	-20.1	-26.1
24	-35.5	-43.8	-43.8	-34.3	-31.3	-37.3
25	-44.3	-43.2	-27.7	-27.5	-24.5	-30.5
26	-43.4	-27.7	-43.9	-27.5	-24.5	-30.5
27	-41.5	-47.1	-47.5	-39.7	-36.7	-42.7
28	-40.2	-48.1	-50.1	-39.2	-36.2	-42.2

Table 2 P_{refl} divided per feeds and per sources

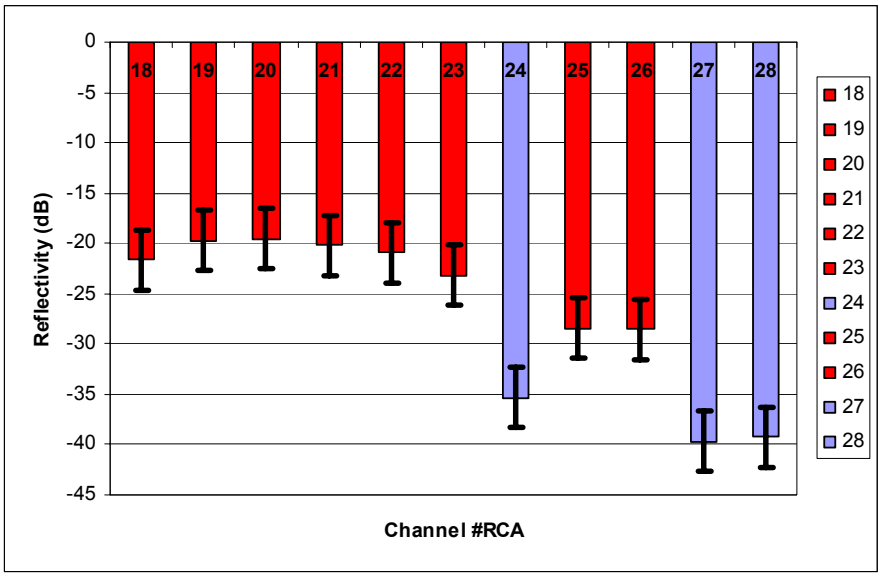

Plot 2 diagram displaying data from Table 2.

	S1	S2	S3
18			
19			
20			
21			
22			
23			
24			
25			
26			
27			
28			

Table 3 Sources MATRIX : red cells indicate that that combination [RCA#-Si] produces a critical reflectivity (Integrated power falling on Si >-30 dB) . RCA 24, 27 and 29 are not affected form by this problem

7 Emissivity (numbers and tables still to be updated)

Basing on results from §6.1.4 and Table 2, applied to formulation described in §4 , it is possible to estimate the effect of CFS presence on total emissivity.
Starting from relation derived in (12), this effect applies mostly to two terms:

$$\int_{CFS} P(\theta) T_A^{CFS}(\theta) d\theta \qquad (14) \qquad \text{and} \qquad \int_{CFS} P(\theta) T_A^{ENV}(\theta) d\theta \qquad (15)$$

The first term represents the lost in the SKL Emissivity (that is a property of material, shape and wavelength) caused by the substitution of a perfectly absorbing material (as the SKL is: the reflectivity of each panel was measured (REF:) to be < -40 dB) with a reflecting material.
Neglecting the real shape of the CFS, we can approximate it here with a reflecting squared surface with Emissivity $\varepsilon_{CFS} = 0.1$ (meaning that only 10% of its thermodynamic power is transmitted); the total thermal power (power due to its thermodynamic temperature) emitted (reaching the feed horn characterized by mismatching $S^H{}_{11}{}^2$) is :

$$P_{CFS}^{TH} = kT_{CFS} \Delta\nu * \varepsilon_{CFS} * S^H{}_{11}{}^2 \qquad (16)$$

It means that, also supposing that the CFS could thermalize at the same temperature of the SKL (4K), the SKL is loosing in thermal Emissivity an amount equal to:

$$P_{LOST}^{TH} = kT_{CFS} \Delta\nu * (\varepsilon_{SKL} - \varepsilon_{CFS}) * S^H{}_{11}{}^2 * \frac{S^{CFS}}{S^{SKL}} \qquad (17)$$

The term ε_{SKL} is > 0.9999 and can be for simplicity taken = 1. S^{CFS} and S^{SKL} are respectively the CFS and SKL cross surfaces.
However, we are interested here not to characterize the global properties of the SKL but only those changes perceived by each feedhorn. Than term P_{LOST}^{TH} must be convolved by the feedhorn power pattern, to gives the individual lost of emissivity appreciated by the generic feedhorn *FH_LFI#*
We get:

$$\left(P_{LOST}^{TH}\right)_{FH\_LFI\#} = kT_{CFS} \Delta\nu * (\varepsilon_{SKL} - \varepsilon_{CFS}) * S^H{}_{11}{}^2 * \cdot \int_{CFS} P_{FH\_LFI\#}(\theta)\, d\theta$$

(18)

Regarding term (15) , it holds everything said for term (14) about convolution times the feedhorn pattern. In add, we can explicit this term by separating it into two components:

$$\int_{CFS} P(\theta) T_A^{ENV}(\theta)\, d\theta = \left(\varepsilon^{EXT\_ENV} \cdot T_A^{EXT\_ENV} + \varepsilon^{FPU} \cdot S_{11}{}^{FH\_LFI\#} \cdot T_A^{FPU} + T_A^{NOISE}\right) \cdot \left(1 - \varepsilon^{CFS}\right) \cdot \int_{CFS} P(\theta)\, d\theta$$

(19)

The first component in left brackets represents radiation not coming from the system FPU plus SKL. It is radiation reflected by the CFS, coming from the baffle (that is expected to stay at 50K with emissivity of about 0.1) and from the internal side of the cryochamber (that is expected to stay at 20K with emissivity of about 1). So we can consider for it the worst case that is T=20K, ε=1)
The second component inside left brackets represents thermal radiation coming from FPU. The FPU stays at 20 K and has expected emissivity lower than 0.1. The term $S_{11}^{FH\_LFI\#}$ is the feedhorn mismatching that here can be neglected and considered equal to unity.
The third term is the noise temperature coming from amplifiers via the feedhorn. The worst case (however not realistic here) is that a feed looks its own noise radiation reflected by the CFS. It is not true, since the CFS should be located approximately coaxial with each feed (or should be a very large object filling the FPU) . What can happen is only that some radiation coming from all other feeds enters the one under test. This implies that the convolution product between the pattern of the feedhorn under test and all the others be performed. This term can hence be written as:

$$T_A^{NOISE} = \cdot \sum_{\substack{i,j=18 \\ i \neq j}}^{i,j=28} \int_{CFS} P^{FH\_LFI\#i}(\theta)\, P^{FH\_LFI\#j}(\theta)\, d\theta \qquad (20)$$

The fourth term inside brackets is the CFS reflectivity (R=0.9)
Results from (19) are summarized in the following table, detailing contributions from each term .

RCA	RF LOSS	TH LOSS	ENV/baffle	Feeds /FPU	coupling	HFI Tn
#	%	mK	mK	mK	mK	mK
18	1.37	49.2	283.2	24.6	38.0	TBC
19	2.14	77.0	442.7	38.5	54.4	TBC
20	2.23	80.4	462.5	40.2	56.2	TBC
21	1.92	69.1	397.1	34.5	50.1	TBC
22	1.61	57.8	332.2	28.9	43.4	TBC
23	0.97	34.8	200.4	17.4	28.0	TBC
24	0.06	2.1	12.1	1.0	1.8	TBC
25	0.28	10.2	58.6	5.1	8.8	TBC
26	0.28	10.1	58.1	5.1	8.7	TBC
27	0.02	0.8	4.5	0.4	0.7	TBC
28	0.02	0.9	5.0	0.4	0.8	TBC

Table 4 Non ideal contributions caused by CFS. Results are obtained by developing equation (19) and evaluating separately each term. From the left, table reports: RCA number, Radiometric degradation in emissivity, Thermal loss (thermodynamic temperature overestimation evaluated for a SKL having T= 4K) , thermal excess coming from the external surrounding (cryo-chamber environment at 20K, Baffle at 50K) , thermal excess from feeds and FPU, RF coupling between the feeds.

The contributions from each source are detailed in the following three tables:

RCA	RF LOSS	TH LOSS	ENV/baffle	Feeds /FPU	coupling	HFI Tn
#	%	mK	mK	mK	mK	mK
18	1.15	41.3	237.6	20.7	29.0	TBC
19	2.06	74.2	426.6	37.1	46.4	TBC
20	2.18	78.4	450.7	39.2	48.3	TBC
21	1.86	67.1	386.0	33.6	43.1	TBC
22	1.53	55.0	316.1	27.5	36.8	TBC
23	0.74	26.8	154.0	13.4	19.7	TBC
24	0.04	1.6	9.3	0.8	1.3	TBC
25	0.01	0.2	1.2	0.1	0.2	TBC
26	0.01	0.3	1.5	0.1	0.2	TBC
27	0.01	0.5	2.9	0.3	0.4	TBC
28	0.02	0.7	3.9	0.3	0.5	TBC

Table 5 Contribution from S1

RCA	RF LOSS	TH LOSS	ENV/baffle	Feeds /FPU	coupling	HFI Tn
#	%	mK	mK	mK	mK	mK
18	0.19	6.9	39.8	3.5	0.2	TBC
19	0.06	2.2	12.9	1.1	0.1	TBC
20	0.04	1.4	7.8	0.7	0.1	TBC
21	0.02	0.7	3.8	0.3	0.0	TBC
22	0.02	0.6	3.3	0.3	0.0	TBC
23	0.03	1.1	6.2	0.5	0.0	TBC
24	0.01	0.2	1.4	0.1	0.0	TBC
25	0.01	0.3	1.6	0.1	0.0	TBC
26	0.27	9.6	55.3	4.8	0.2	TBC
27	0.00	0.1	0.8	0.1	0.0	TBC
28	0.00	0.1	0.6	0.1	0.0	TBC

Table 6 Contribution from S2

RCA	RF LOSS	TH LOSS	ENV/baffle	Feeds /FPU	coupling	HFI Tn
#	%	mK	mK	mK	mK	mK
18	0.03	1.0	5.8	0.5	0.0	TBC
19	0.02	0.6	3.2	0.3	0.0	TBC
20	0.02	0.7	4.0	0.3	0.0	TBC
21	0.04	1.3	7.3	0.6	0.1	TBC
22	0.06	2.2	12.8	1.1	0.1	TBC
23	0.19	7.0	40.2	3.5	0.2	TBC
24	0.01	0.2	1.4	0.1	0.0	TBC
25	0.27	9.7	55.8	4.9	0.2	TBC
26	0.01	0.2	1.3	0.1	0.0	TBC
27	0.00	0.1	0.7	0.1	0.0	TBC
28	0.00	0.1	0.4	0.0	0.0	TBC

Table 7 Contribution from S3

Only for comparison, the nominal case in which the SKL reflectivity is lower than -30 dB is proposed in the table below: this is also the case in which the SKL sources are located in regions outside the -30 dB power contour.

RCA	RF LOSS	TH LOSS	ENV/baffle	Feeds /FPU	coupling	HFI Tn
#	%	mK	mK	mK	mK	mK
18	0.1	3.6	20.7	1.8	0.2	TBC
19	0.1	3.6	20.7	1.8	0.2	TBC
20	0.1	3.6	20.7	1.8	0.2	TBC
21	0.1	3.6	20.7	1.8	0.2	TBC
22	0.1	3.6	20.7	1.8	0.2	TBC
23	0.1	3.6	20.7	1.8	0.2	TBC
24	0.1	3.6	20.7	1.8	0.2	TBC
25	0.1	3.6	20.7	1.8	0.2	TBC
26	0.1	3.6	20.7	1.8	0.2	TBC
27	0.1	3.6	20.7	1.8	0.2	TBC
28	0.1	3.6	20.7	1.8	0.2	TBC

Table 8 ideal case: SKL reflectivity <-30 dB (SKL with CFSs external to the -30 dB level).

8 Preliminary conclusions

As it was already foreseen by the results presented in Issue 0.1, any non ideally absorbing object placed not in the neighborhood of the SKL centre can produce interference with LFI feeds, at different levels, depending on the considered feed and source. This interference has different natures and can consequently have different impact on the LFI operations. Expected modifications are in terms of :

Emissivity loss of the SKL (causing a signal seen from the feeds lower than expected by 1-2%): this is maybe the less problematic features, since it acts on the estimation of SKL absolute temperature.

Spurious signals reflected toward the LFI (100-500 mK) coming from the surrounding environment and correlated with the cryofacility characteristic fluctuations .

Spurious signals reflected toward the LFI coming from the LFI itself (thermal from FPU and radiometric- from amplifiers- signals) causing a cross correlation LFI-LFI (40-80 mK)

Spurious signals reflected toward the LFI coming from the HFI (thermal from feeds and radiometric- details should be known to investigate this contribution) causing a cross correlation LFI-HFI: I am not able to make an estimation of this contribution without additional infos from HFI.

Moreover, the analysis presented above has, up to now, a large uncertainty due to the kind of solution required (the SKL is located in the limit of the very near field region for several feeds) , of the method (to be investigated deeper) used to get the fields of FM feeds, of the many approximations used, of the time required to perform all these analysis with a large degree of confidence. All this contributions can be at present estimated as a ±3 dB uncertainty bar: it suggests that any reflecting object should be located at least outside the -30 dB contour ('safe region'.

The safe region (to be thought as a weak interference region) is displayed in white color in the two figures 9 and 10. In figure 9 is also displayed the -20 dB contour level. Following the argumentations above, the two levels must be read as:
[-27 dB : -33 dB] and [-17 dB : -23 dB]

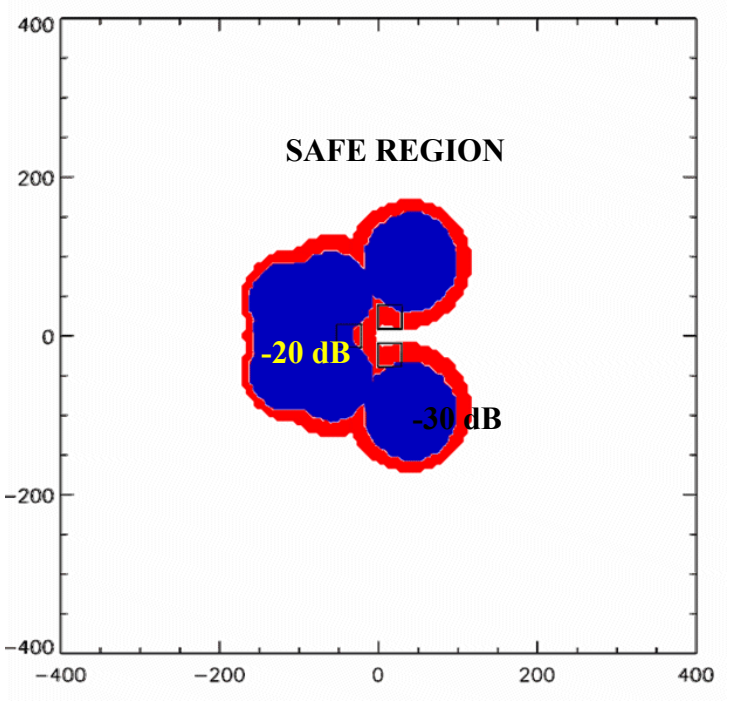

Figure 11

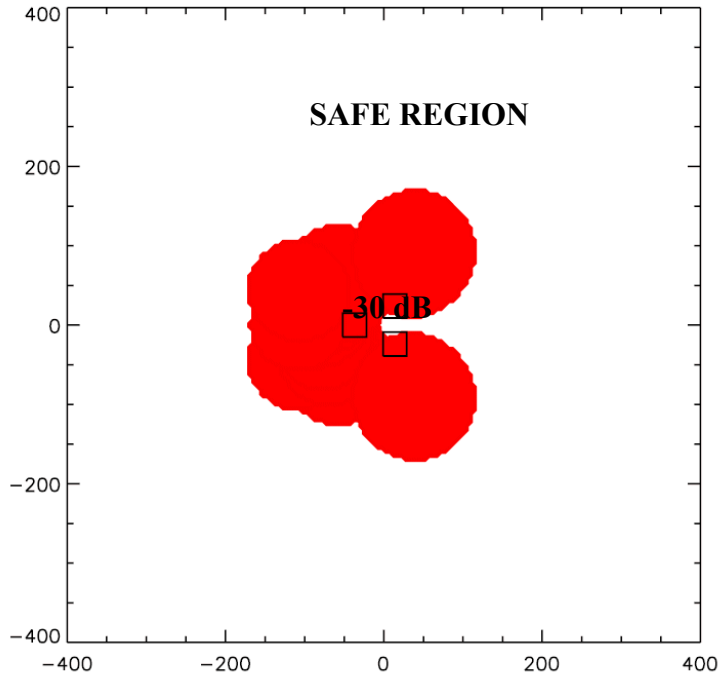

Figure 12

9 Conclusions

This works wants to be an attempt to estimate the effects produced on LFI instrument by the substitution of several pyramids in the PLANCK Cold Load with a carbon fibre noise source. The noise source is supposed here to be switched OFF during LFI observation time and is treated only as a passive device.
Simulations have been run using GRASP-8 and GRASP-9 software to evaluate the near field projection onto the Cold Load plane. Results have been applied to an analytical model taking into account the various contributions affecting the cold load performances and producing non ideal behaviours.
Contributions to non ideal performances are of two genres: degradation of the cold load emissivity and excess of noise coming from sources external to the cold load.
This result suggests that 3 sources (located as proposed by HFI) can create unwanted non ideal behaviours in LFI radiometers, especially in terms of spurious cross correlations.
Most of the undesired interference is due to one source (namely S1) acting especially on 70 GHz channels. Other sources (S2 and S3) can impact on RCA 25 and RCA 26 performances.
One source, located near the centre, seems otherwise to be acceptable, also without additional analysis.
Possible solutions to mitigate the interference by implementing absorbing shields are beyond the scope of this preliminary work and are eventually leaved to another Issue of the same document.

Output of this work, besides of the numerical solutions, is a map of the 'weak interference regions' (white region of Fig. 10) where it is possible to locate sources without creating a considerable effect on LFI. Obviously, also in the case of sources located in this region, the specific case (number of sources , dimensions) mast be considered deeper.

ANNEX1: ABOUT THE ENVIRONMENTAL COMPONENT CALCULATED IN PL-LFI-PST-XXX Issue 0.3

F. Cuttaia, 21/03/2007

Here follows a brief rough description of calculations made to estimate the contribution from environment.

Each CFS (Carbon Fibre Source) **emits two main contributions (power P):**

Due to its thermodynamic temperature (about 4K) with very poor efficiency (ε <0.1) – (the blue arrow): **$P \approx 4K*\varepsilon_{CFS}$**
Reflected radiation coming from the surrounding at a certain temperature T? K, with high efficiency >0.9 (the red arrow): **$P \approx T?K*(1-\varepsilon_{CFS})$**

Both these contributions must be multiplied times the fraction (P_{CFS}) of the total power effectively reaching each horn. This fraction (schematised with the colour scale in figure) was calculated in the report as:

$$P_{\_CFS} = \frac{\int \text{power falling on source surface}}{\int \text{power falling on entire SKL surface}} < 1$$

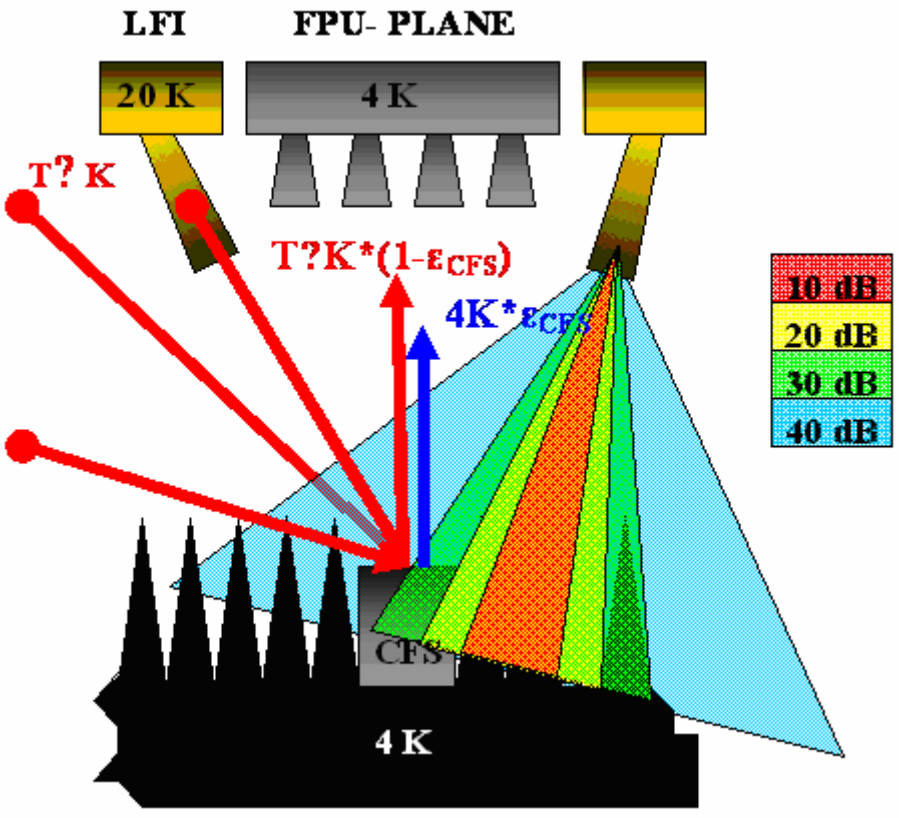

The geometry of the environment surrounding the SKL is very complicated: only a rough estimation of T?K can be done.
Maybe a cross check with data available to HFI can provide a more accurate solution.
A deeper analysis would require to implement a detailed model using GRASP , launching a plane wave from each CFS and analysing how much of this radiation is blocked-reflected by each object.
This is unfeasible at this stage (meaning to clarify the best positioning of CFSs) and in the short time available.

Scope of this brief note is to present a rough estimation of the contribution coming from the surrounding.
It is here defined **SURROUNDING**: everything except the SKL and the objects at 4K (FPU plane where the HFI horns are mounted and the HFI feed). In the following table are reported all elements belonging to the surrounding, together with their emissivity . Concerning the telescope, its emissivity is for me at present unknown (? In the table) , since I ignore the setup condition in CSL (will it be tested in nominal conditions or covered to avoid contamination?)

PART	T (K)	ε
LFI FEEDS & MAIN FRAME	20	< 0.1
BAFFLE	50	< 0.1
TELESCOPE	50	< 0.01 / ?
CRYO CHAMBER	20	1

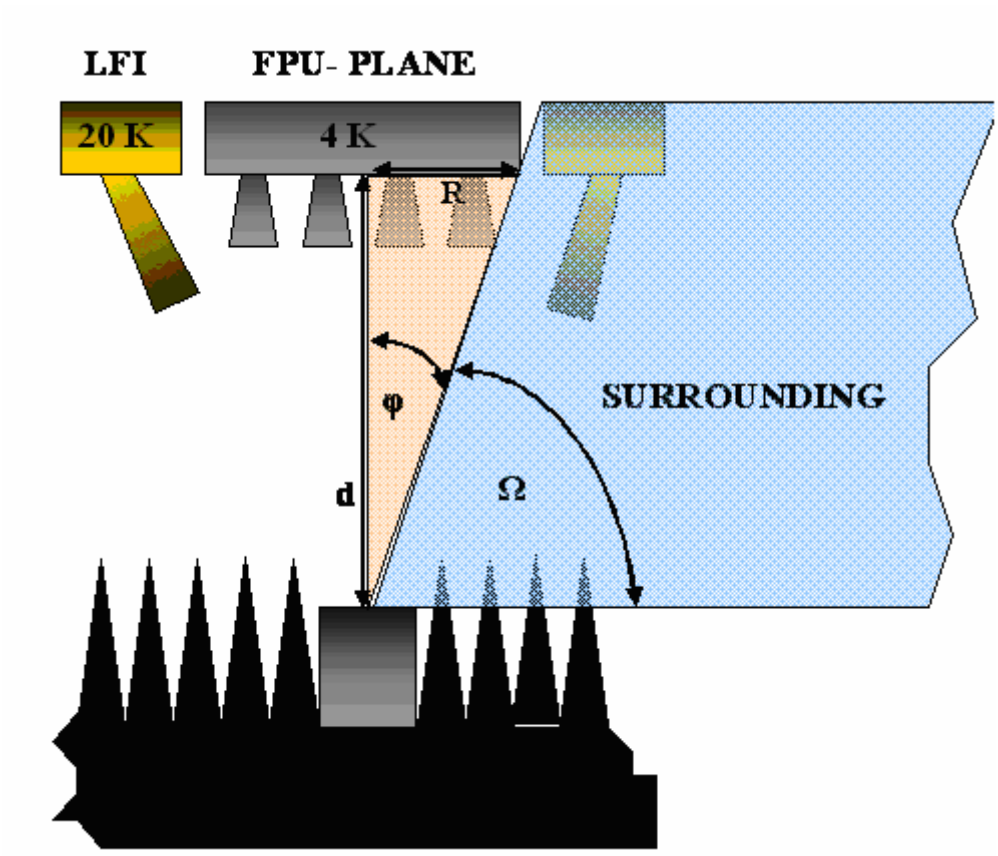

The power coming from environment (surrounding) is then defined as:

(Temperature of the emitting object) * (emissivity of the object* reflectivity of the CFS) * (percentage of the power entering the feed)* (percentage ψ of the whole solid angle subtended by that source)
That is:

$$P\_{ENV} = T?K * \varepsilon_{T?K} * \left(1 - \varepsilon\_{CFS}\right) * P\_{CFS} * \Psi$$

The last term ψ is the most uncertain point, since we do not know exactly the thermal distribution of the surrounding and how radiation propagates among the different stages.

With reference to the figure above we can state that:

Each CFS is positioned about in the centre of the SKL.
d = distance from CFS mouth to FPU plate (backing HFI feeds) ~ 180 mm (at this purpose I will need further confirmations by HFI and ALCATEL-CSL cause a discrepancy , around 20 mm , that I found with data in my possess)
R= FPU_plate radius ~100 mm
φ = linear angle subtended by the FPU_plate ~ 29 °
Ω= 1- φ = linear angle subtended by the surrounding
Ψ' = e fraction of solid angle subtended by the FPU_plate is:

$$\Psi' = \frac{\int_{\beta=0}^{2\pi}\int_{\vartheta=0}^{\varphi}\sin\vartheta\cdot d\theta\cdot d\beta}{\int_{\beta=0}^{2\pi}\int_{\vartheta=0}^{\vartheta=\pi/2}\sin\vartheta\cdot d\theta\cdot d\beta} = 1-\cos(\phi)\cong 0.125$$

Then, the view factor, that is the fraction of solid angle subtended by the surrounding, is:
ψ = (1- ψ') ~ 0.875

It is absolutely not straightforward to guess what is the effective thermal contribution falling on the CFS.

From the figure below, three possible frames can be guessed. Probably the real frame is something in the middle.

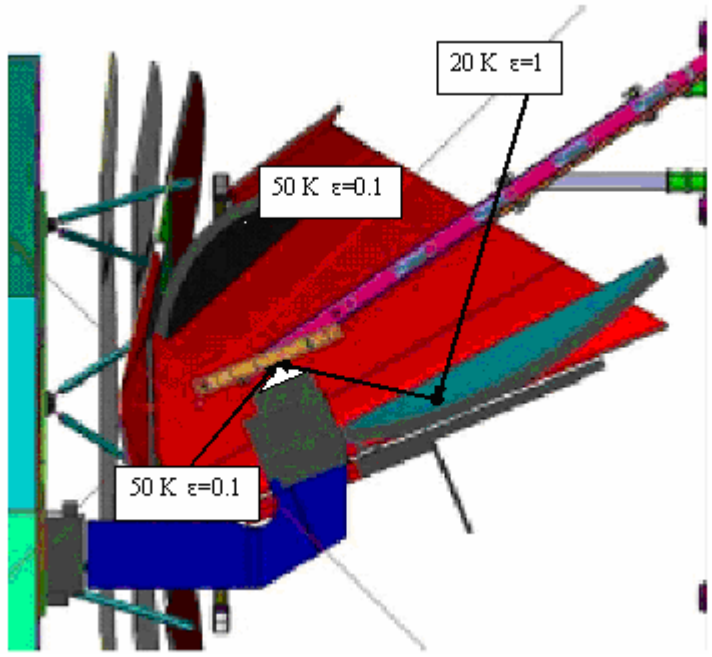

1st FRAME:
the SKL is considered surrounded by a 50 K perfect cavity (the baffle). This cavity, although has reflective walls, acts like an integrating sphere. Radiation from this ideal sphere is:

Perfectly absorbed by the sky load, that is expected to increases only marginally its temperature (paying a larger helium consumption)
About perfectly reflected by each CFS : power entering the feeds from CFS is then :
$P \approx 50 * 1 * (1 - 0.1) * P_{\_CFS} * 1$

For example, if:

$P_{\_CFS}$ = 0.1 gives : P~ 4.5 K
$P_{\_CFS}$ = 0.01 gives : P~ 0.45 K
$P_{\_CFS}$ = 0.001 gives : P~ 0.045 K

2nd FRAME:
The SKL is considered surrounded by an open reflecting cavity (baffle, FPU plate, feeds, telescope) opened to a mixed environment mainly at 20 K Under this fram,e each CFS acts as a source at power entering the feeds from CFS is then :

$P \approx 20 * 1 * (1 - 0.1) * P_{\_CFS} * 1$

For example, if:

$P_{\_CFS}$ = 0.1 gives : P~ 1.8 K
$P_{\_CFS}$ = 0.01 gives : P~ 0.18 K

$P\__{CFS}$ = 0.001 gives : P~ 0.018 K

3rd FRAME:
It is an intermediate situation: the CFS reflects radiation coming from the objects that directly observes, weighted by the emissivity of the observed object and the solid angle subtended. Since we do not know what is actually emitting in front of the SKL the we can suppose here:

$$P \approx (50 * 0.1 + 20 * 1) * (0.9) * P\_{CFS} * 0.875$$

For example, if:

$P\__{CFS}$ = 0.1 gives : P~ 1.96 K
$P\__{CFS}$ = 0.01 gives : P~ 0.196 K
$P\__{CFS}$ = 0.001 gives : P~ 0.019K

The remaining part is supposed to be emitted by the 4K FPU (subtending a fraction of the solid angle 0.125)

The true value could be guessed **to be an average (AV)** of the three frames (indicated as FR1 , FR2. FR3) presented; results from the three models, using the true values for $P\__{CFS}$, are reported in the table below.

RCA	RF LOSS	FR1	FR2	FR3	AV
#	%	mK	mK	mK	mK
18	1.37	612.5	243.1	272.2	375.9
19	2.14	957.6	380.1	425.5	587.7
20	2.23	1000.4	397.1	444.5	614.0
21	1.92	858.8	340.9	381.6	527.1
22	1.61	718.6	285.3	319.3	441.1
23	0.97	433.4	172.0	192.6	266.0
24	0.06	26.1	10.4	11.6	16.0
25	0.28	126.8	50.3	56.3	77.8
26	0.28	125.7	49.9	55.9	77.2
27	0.02	9.6	3.8	4.3	5.9
28	0.02	10.7	4.3	4.8	6.6

In every frames above the maximum contribution to environmental radiation falls between 400 mK and 1 K. As already said in the TN, this contribution affects mostly the 70 GHz channels and RCA25 and RCA26.

As it is clear, the problem is related with the damping factor given by the term P_CFS: it reduces strongly when P_CFS < 0.001 (RF LOSS < 0.1%), resizing strongly the importance of thermal distribution and view factors in the final result.

ANNEX1: ABOUT THE ENVIRONMENTAL COMPONENT CALCULATED IN PL-LFI-PST-XXX Issue 0.3

F. Cuttaia, 21/03/2007

Here follows a brief rough description of calculations made to estimate the contribution from environment.

Each CFS (Carbon Fibre Source) **emits two main contributions (power P):**

Due to its thermodynamic temperature (about 4K) with very poor efficiency (ε <0.1) – (the blue arrow): $\mathbf{P \approx 4K*\varepsilon_{CFS}}$
Reflected radiation coming from the surrounding at a certain temperature T? K, with high efficiency >0.9 (the red arrow): $\mathbf{P \approx T?K*(1-\varepsilon_{CFS})}$

Both these contributions must be multiplied times the fraction ($P_{\_CFS}$) of the total power effectively reaching each horn. This fraction (schematised with the colour scale in figure) was calculated in the report as:

$$P_{\_CFS} = \frac{\int \text{power falling on source surface}}{\int \text{power falling on entire SKL surface}} < 1$$

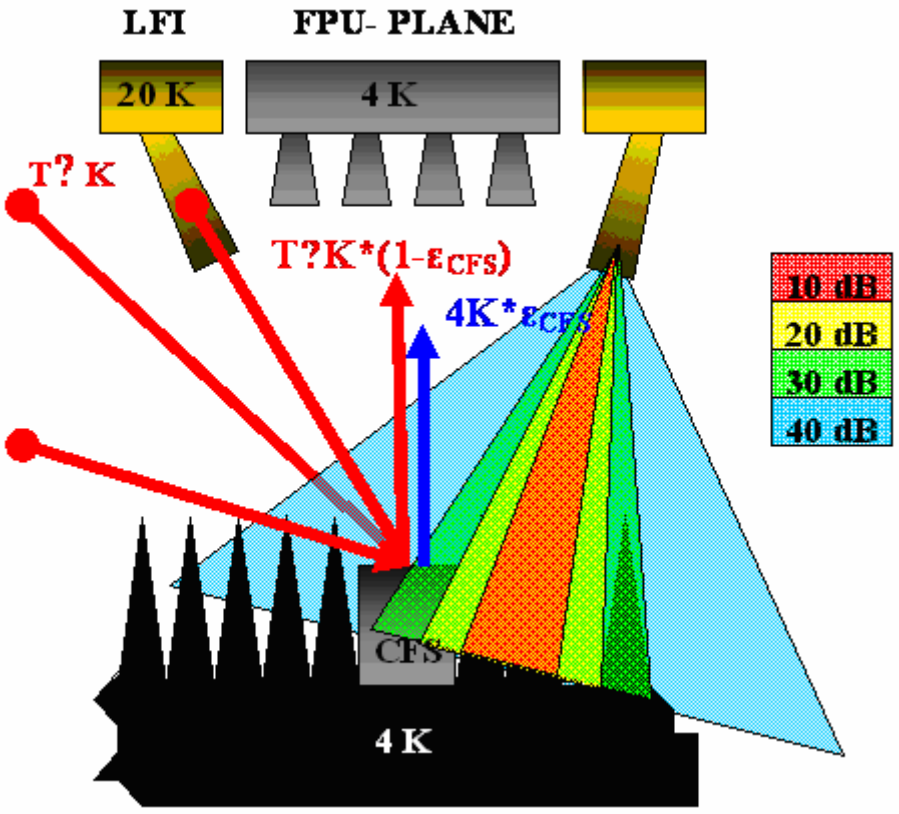

The geometry of the environment surrounding the SKL is very complicated: only a rough estimation of T?K can be done.
Maybe a cross check with data available to HFI can provide a more accurate solution.
A deeper analysis would require to implement a detailed model using GRASP , launching a plane wave from each CFS and analysing how much of this radiation is blocked-reflected by each object.
This is unfeasible at this stage (meaning to clarify the best positioning of CFSs) and in the short time available.

Scope of this brief note is to present a rough estimation of the contribution coming from the surrounding.
It is here defined **SURROUNDING**: everything except the SKL and the objects at 4K (FPU plane where the HFI horns are mounted and the HFI feed). In the following table are reported all elements belonging to the surrounding, together with their emissivity . Concerning the telescope, its emissivity is for me at present unknown (? In the table) , since I ignore the setup condition in CSL (will it be tested in nominal conditions or covered to avoid contamination?)

PART	T (K)	ε
LFI FEEDS & MAIN FRAME	20	< 0.1
BAFFLE	50	< 0.1
TELESCOPE	50	< 0.01 / ?
CRYO CHAMBER	20	1

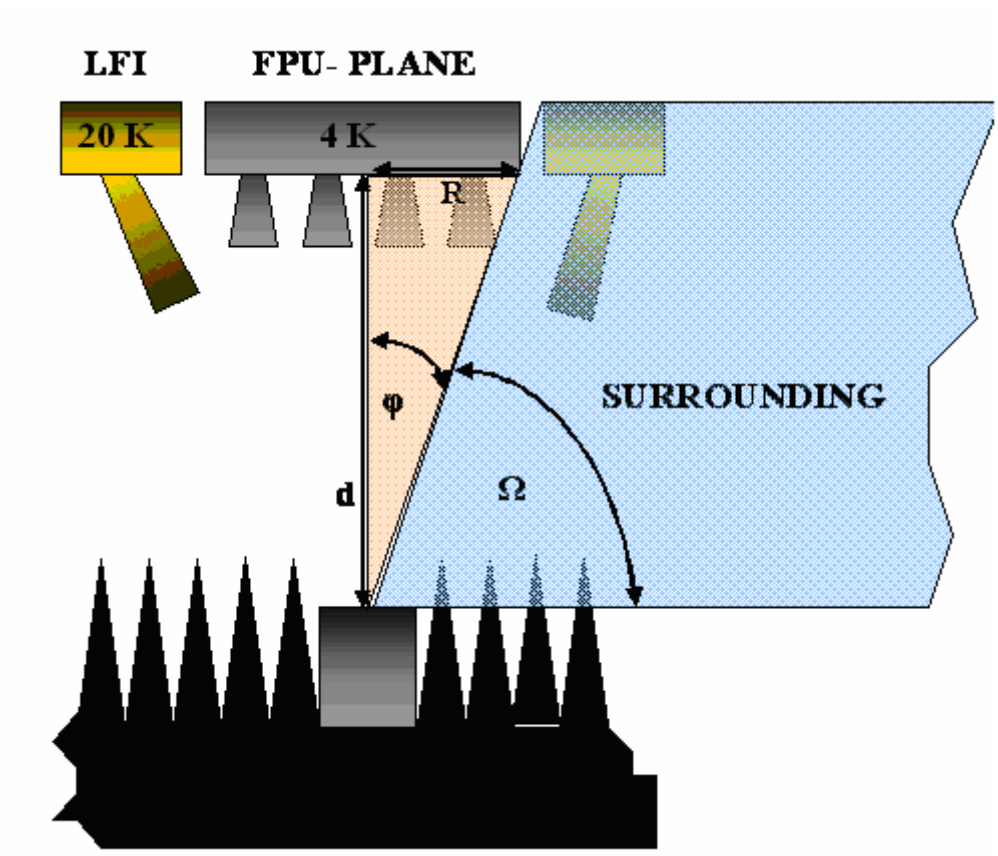

The power coming from environment (surrounding) is then defined as:

(Temperature of the emitting object) * (emissivity of the object* reflectivity of the CFS) * (percentage of the power entering the feed)* (percentage ψ of the whole solid angle subtended by that source)
That is:

$$P\_{ENV} = T?K * \varepsilon_{T?K} * \left(1 - \varepsilon\_{CFS}\right) * P\_{CFS} * \Psi$$

The last term ψ is the most uncertain point, since we do not know exactly the thermal distribution of the surrounding and how radiation propagates among the different stages.

With reference to the figure above we can state that:

Each CFS is positioned about in the centre of the SKL.
d = distance from CFS mouth to FPU plate (backing HFI feeds) ~ 180 mm (at this purpose I will need further confirmations by HFI and ALCATEL-CSL cause a discrepancy , around 20 mm , that I found with data in my possess)
R= FPU_plate radius ~100 mm
φ = linear angle subtended by the FPU_plate ~ 29 °
Ω= 1- φ = linear angle subtended by the surrounding
Ψ' = e fraction of solid angle subtended by the FPU_plate is:

$$\Psi' = \frac{\int_{\beta=0}^{2\pi}\int_{\vartheta=0}^{\varphi}\sin\vartheta\cdot d\theta\cdot d\beta}{\int_{\beta=0}^{2\pi}\int_{\vartheta=0}^{\vartheta=\pi/2}\sin\vartheta\cdot d\theta\cdot d\beta} = 1-\cos(\phi)\cong 0.125$$

Then, the view factor, that is the fraction of solid angle subtended by the surrounding, is:
ψ = (1- ψ') ~ 0.875

It is absolutely not straightforward to guess what is the effective thermal contribution falling on the CFS.

From the figure below, three possible frames can be guessed. Probably the real frame is something in the middle.

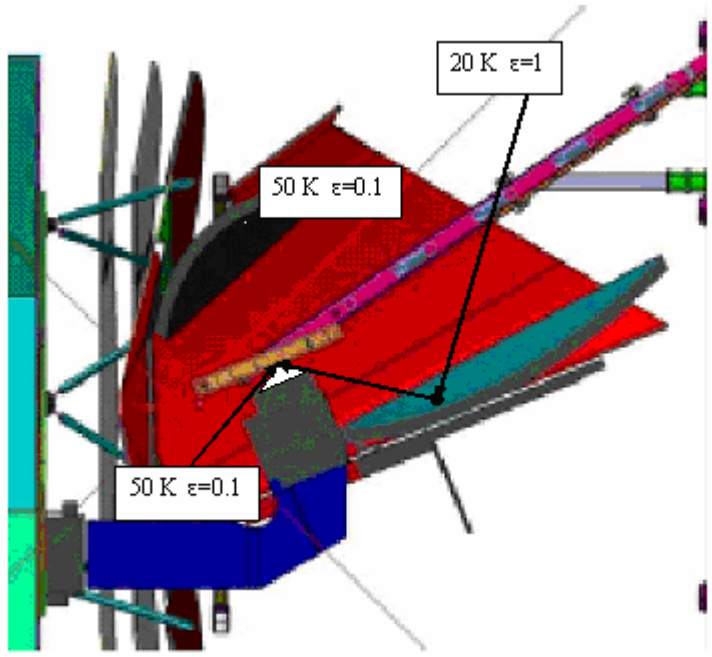

1st FRAME:
the SKL is considered surrounded by a 50 K perfect cavity (the baffle). This cavity, although has reflective walls, acts like an integrating sphere. Radiation from this ideal sphere is:

Perfectly absorbed by the sky load, that is expected to increases only marginally its temperature (paying a larger helium consumption)
About perfectly reflected by each CFS : power entering the feeds from CFS is then :
$P \approx 50 * 1 * (1 - 0.1) * P_{\_CFS} * 1$

For example, if:

$P_{\_CFS}$ = 0.1 gives : P~ 4.5 K
$P_{\_CFS}$ = 0.01 gives : P~ 0.45 K
$P_{\_CFS}$ = 0.001 gives : P~ 0.045 K

2nd FRAME:
The SKL is considered surrounded by an open reflecting cavity (baffle, FPU plate, feeds, telescope) opened to a mixed environment mainly at 20 K Under this fram,e each CFS acts as a source at power entering the feeds from CFS is then :

$P \approx 20 * 1 * (1 - 0.1) * P_{\_CFS} * 1$

For example, if:

$P_{\_CFS}$ = 0.1 gives : P~ 1.8 K
$P_{\_CFS}$ = 0.01 gives : P~ 0.18 K

$P\__{CFS}$ = 0.001 gives : P~ 0.018 K

3rd FRAME:
It is an intermediate situation: the CFS reflects radiation coming from the objects that directly observes, weighted by the emissivity of the observed object and the solid angle subtended. Since we do not know what is actually emitting in front of the SKL the we can suppose here:

$$P \approx (50 * 0.1 + 20 * 1) * (0.9) * P\_{CFS} * 0.875$$

For example, if:

$P\__{CFS}$ = 0.1 gives : P~ 1.96 K
$P\__{CFS}$ = 0.01 gives : P~ 0.196 K
$P\__{CFS}$ = 0.001 gives : P~ 0.019K

The remaining part is supposed to be emitted by the 4K FPU (subtending a fraction of the solid angle 0.125)

The true value could be guessed **to be an average (AV)** of the three frames (indicated as FR1 , FR2. FR3) presented; results from the three models, using the true values for $P\__{CFS}$, are reported in the table below.

RCA	RF LOSS	FR1	FR2	FR3	AV
#	%	mK	mK	mK	mK
18	1.37	612.5	243.1	272.2	375.9
19	2.14	957.6	380.1	425.5	587.7
20	2.23	1000.4	397.1	444.5	614.0
21	1.92	858.8	340.9	381.6	527.1
22	1.61	718.6	285.3	319.3	441.1
23	0.97	433.4	172.0	192.6	266.0
24	0.06	26.1	10.4	11.6	16.0
25	0.28	126.8	50.3	56.3	77.8
26	0.28	125.7	49.9	55.9	77.2
27	0.02	9.6	3.8	4.3	5.9
28	0.02	10.7	4.3	4.8	6.6

In every frames above the maximum contribution to environmental radiation falls between 400 mK and 1 K. As already said in the TN, this contribution affects mostly the 70 GHz channels and RCA25 and RCA26.

As it is clear, the problem is related with the damping factor given by the term P_CFS: it reduces strongly when P_CFS < 0.001 (RF LOSS < 0.1%), resizing strongly the importance of thermal distribution and view factors in the final result.

ANNEX-2 to TN PL-LFI-PST-XXX ISSUE 0.3 (Planck cold load performance degradation at LFI frequency caused by HFI carbon fibre noise source)

F. Cuttaia, 26-03-07

A new analysis based on the new setup proposed by IAS (Email from J.M. Lamarre, 22-03-2007), is here described (RD1).
The 3 large sources (30 * 30 mm) of the last configuration have been replaced with 3 small sources (Diameter D=9mm), disposed as a cluster, embedded in an absorbing plate (size about 50*50 mm) made of ECCOSORB CR110. The Eccosorb plate shields the mounting structure of the sources and allows RF propagation throughout holes practiced in the surface, corresponding to the sources' mouth. The design is displayed in Fig. 1.
The distance FPU-Sources changed w.r.t. the old configuration (RD3t comes by comparing Tab. 1 and Tab. 2.

				S1	S2	S3
Position source dans RDP			X	10.000	10.000	-10.000
			Y	12.500	-12.500	0.000
			Z	156.000	156.000	156.000

Table 9 NEW setup

X	-37	14	14
Y	0	-24	24
Z	168,4	168,4	168,4

Table 10 Old setup

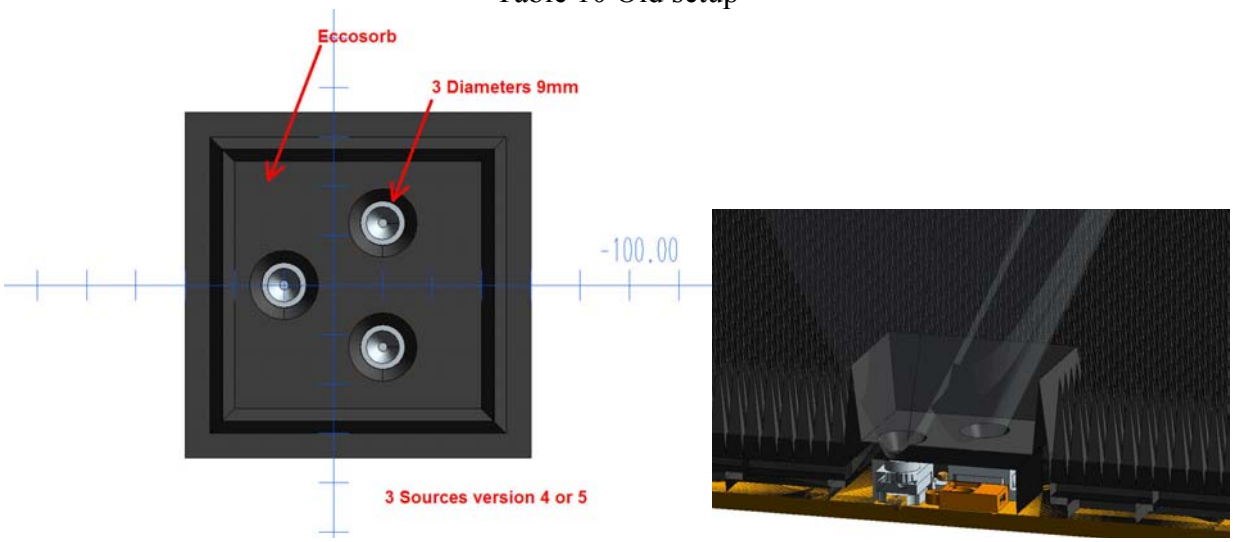

Figure 13

Moreover, a discrepancy (about 20 mm) was found w.r.t. the indications provided by AAS and ESA in jan-2004 (RD2). Actually, until now, information available to LFI (RD1) reported the clearance

LFI-Eccsorb tips to be 70 mm whilst in RD3 it si declared to be >90 mm. It obviously has impact on the beam size.
So, in accordance with data from Tab 1 , a new simulation was run using Grasp 9 to calculate beams at the new distance.
Following the same method describe in the TN, all the different non ideal contributions have been evaluated, basing on the following assumptions:
-each CFS is represented as a reflecting disk with diameter 9 mm and reflectivity = 0.9
- the Eccosorb shield is represented as a flat surface with variable reflectivity and transmittivity, depending on frequency (RD4). Values are reported in Tab. 3 (linear scale).
- the Eccosorb plate is considered in two different frames, depending on the thickness: d= 5mm and d= 10mm. In the Solution proposed by IAS it looks to be very close to 5 mm.

	GHZ	30.0	44.0	70.0
REFL		0.13	0.13	0.10
TRANSM	0.5 cm	0.62	0.45	0.37
	1cm	0.24	0.00	0.00

Table 11 Eccosorb parameters used in the model. Whilst R changes largely with d and frequency, the reflection coefficient remains quite stable.

The case d=10 mm was considered since:

- a considerable amount of radiation is not fully absorbed by a 5 mm tick Eccosorb layer and is back scattered by the metal structure: a 5 mm seems to be insufficient for the purpose.
- - the increased thickness does not impact on performance of the sources.

In order to relax a little the LFI requirement, the simulation was performed in the central frequency of each channel, considering that the total power entering each feed is averaged within the bandwidth (and then among different beam sizes). It seems to be a good trade off considering time available.
Results are displayed, feed by feed, in plot 1, allowing to appreciate the contribution given by each source and by the absorbing plate.
The maximum normalized power (normalization is made per feed: the maximum power of each feed accounts for 0dB) falling on each pixel is displayed in Plot 2.
Plot 3 describes the power reflected by the 3 sources and the absorbing plate (without the sources) considered 5mm thick.
Plot 4 describes the power reflected by absorbing plate (without the sources) considered 10 mm thick and the total power reflected (sources + absorbing plate)
Table 4 reports the detailed contributions in both configurations of the Eccosorb plate (5 mm left column, 10 mm right column) in the four frames considered in the TN. 50 K cavity; 20 K cavity; mixed model considering the view factor of each source; average.
Table 5 reports the summary of only contributions from environment in the four frames and in the both configs. of Eccosorb plate.
Plot 5 and Plot 6 are useful to compare the present setup and the old : only -20 dB and -30 dB envelope are represented. Both plots are calculated at the new updated distance.

Results indicate that the solution proposed by HFI (3 sources embedded in Eccosorb baffle) with the increased thickness (from 5 mm to 10 mm) helps to reduce strongly possible spurious contributions entering the LFI feeds.

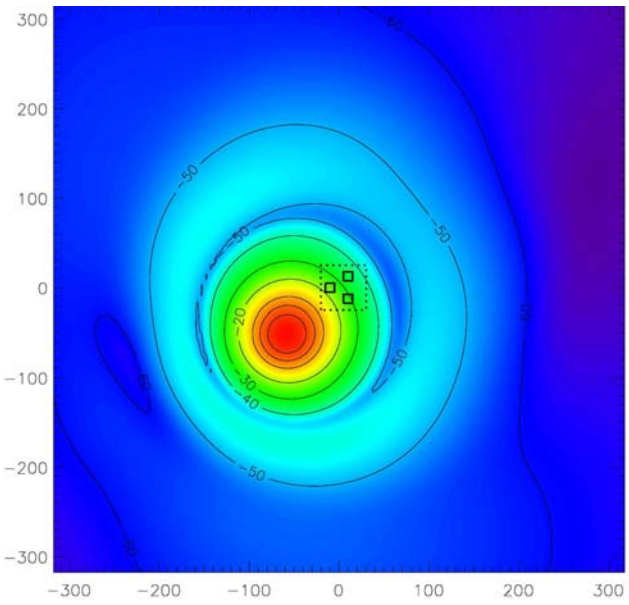

FH_LFI18

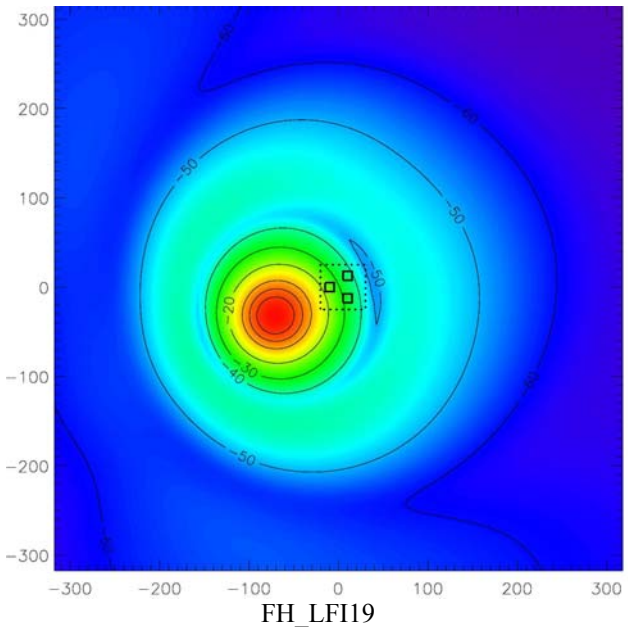

FH_LFI19

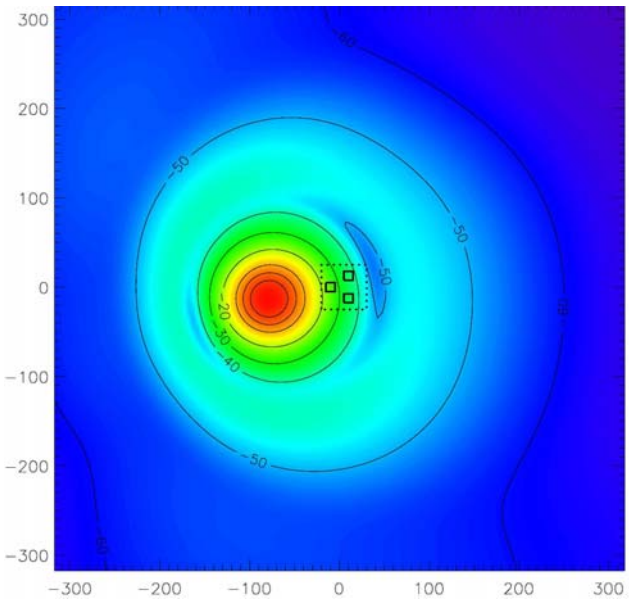

FH_LFI20

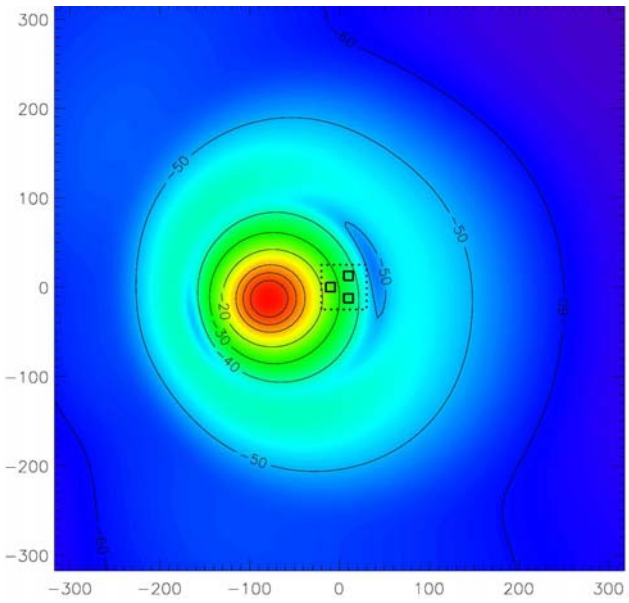

FH_LFI21

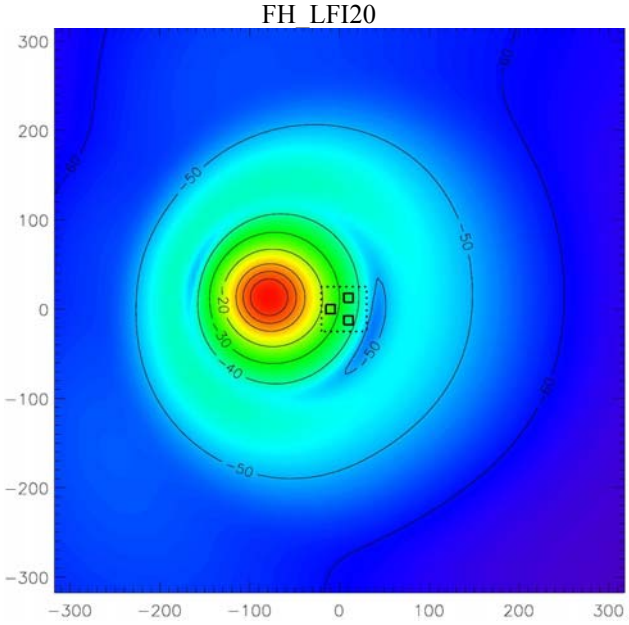

FH_LFI22

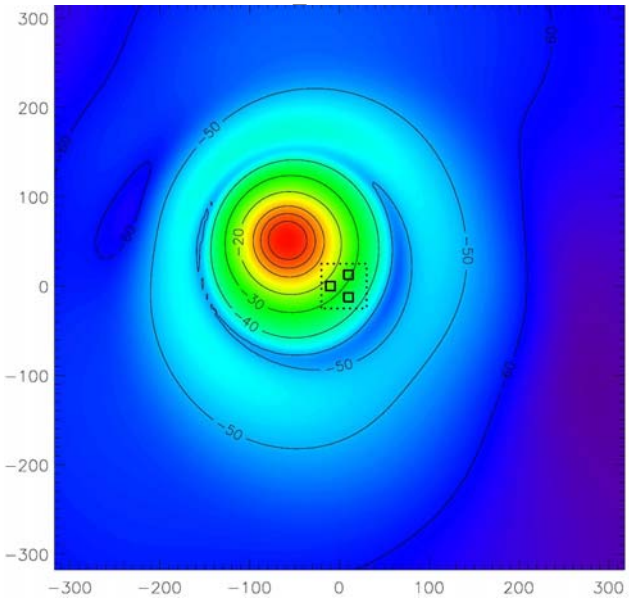

FH_LFI23

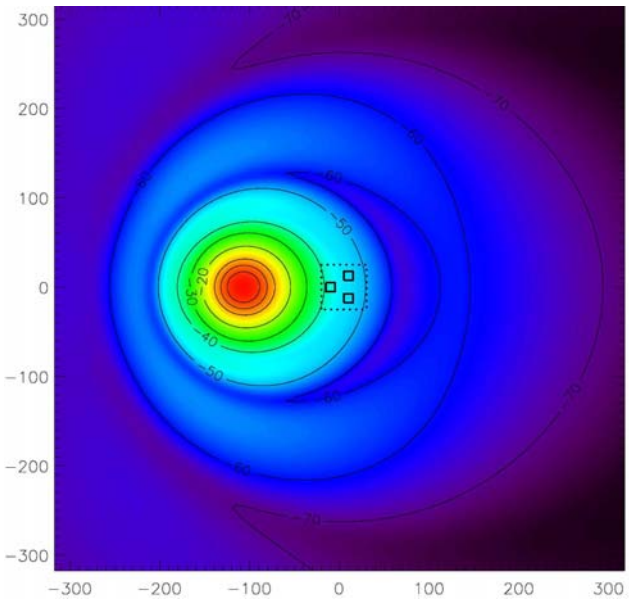

FH_LFI24

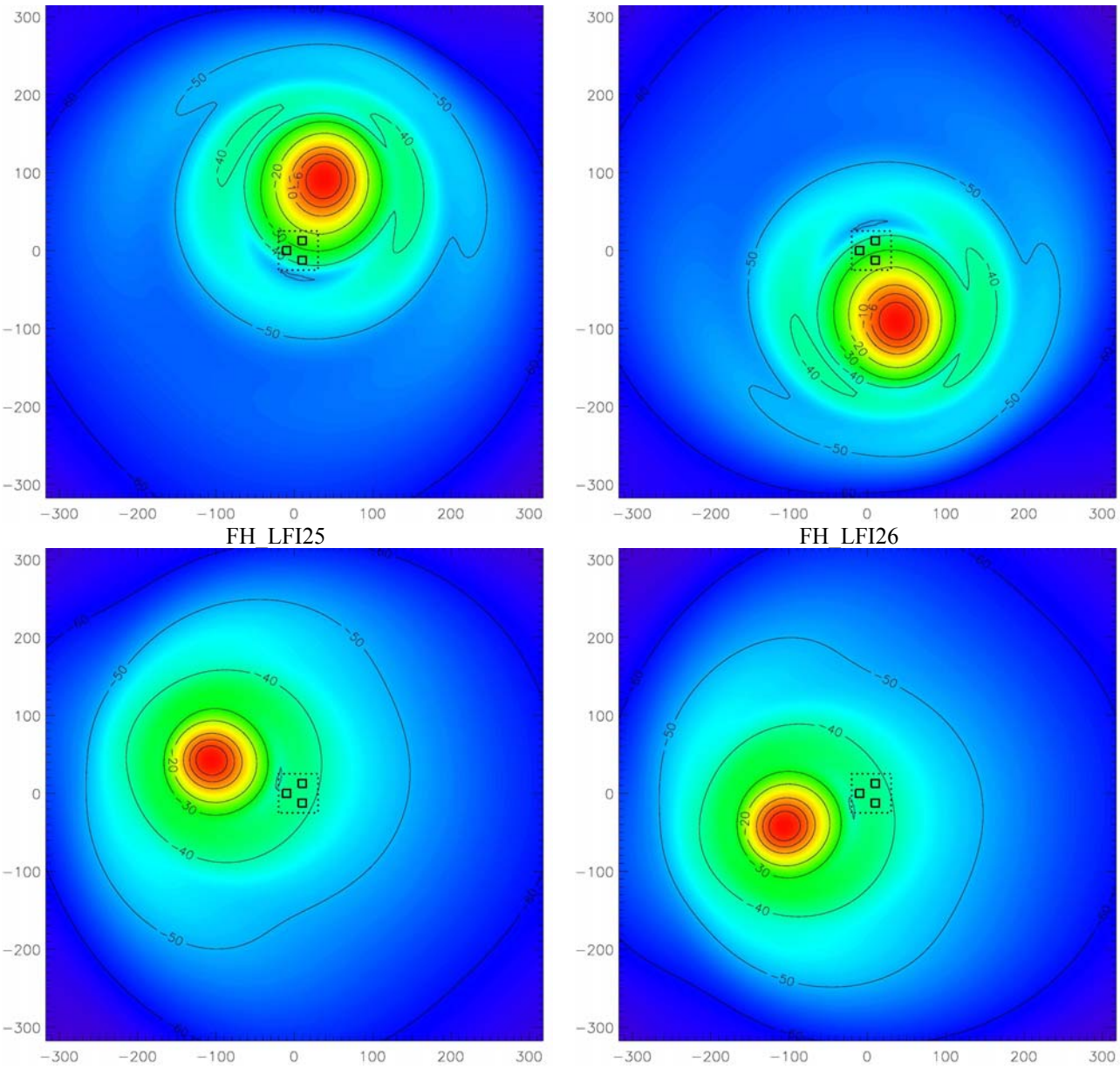

Plot 3 power contour on the SKL surface. S1, S2 S3 (square) and Eccosorb baffle (dot line square) are displayed.

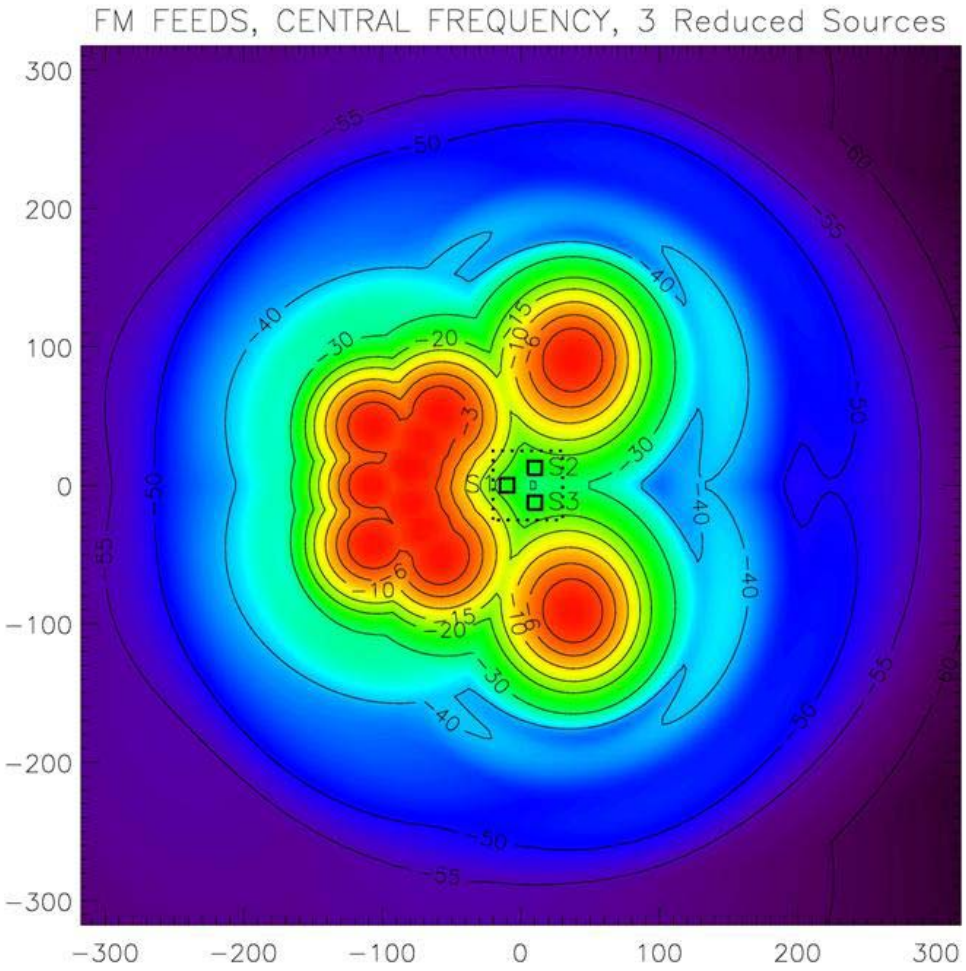

Plot 4 Power envelope: maximum normalized (to the maximum of each channel) power per pixel is represented.

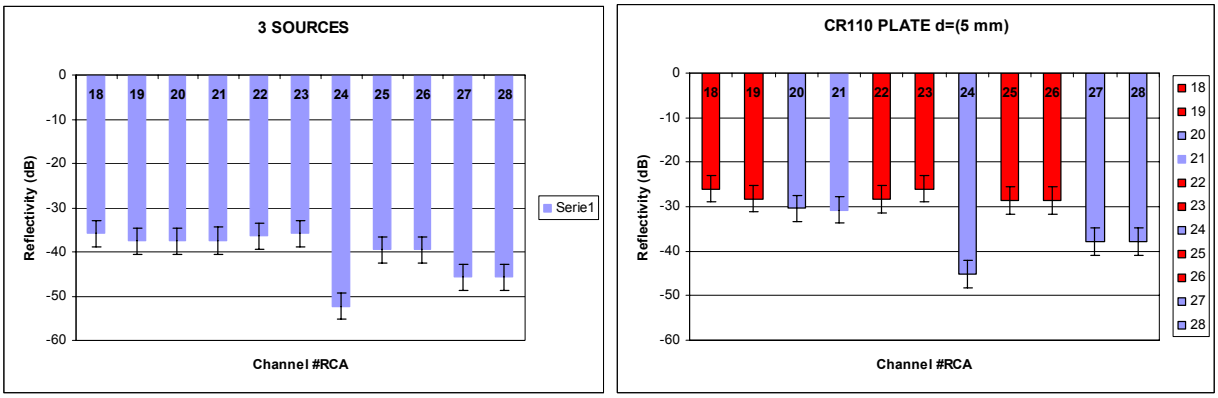

Plot 5 reflected power from 3 sources (left) and from CR110 plate 5 mm tick (right). Uncertainty bars displayed

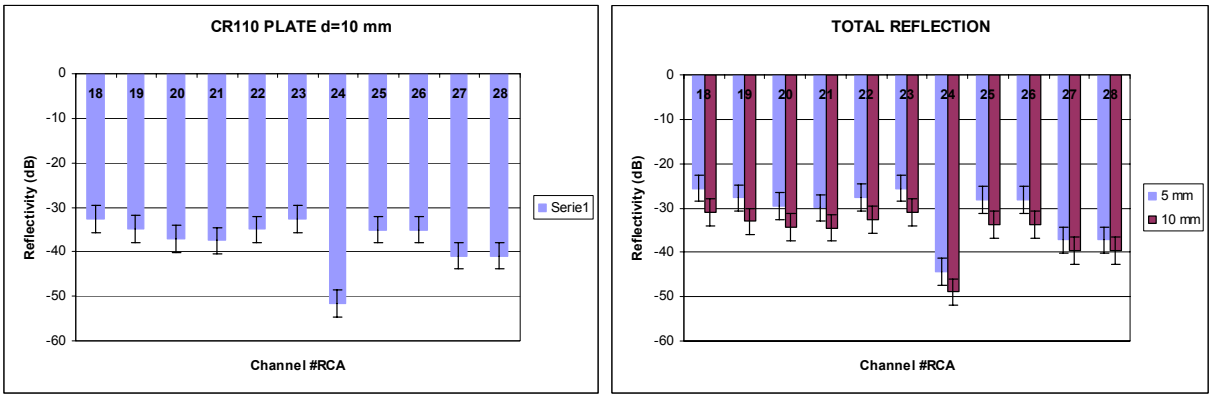

Plot 6 reflected power from CR110 plate 10 mm tick (left) and total reflection (right). Uncertainty bars displayed

MIXED						
RCA	RF LOSS	TH LOSS	ENV/baffle	Feeds /FPU	coupling	HFI Tn
#	%	mK	mK	mK	mK	mK
18	0.6	20.0	110.6	1.3	3.4	TBC
19	0.3	12.1	67.1	0.8	2.3	TBC
20	0.2	7.9	43.5	0.5	1.6	TBC
21	0.2	7.3	40.3	0.5	1.5	TBC
22	0.3	12.3	67.8	0.8	2.3	TBC
23	0.6	20.0	110.6	1.3	3.4	TBC
24	0.0	0.3	1.5	0.0	0.1	TBC
25	0.3	10.7	59.3	0.7	2.1	TBC
26	0.3	10.7	59.3	0.7	2.1	TBC
27	0.0	1.4	7.5	0.1	0.3	TBC
28	0.0	1.4	7.5	0.1	0.3	TBC

MIXED						
RCA	RF LOSS	TH LOSS	ENV/baffle	Feeds /FPU	coupling	HFI Tn
#	%	mK	mK	mK	mK	mK
18	0.16	5.7	31.6	0.4	0.3	TBC
19	0.10	3.6	19.7	0.2	0.2	TBC
20	0.07	2.7	14.7	0.2	0.2	TBC
21	0.07	2.6	14.1	0.2	0.2	TBC
22	0.11	3.9	21.6	0.2	0.2	TBC
23	0.16	5.7	31.6	0.4	0.3	TBC
24	0.00	0.1	0.5	0.0	0.0	TBC
25	0.08	3.0	16.7	0.2	0.2	TBC
26	0.08	3.0	16.7	0.2	0.2	TBC
27	0.02	0.8	4.3	0.0	0.0	TBC
28	0.02	0.8	4.3	0.0	0.0	TBC

50 K						
RCA	RF LOSS	TH LOSS	ENV/baffle	Feeds /FPU	coupling	HFI Tn
#	%	mK	mK	mK	mK	mK
18	0.56	20.0	248.9	1.3	3.4	TBC
19	0.34	12.1	151.1	0.8	2.3	TBC
20	0.22	7.9	97.9	0.5	1.6	TBC
21	0.20	7.3	90.8	0.5	1.5	TBC
22	0.34	12.3	152.5	0.8	2.3	TBC
23	0.56	20.0	248.9	1.3	3.4	TBC
24	0.01	0.3	3.3	0.0	0.1	TBC
25	0.30	10.7	133.5	0.7	2.1	TBC
26	0.30	10.7	133.5	0.7	2.1	TBC
27	0.04	1.4	17.0	0.1	0.3	TBC
28	0.04	1.4	17.0	0.1	0.3	TBC

50 K						
RCA	RF LOSS	TH LOSS	ENV/baffle	Feeds /FPU	coupling	HFI Tn
#	%	mK	mK	mK	mK	mK
18	0.16	5.7	71.1	0.4	0.3	TBC
19	0.10	3.6	44.4	0.2	0.2	TBC
20	0.07	2.7	33.0	0.2	0.2	TBC
21	0.07	2.6	31.8	0.2	0.2	TBC
22	0.11	3.9	48.5	0.2	0.2	TBC
23	0.16	5.7	71.1	0.4	0.3	TBC
24	0.00	0.1	1.1	0.0	0.0	TBC
25	0.08	3.0	37.6	0.2	0.2	TBC
26	0.08	3.0	37.6	0.2	0.2	TBC
27	0.02	0.8	9.6	0.0	0.0	TBC
28	0.02	0.8	9.6	0.0	0.0	TBC

20 K						
RCA	RF LOSS	TH LOSS	ENV/baffle	Feeds /FPU	coupling	HFI Tn
#	%	mK	mK	mK	mK	mK
18	0.56	20.0	98.8	1.3	3.4	TBC
19	0.34	12.1	60.0	0.8	2.3	TBC
20	0.22	7.9	38.8	0.5	1.6	TBC
21	0.20	7.3	36.0	0.5	1.5	TBC
22	0.34	12.3	60.5	0.8	2.3	TBC
23	0.56	20.0	98.8	1.3	3.4	TBC
24	0.01	0.3	1.3	0.0	0.1	TBC
25	0.30	10.7	53.0	0.7	2.1	TBC
26	0.30	10.7	53.0	0.7	2.1	TBC
27	0.04	1.4	6.7	0.1	0.3	TBC
28	0.04	1.4	6.7	0.1	0.3	TBC

20 K						
RCA	RF LOSS	TH LOSS	ENV/baffle	Feeds /FPU	coupling	HFI Tn
#	%	mK	mK	mK	mK	mK
18	0.16	5.7	28.2	0.4	0.3	TBC
19	0.10	3.6	17.6	0.2	0.2	TBC
20	0.07	2.7	13.1	0.2	0.2	TBC
21	0.07	2.6	12.6	0.2	0.2	TBC
22	0.11	3.9	19.3	0.2	0.2	TBC
23	0.16	5.7	28.2	0.4	0.3	TBC
24	0.00	0.1	0.5	0.0	0.0	TBC
25	0.08	3.0	14.9	0.2	0.2	TBC
26	0.08	3.0	14.9	0.2	0.2	TBC
27	0.02	0.8	3.8	0.0	0.0	TBC
28	0.02	0.8	3.8	0.0	0.0	TBC

AVERAGE						
RCA	RF LOSS	TH LOSS	ENV/baffle	Feeds /FPU	coupling	HFI Tn
#	%	mK	mK	mK	mK	mK
18	0.56	20.0	152.8	1.3	3.4	TBC
19	0.34	12.1	92.7	0.8	2.3	TBC
20	0.22	7.9	60.1	0.5	1.6	TBC
21	0.20	7.3	55.7	0.5	1.5	TBC
22	0.34	12.3	93.6	0.8	2.3	TBC
23	0.56	20.0	152.8	1.3	3.4	TBC
24	0.01	0.3	2.0	0.0	0.1	TBC
25	0.30	10.7	81.9	0.7	2.1	TBC
26	0.30	10.7	81.9	0.7	2.1	TBC
27	0.04	1.4	10.4	0.1	0.3	TBC
28	0.04	1.4	10.4	0.1	0.3	TBC

AVERAGE						
RCA	RF LOSS	TH LOSS	ENV/baffle	Feeds /FPU	coupling	HFI Tn
#	%	mK	mK	mK	mK	mK
18	0.16	5.7	43.6	0.4	0.3	TBC
19	0.10	3.6	27.2	0.2	0.2	TBC
20	0.07	2.7	20.3	0.2	0.2	TBC
21	0.07	2.6	19.5	0.2	0.2	TBC
22	0.11	3.9	29.8	0.2	0.2	TBC
23	0.16	5.7	43.6	0.4	0.3	TBC
24	0.00	0.1	0.7	0.0	0.0	TBC
25	0.08	3.0	23.1	0.2	0.2	TBC
26	0.08	3.0	23.1	0.2	0.2	TBC
27	0.02	0.8	5.9	0.0	0.0	TBC
28	0.02	0.8	5.9	0.0	0.0	TBC

Table 12 Contributions (expressed in mK) from different sources. Two cases are summarized: Eccosorb thickness d= 0.5 mm (left table) and d=10 mm (right table)

RCA	RF LOSS	FR1	FR2	FR3	AV
#	%	mK	mK	mK	mK
18	0.56	248.9	98.8	110.6	152.8
19	0.34	151.1	60.0	67.1	92.7
20	0.22	97.9	38.8	43.5	60.1
21	0.20	90.8	36.0	40.3	55.7
22	0.34	152.5	60.5	67.8	93.6
23	0.56	248.9	98.8	110.6	152.8
24	0.01	3.3	1.3	1.5	2.0
25	0.30	133.5	53.0	59.3	81.9
26	0.30	133.5	53.0	59.3	81.9
27	0.04	17.0	6.7	7.5	10.4
28	0.04	17.0	6.7	7.5	10.4

RCA	RF LOSS	FR1	FR2	FR3	AV
#	%	mK	mK	mK	mK
18	0.16	71.1	28.2	31.6	43.6
19	0.10	44.4	17.6	19.7	27.2
20	0.07	33.0	13.1	14.7	20.3
21	0.07	31.8	12.6	14.1	19.5
22	0.11	48.5	19.3	21.6	29.8
23	0.16	71.1	28.2	31.6	43.6
24	0.00	1.1	0.5	0.5	0.7
25	0.08	37.6	14.9	16.7	23.1
26	0.08	37.6	14.9	16.7	23.1
27	0.02	9.6	3.8	4.3	5.9
28	0.02	9.6	3.8	4.3	5.9

Table 13 External Spillover (reflected component) in the four frames considered. Two cases are summarized: Eccosorb thickness d= 0.5 mm (left table) and d=10 mm (right table)

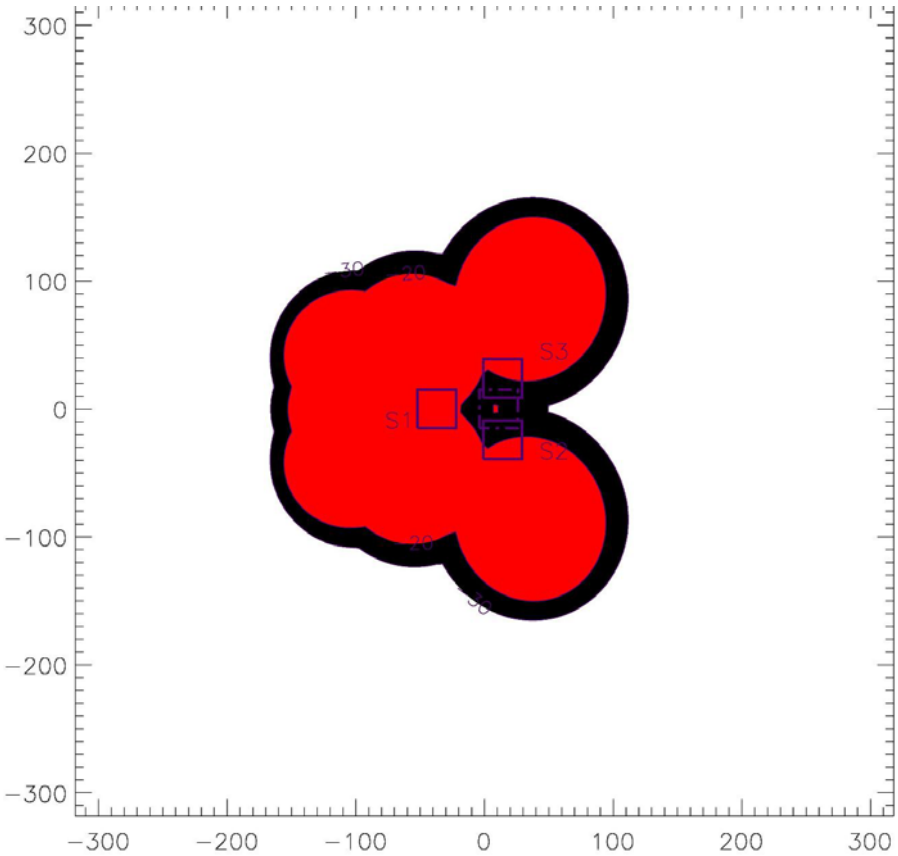

Plot 7 20 dB (red) and 30 dB (black) power envelope in the old configuration (3 sources 30mm*30 mm)

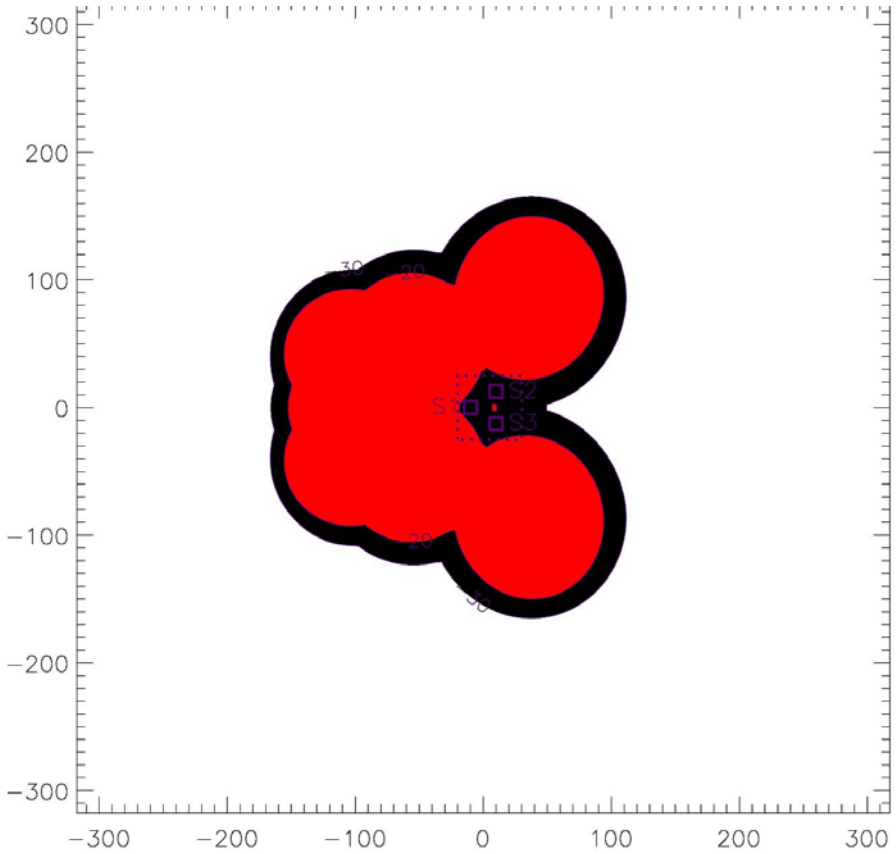

Plot 8 20 dB (red) and 30 dB (black) power envelope in the NEW configuration (3 sources D=9mm and ECCOSORB baffle, dot line)

REFERENCE DOCUMENTS

RD1 E-mail from J.M. Lamarre, 22-03-2207
RD2 Fax from ESA, SCIPT/23808, Jan- 2004
RD3 SP-PH700916-IAS , RATIONALE FOR IMPLEMENTING MEASUREMENT OF LOW FREQUENCY EXCESS RESPONSE OF HFI – PART 2
RD4 PL-LFI-PST-TN 047 , F. Cuttaia , Aug. 2003, RF COMPARATIVE ANALYSIS OF MATERIALS AND DESIGN FOR THE PLANCK COLD LOAD
RD5 Annex 1 to TN PL-LFI-PST-XXX Issue 0.3

ANNEX 3 to TN PL-LFI-PST-XXX ISSUE 0.3 (Planck cold load performance degradation at LFI frequency caused by HFI carbon fibre noise source)

29-05-2007, F. CUTTAIA
IASF-bo INAF

SCOPE

The new sky load design with the 3 CFS sources requires to know, with a certain accuracy, the positioning of the optical shield in front of the HFI/LFI FPU. This arises from:
The panel, once the 3 CFS sources have replaced somewhere the Eccosorb bed of pyramids, has no more isotropic properties in terms of emissivity / reflectivity.
The CFS sources must provide the HFI feeds with a certain power
The straylight effects and the non ideal black body emission towards the LFI feeds must be below a certain level..
Since accuracy in the SKL positioning is still unknown, and depends on the techniques will be used to perform the measurement, LFI Team was asked to evaluate the effect having a displacement of the CFS along the [XY] plane (that is the plane of the optical shield).

ANALYSIS

The same calculations and assumptions made in the main document and in the last updates presented in ANNEX 2 are here applied.
The design which the analysis is applied to is very near to that in ANNEX 2. Following a private communication from HFI instrument team (E-mail from G. Guyot) , the diameter of each CFS source was changed from 9 mm to 12 mm, consistently with the last updates in the main design (comparison shown in Fig 1). The position of CFS mouths is assumed about co-planar with the Eccosorb 10mm thick layer, as it was in Annex 2; the same is for nominal position on the plane [XY].
The three sources have been moved along the plane per steps of 5 mm as a rigid body . The full range : [X= nominal +/- 30 mm , Y= nominal +/- 30 mm] has been explored, evaluating the changes in reflectivity (in dB) and in thermal emission (mK) in all the possible 144 different configurations. The range was to explore was arbitrary decided, doubling, only for completeness, the possible error in accuracy guessed by ESA, following discussions with CSL people (L. Perez Cuevas E-mail communication)
For each position , for each feedhorn, have been calculated:

1) Return Loss : it comes out as sum of the three components:
- RL from the bed of pyramids,
- RL from the CR110 flat layer masking the metal mounting structures of CFS. This term was calculated in two different scenarios: layer 5mm or 10 mm thick.
- RL from metal surface of the CFS facing the FPU.

2) Thermal loss: without CFS, the PSkL is a black body at least within >99,97% at the LFI frequencies. Introducing any metal object causes a degrading of emission properties, shown as a thermal loss (mK) with respect to the ideal 4K thermodynamic temperature.

3) Straylight radiation: is the sum of the possible thermal contribution coming from the outside (environment) and from the FPU (thermal emission from the feeds and from the main frame) via reflections on the PSkL surface. This therm is here calculated as the average of the three scenarios presented in annex 2. It is strictly depending on the term 1).
4) Coupling radiation: it measures the noise power emitted by 10 feeds and reflected on the 11th not included in the sum. Although in ANNEX 2 it was calculated feed by feed, here, for simplicity, a unique value is given averaging on all feeds (values are however very similar)
5) SUM: it simply sums contributions from 3 and 4. Represents the total spurious radiation entering the feeds.
The above contributions have been calculated in both the cases, Eccosorb layer 5mm and 10 mm thick. It is quite evident from the graphs below that, was already observed in the previous document, a net difference does exist. This is due to the fact that 5 mm thickness is not fully able to absorb the incoming radiation end reflects a certain percentage of that, varying mostly with frequency. Hence, the contribution from the Eccosorb CR110 flat layer masking the mounting structure of the sources is the sum of:
-the component reflected by the Eccosorb surface (quite constant in frequency)
-the component absorbed from 5mm Eccosorb layer , back reflected from the CFS structure , absorbed again from the 5mm layer and then emitted towards the feeds.

In the followings, the two cases 5mm and 10 mm layer are represented and compared in each page. The displacement region [X= nominal +/- 30 mm , Y= nominal +/- 30 mm] is displayed using by contour plots in scale of colours. The central position is the nominal one. The nominal value is displayed.
Main results are summarized in Table 1 to provide the reader with a quick look display of the quantities involved.

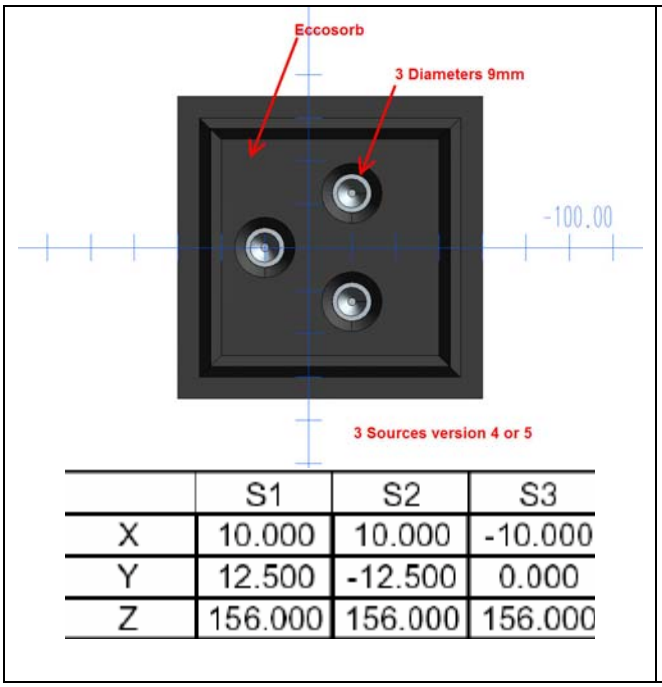

	S1	S2	S3
X	10.000	10.000	-10.000
Y	12.500	-12.500	0.000
Z	156.000	156.000	156.000

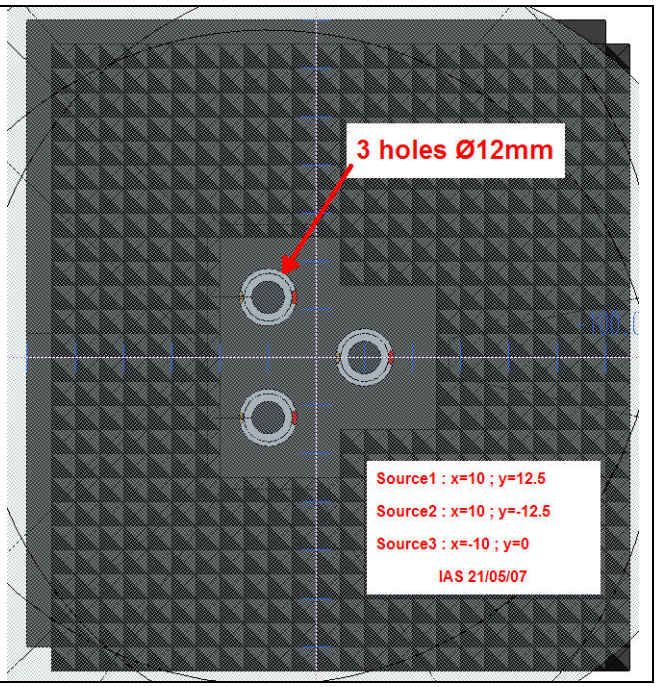

Fig 1: on the left side: the last setup before this document (i.e. that analysed in ANNEX 2). On the right side: the new setup , with larger sources; diameter passed from 9 mm to 12 mm (total reflecting surface increased by about 1.7) . The nominal position of each source remained unmodified. The region surrounding the sources , where the absorber shape is flat, involves about 10X9 pyramids (considering the total envelope), that is a rectangular region 50mm X 45 mm.

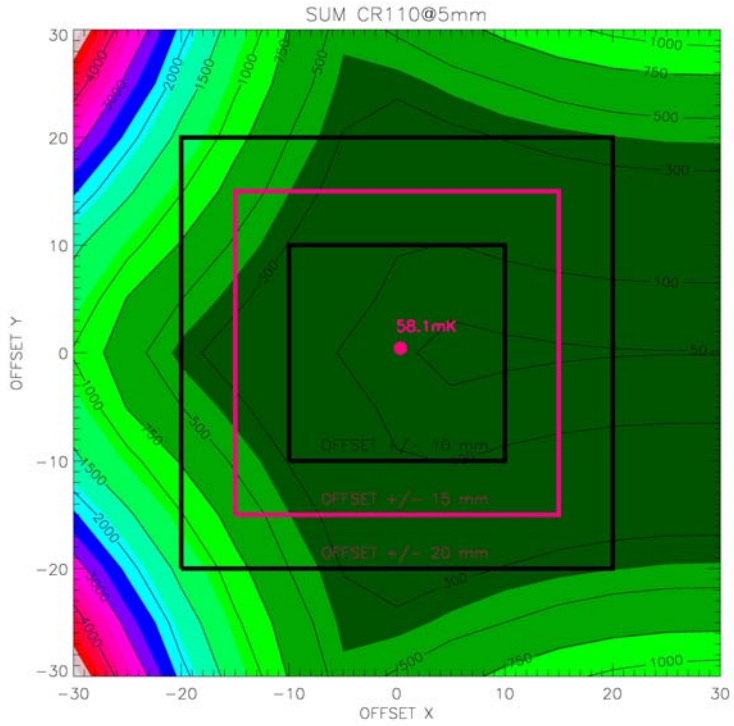

Figure 14 Total maximum thermal excess perceived from LFI feeds with displacement (CR110 layer 5mm thick) ; values in mK; the three offest regions [X=+/- 10 mm , Y=+/- 10 mm], [X=+/- 15 mm , Y=+/- 15 mm], [X=+/- 20 mm , Y=+/- 20 mm] are displayed

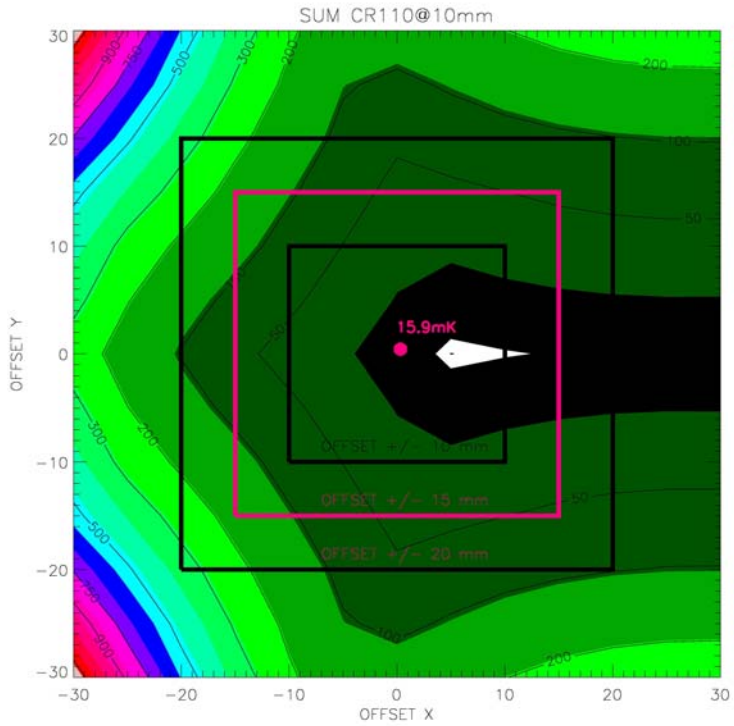

Figure 15 Total maximum thermal excess perceived from LFI feeds with displacement (CR110 layer 10 mm thick) ; values in mK; the three offest regions [X=+/- 10 mm , Y=+/- 10 mm], [X=+/-

15 mm , Y=+/- 15 mm], [X=+/- 20 mm , Y=+/- 20 mm] are displayed

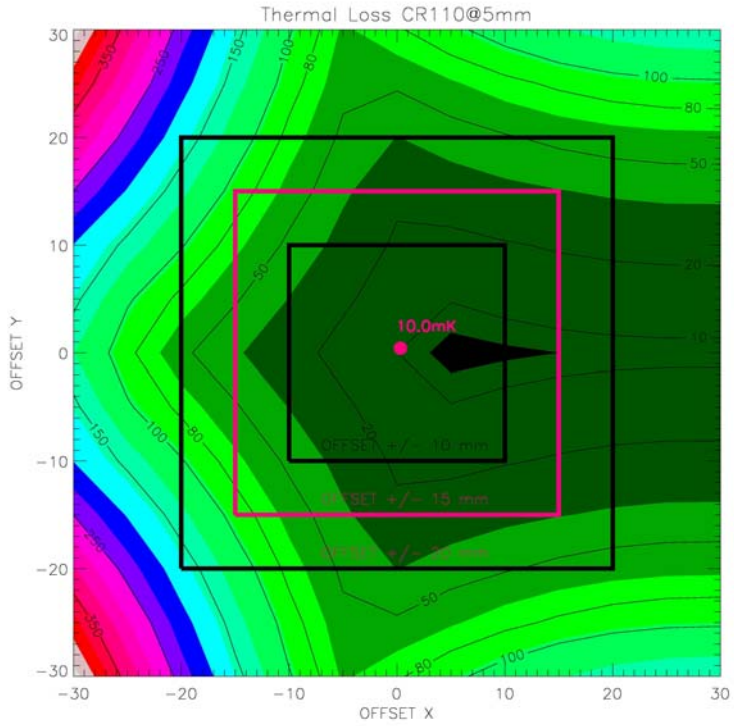

Figure 16 Maximum thermal LOSS (w.r.t. a load @4K) perceived from LFI feeds with displacement (CR110 layer 5mm thick) ; values in mK; the three offest regions [X=+/- 10 mm , Y=+/- 10 mm], [X=+/- 15 mm , Y=+/- 15 mm], [X=+/- 20 mm , Y=+/- 20 mm] are displayed

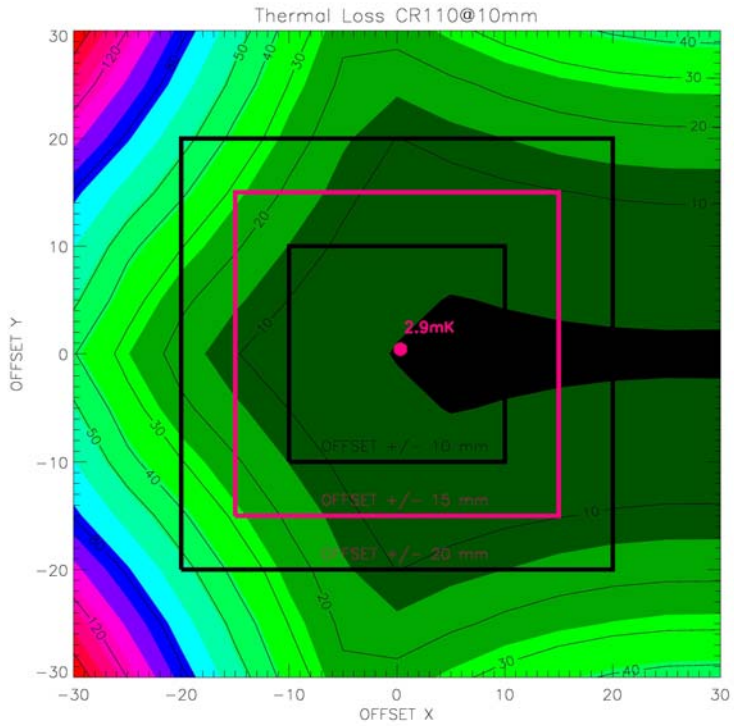

Figure 17 Maximum thermal LOSS (w.r.t. a load @4K) perceived from LFI feeds with displacement (CR110 layer 10 mm thick) ; values in mK; the three offest regions [X=+/- 10 mm ,

Y=+/- 10 mm], [X=+/- 15 mm , Y=+/- 15 mm], [X=+/- 20 mm , Y=+/- 20 mm] are displayed

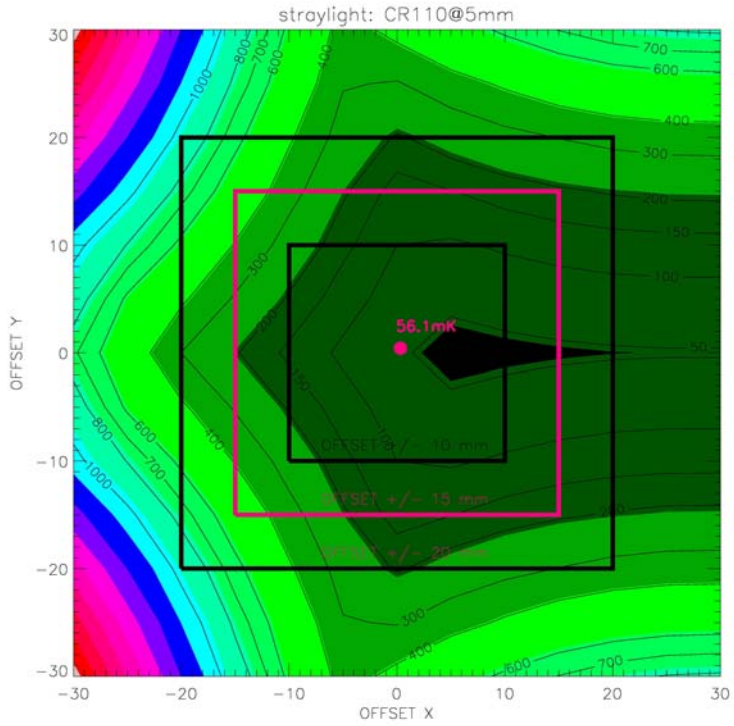

Figure 18 Maximum straylight contribution perceived from LFI feeds with displacement (CR110 layer 5mm thick) ; values in mK; the three offest regions [X=+/- 10 mm , Y=+/- 10 mm], [X=+/- 15 mm , Y=+/- 15 mm], [X=+/- 20 mm , Y=+/- 20 mm] are displayed

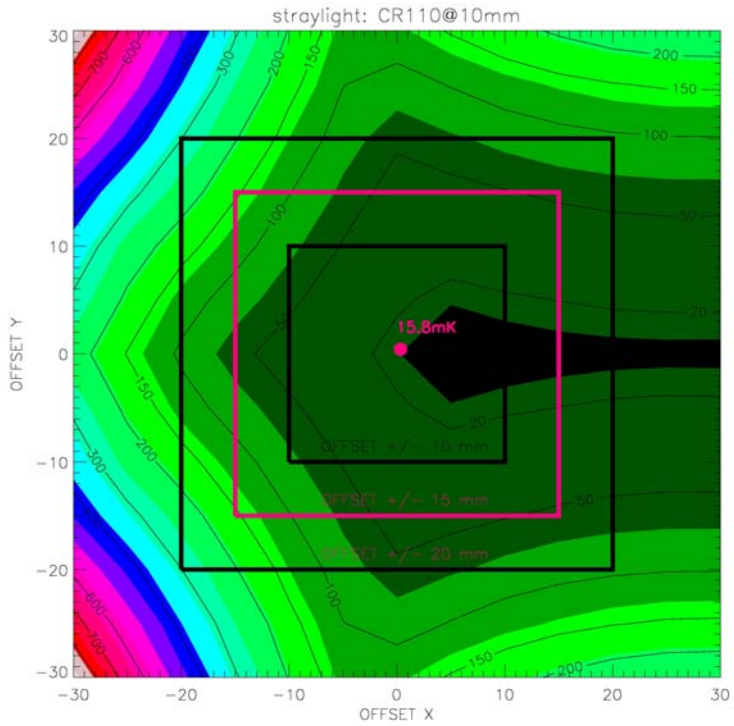

Figure 19 Maximum straylight contribution perceived from LFI feeds with displacement (CR110 layer 10 mm thick) ; values in mK; the three offest regions [X=+/- 10 mm , Y=+/- 10 mm], [X=+/-

15 mm , Y=+/- 15 mm], [X=+/- 20 mm , Y=+/- 20 mm] are displayed

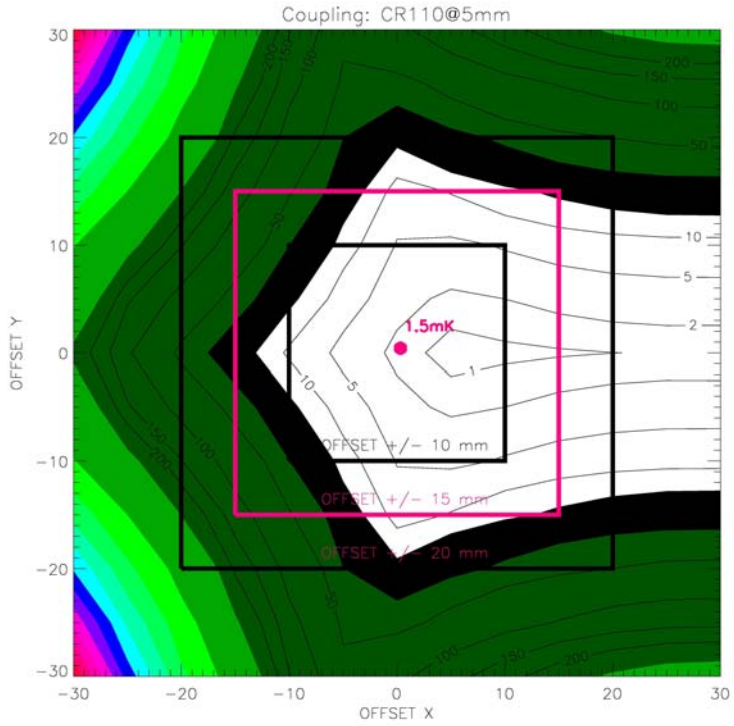

Figure 20 Maximum coupling between LFI feeds, depending on displacement (CR110 layer 5mm thick) ; values in mK; the three offest regions [X=+/- 10 mm , Y=+/- 10 mm], [X=+/- 15 mm , Y=+/- 15 mm], [X=+/- 20 mm , Y=+/- 20 mm] are displayed

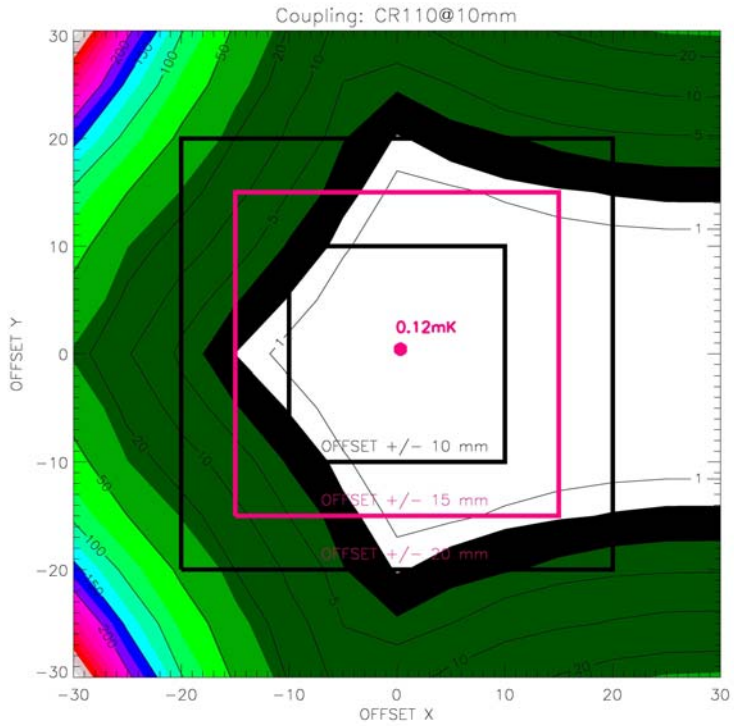

Figure 21 Maximum coupling between LFI feeds, depending on displacement (CR110 layer 10 thick) ; values in mK; the three offest regions [X=+/- 10 mm , Y=+/- 10 mm], [X=+/- 15 mm ,

Y=+/- 15 mm], [X=+/- 20 mm , Y=+/- 20 mm] are displayed

The changes in Sky Load reflectivity, as perceived from each LFI feed, are displayed in the following plots. Only the frame with Eccosorb layer thickness = 5 mm is shown. It is evident that the displacement affects mostly the 70 GHz channels, pushing reflectivity sometimes below -10 dB

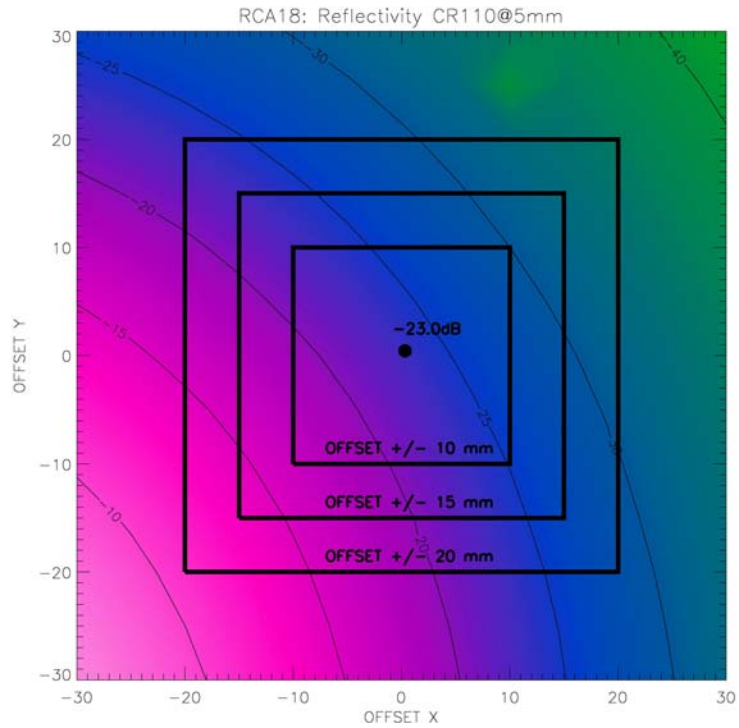

Figure 22 Sky Load reflectivity perceived from LFI #18, depending on displacement (CR110 layer 10 thick) ; values in dB; the three offest regions [X=+/- 10 mm , Y=+/- 10 mm], [X=+/- 15 mm , Y=+/- 15 mm], [X=+/- 20 mm , Y=+/- 20 mm] are displayed

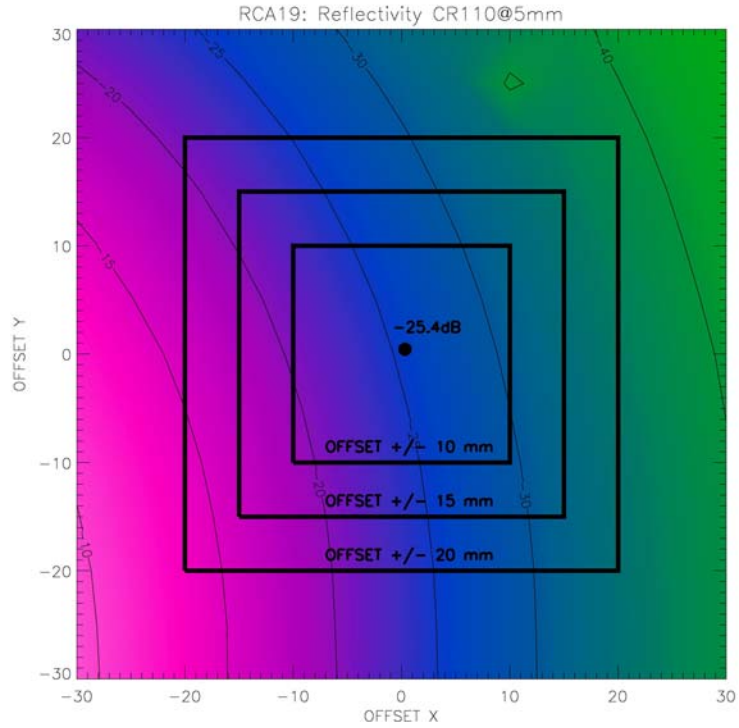

Figure 23 Sky Load reflectivity perceived from LFI #19, depending on displacement (CR110 layer 10 thick) ; values in dB; the three offest regions [X=+/- 10 mm , Y=+/- 10 mm], [X=+/- 15 mm , Y=+/- 15 mm], [X=+/- 20 mm , Y=+/- 20 mm] are displayed

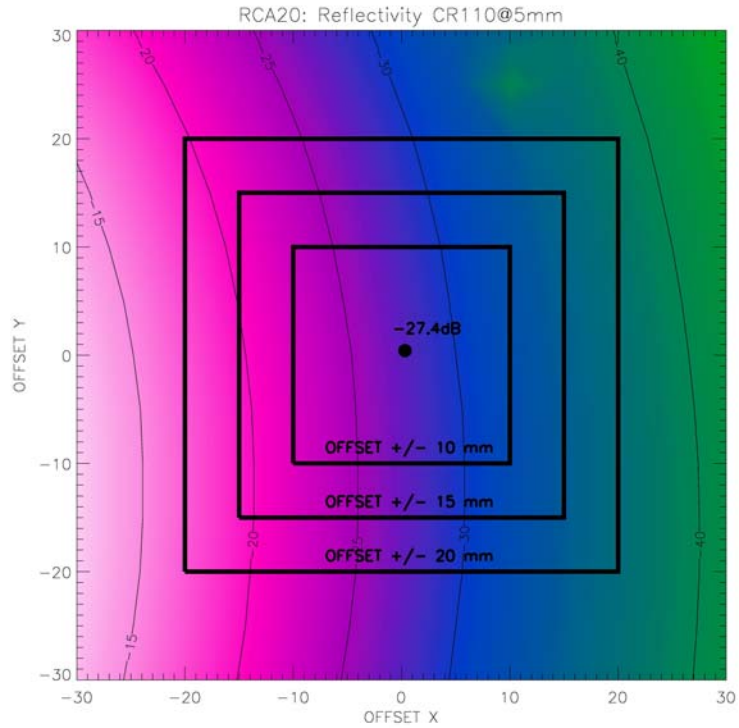

Figure 24 Sky Load reflectivity perceived from LFI #20, depending on displacement (CR110 layer 10 thick) ; values in dB; the three offest regions [X=+/- 10 mm , Y=+/- 10 mm], [X=+/- 15 mm ,

Y=+/- 15 mm], [X=+/- 20 mm , Y=+/- 20 mm] are displayed

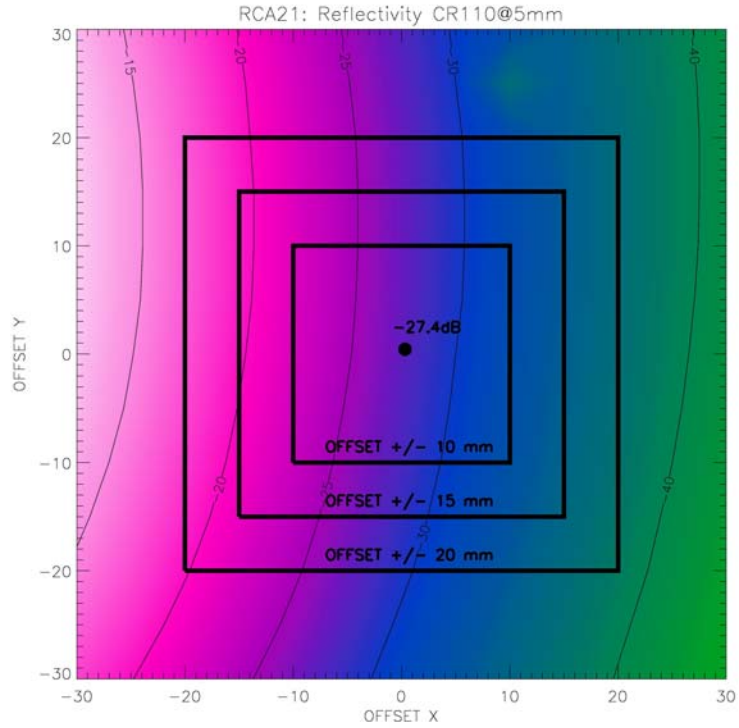

Figure 25 Sky Load reflectivity perceived from LFI #21, depending on displacement (CR110 layer 10 thick) ; values in dB; the three offest regions [X=+/- 10 mm , Y=+/- 10 mm], [X=+/- 15 mm , Y=+/- 15 mm], [X=+/- 20 mm , Y=+/- 20 mm] are displayed

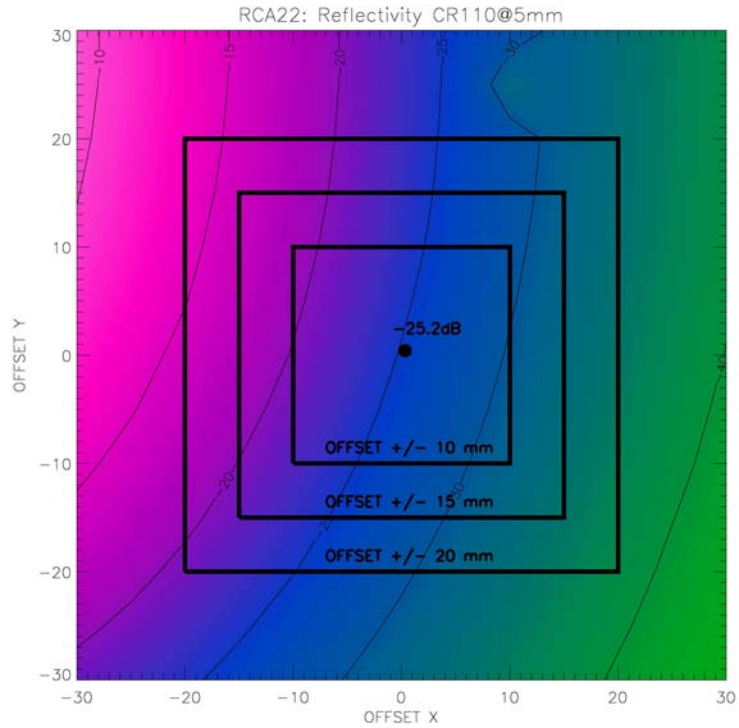

Figure 26 Sky Load reflectivity perceived from LFI #22, depending on displacement (CR110 layer 10 thick) ; values in dB; the three offest regions [X=+/- 10 mm , Y=+/- 10 mm], [X=+/- 15 mm ,

Y=+/- 15 mm], [X=+/- 20 mm , Y=+/- 20 mm] are displayed

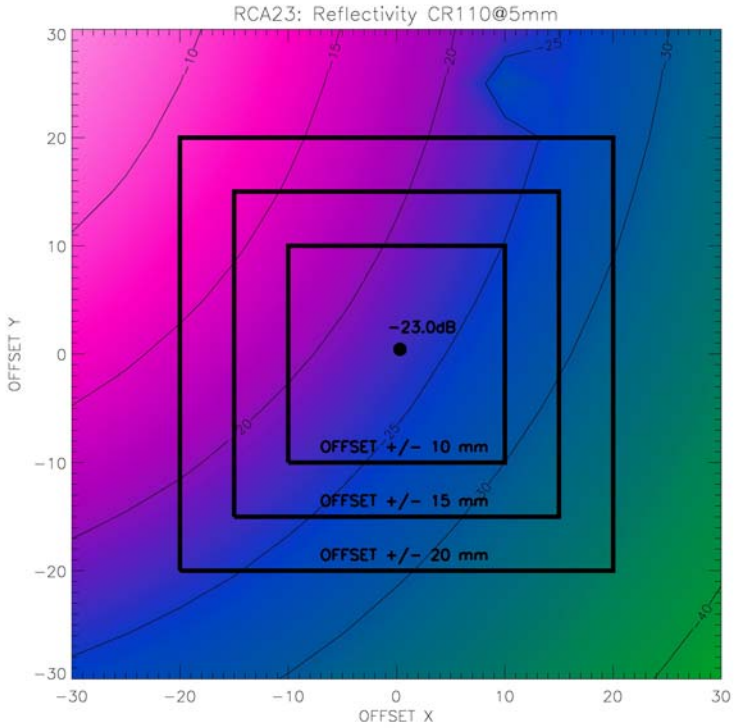

Figure 27 Sky Load reflectivity perceived from LFI #23, depending on displacement (CR110 layer 10 thick) ; values in dB; the three offest regions [X=+/- 10 mm , Y=+/- 10 mm], [X=+/- 15 mm , Y=+/- 15 mm], [X=+/- 20 mm , Y=+/- 20 mm] are displayed

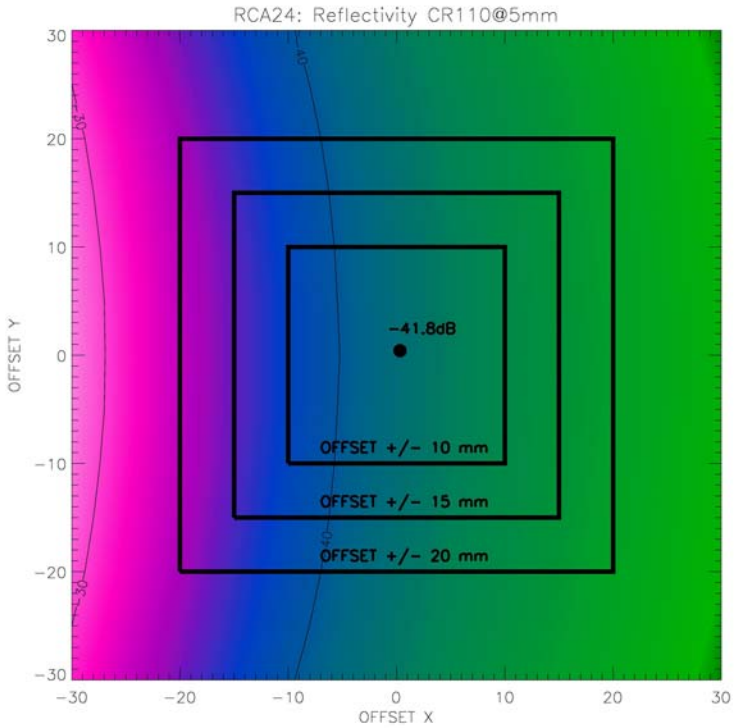

Figure 28 Sky Load reflectivity perceived from LFI #24, depending on displacement (CR110 layer 10 thick) ; values in dB; the three offest regions [X=+/- 10 mm , Y=+/- 10 mm], [X=+/- 15 mm ,

Y=+/- 15 mm], [X=+/- 20 mm , Y=+/- 20 mm] are displayed

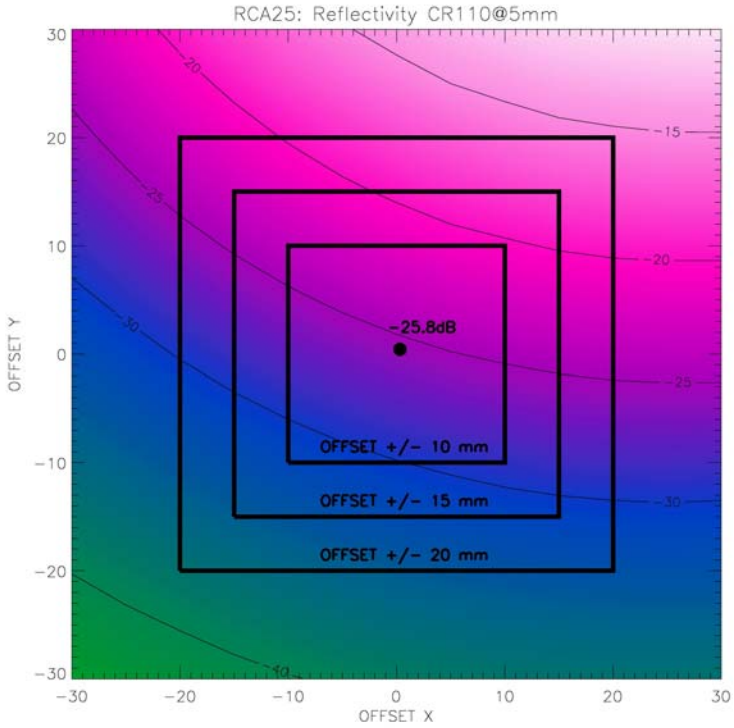

Figure 29 Sky Load reflectivity perceived from LFI #25, depending on displacement (CR110 layer 10 thick) ; values in dB; the three offest regions [X=+/- 10 mm , Y=+/- 10 mm], [X=+/- 15 mm , Y=+/- 15 mm], [X=+/- 20 mm , Y=+/- 20 mm] are displayed

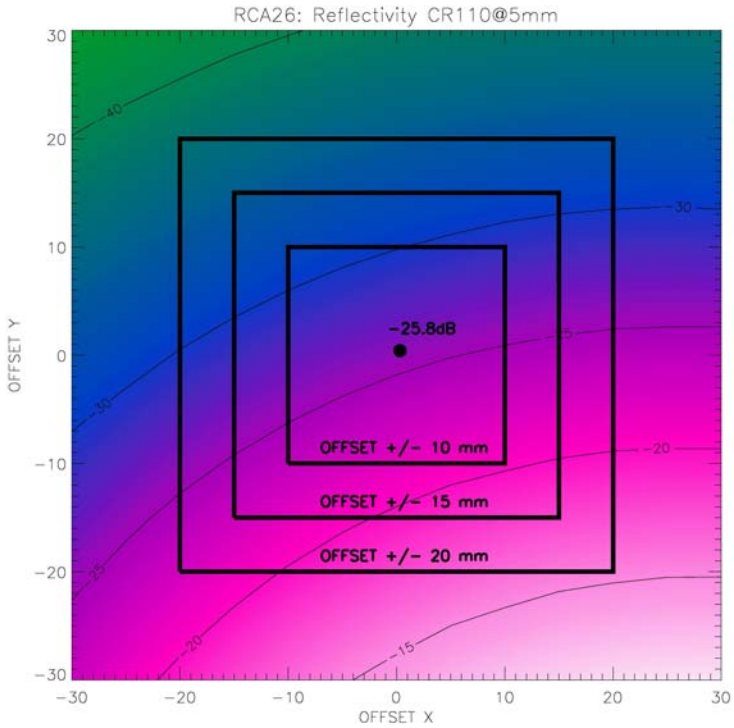

Figure 30 Sky Load reflectivity perceived from LFI #26, depending on displacement (CR110 layer 10 thick) ; values in dB; the three offest regions [X=+/- 10 mm , Y=+/- 10 mm], [X=+/- 15 mm ,

Y=+/- 15 mm], [X=+/- 20 mm , Y=+/- 20 mm] are displayed

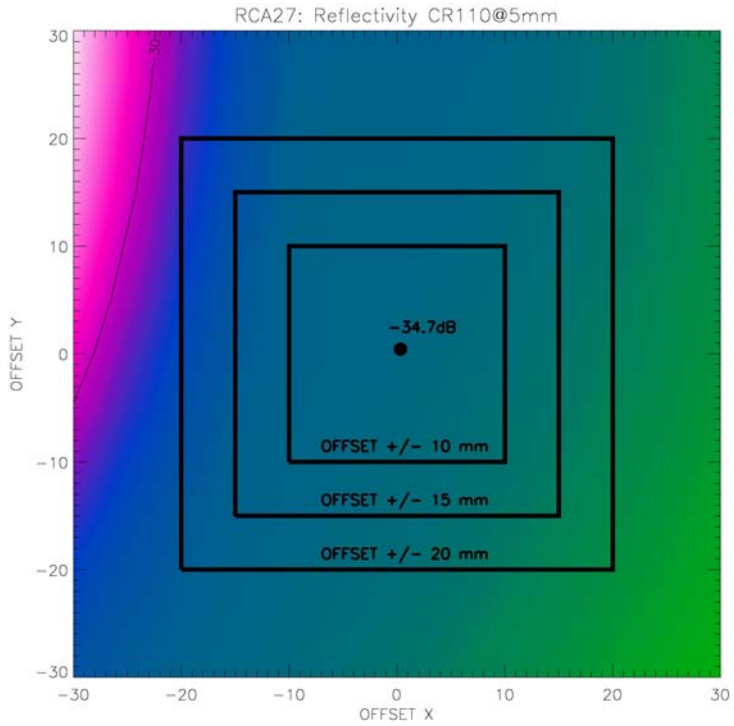

Figure 31 Sky Load reflectivity perceived from LFI #27, depending on displacement (CR110 layer 10 thick) ; values in dB; the three offest regions [X=+/- 10 mm , Y=+/- 10 mm], [X=+/- 15 mm , Y=+/- 15 mm], [X=+/- 20 mm , Y=+/- 20 mm] are displayed

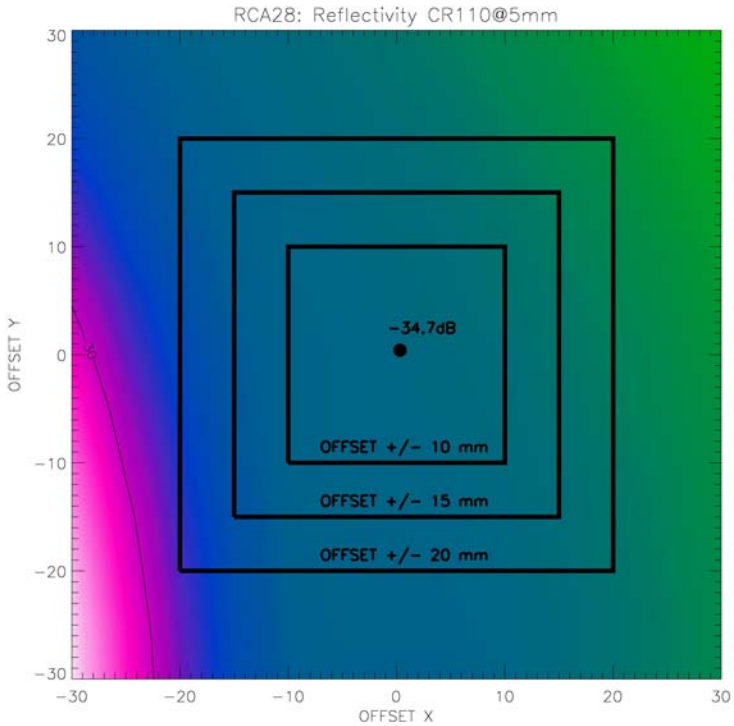

Figure 32 Sky Load reflectivity perceived from LFI #28, depending on displacement (CR110 layer 10 thick) ; values in dB; the three offest regions [X=+/- 10 mm , Y=+/- 10 mm], [X=+/- 15 mm ,

Y=+/- 15 mm], [X=+/- 20 mm , Y=+/- 20 mm] are displayed

The maximum reflectivity, as perceived from the LFI feeds, is displayed in the two following graphs: it is evident that the position considered as 'nominal' up to now (that is X=0, Y=0, in offset units) is very close to the best available within the explored grid (that is X=0.5, Y=0) . This was already known before this last work, as documented in the main document.

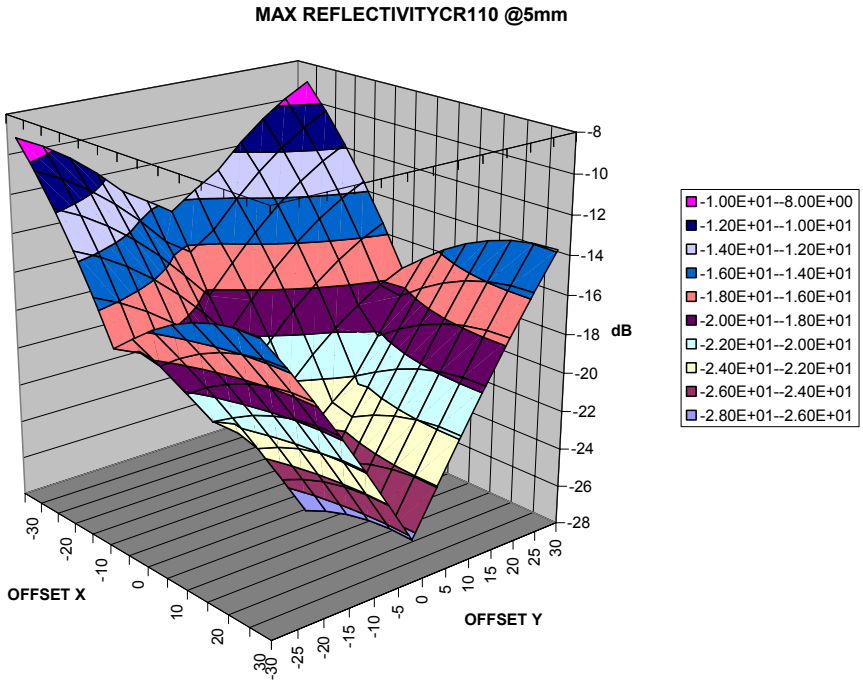

Figure 33 Sky Load maximum reflectivity perceived from the whole LFI, depending on displacement (CR110 layer 5 thick) ; values in dB; the three offest regions [X=+/- 10 mm , Y=+/- 10 mm], [X=+/- 15 mm , Y=+/- 15 mm], [X=+/- 20 mm , Y=+/- 20 mm] are displayed

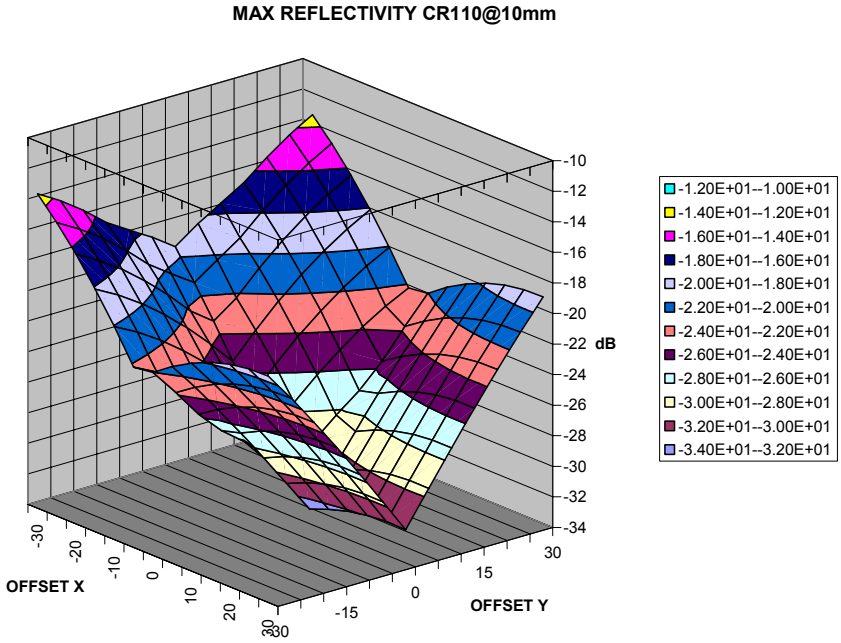

Figure 34 Sky Load maximum reflectivity perceived from the whole LFI, depending on displacement (CR110 layer 10 thick) ; values in dB; the three offest regions [X=+/- 10 mm , Y=+/- 10 mm], [X=+/- 15 mm , Y=+/- 15 mm], [X=+/- 20 mm , Y=+/- 20 mm] are displayed

Parameter	Nominal (mK)		+/-10 mm (mK)		+/-15mm (mK)		+/-20 mm (mK)		+/-30 mm (mK)	
Th Loss	10.0	2.9	>50	<15	<100	<30	<150	<50	<400	<150
Coupling	1.5	0.12	15	<5	<100	<10	<250	<50	<390	250
Straylight	56.1	15.8	<200	<50	<400	<100	<800	<200	<3000	<800
Total	58.1	15.9	<300	<50	<500	<100	<900	<300	>3000	<1000

Table 14 effect on main thermal contributions due to the displacement of sources along the plane [X,Y]. For each contribution and offset, two columns are displayed, depending on the Eccosorb layer thickness : the left one is relative to a layer 5mm thick, the right one 10 mm thick.

EFFECT ON THE LFI PERFORMANCES

Here we try to analize the impact having the non idealities described before on the LFI performances. Here the word ‘performance’ has to be red also as capability to check the instrument

health, to put the LFI in its conditions of best tuning, to compare with previous tests performed at Instrument Level in order to investigate if any change occurred.
Namely, the LFI will be tuned by optimizing the radiometers noise temperature (using the Y-factor method) . It is then necessary to compare between two tests, one performed with the 4K Reference Load at high (about 30 K) and the other at low (4.5 K) temperature.
How longer the SKL is far to be a black body so much the contribution from external sources will be visible to the LFI radiometers.
In particular:

-the straylight temperature (due to the baffle @20 K and to the environment @50K) will reflect as an offset on the Noise temperature (since it weights in the same way on the hot and cold states) , mimicking a true temperature excess signal. This effect is shown in plots in Figure 35 and Figure 36 .
-The FPU emission changes when the 4K stage is passing from 30 K to 4.5 K. This effect is asymmetric and acts with different weights on hot and cold states. It mimic a higher Gain of the radiometer and behaves as a lower noise temperature. However, since the FPU emission is here supposed about 0.2, and the effect is weighted by the solid angle subtended by the FPU (that is less than 13% of the total solid angle) , it does not change considerably the best tuning condition.
Depending on the channel considered, we can estimate that average variation by about 1% in the capability to estimate the scientific output is associated with one step (1 LSB) in the Gate tuning procedure. From Plots in Figure 37 and Figure 38 it arises that the maximum error committed, due to the HFI FPU temperature variation during the Tuning procedure, is less than 2 LSB.
- Coupling between LFI radiometers: it increases with reflectivity and is maximized when the beams of the receiving feed and of the emitting feeds overlap on the region interested by the sources and the eccosorb flat layer. This effect is symmetric. However it changes, lowering from Gate 1 to Gate 2 Tuning , since the Noise temperature reduces after Gate 1 tuning. It can be supposed to act mostly as an offset applied to the total noise temperature. This effect was already taken into account in the straylight contribution but can be separately considered in the plots shown in Figure 20 and Figure 21.
- The scientific output can be also very different from that expected under the same conditions , from the test campaign measurements at instrument level. This difference accounts in percentage diversely depending on the 4K reference load stays at 30 K or at 20 K. Results are shown in Figure 39, Figure 40, Figure 41, Figure 42 (depending on Eccosorb layer thickness and on 4K source temperature) .
- Possible saturation at higher temperatures (30K) due to the combined effect of high noise Temperature and RF coupling. During Calibration tests at Instrument level , some channels, as RCA 28 (for example channel 28,10 @26K is about 2.3 V) and 27, were very close to the DAE saturation limit (2.5 V)
- with exception for the HFI FPU temperature change (needed to execute the radiometers tuning procedure) all the other sources of thermal excess are here considered under a stationary frame. This is since more data where not available in the short time of this analysis. However, it must be considered that each fluctuation in the environment (cryo chamber stage @50 K, telescope (50K) and baffle (20K)) can have the same effect of the FPU fluctuation , that is for example to distort the Radiometer tuning curves or to create correlate spurious signals on the radiometer.

To test the model, a radiometer representative of the average properties channels has been used (Noise temperature =15 K, Y factor calculated between 30K and 4K).
All the above results are summarized in the following table:

mm	T NOISE EXCESS (%)	Bias error (%)	V out 30K	V out @4K
10	2.49	-0.13	0.82	1.95
15	5.43	-0.30	1.80	4.27
20	11.66	-0.60	3.88	9.19
30	48.12	-1.68	16.03	37.97

Table 15 Summary of average results from plots displayed in FIGs. From 22 to 31. From the left column: Maximum displacement from the nominal position (along X and Y direction) , Excess in the noise temperature (in percentage of a nominal noise temperature Tn=15K) , Error in the optimum bias estimation

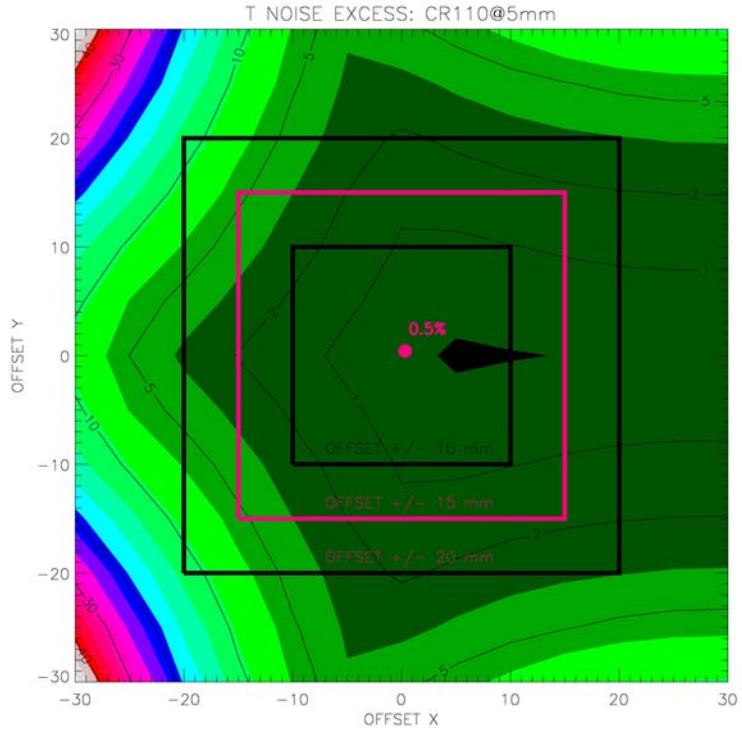

Figure 35 maximum error committed on Noise temperature extimation due to the sky load increased reflectivity , varying with displacement (CR110 layer 5 thick) ; values are in percentage of the nominal noise temperature used here for the test (15K); the three offest regions [X=+/- 10 mm , Y=+/- 10 mm], [X=+/- 15 mm , Y=+/- 15 mm], [X=+/- 20 mm , Y=+/- 20 mm] are displayed

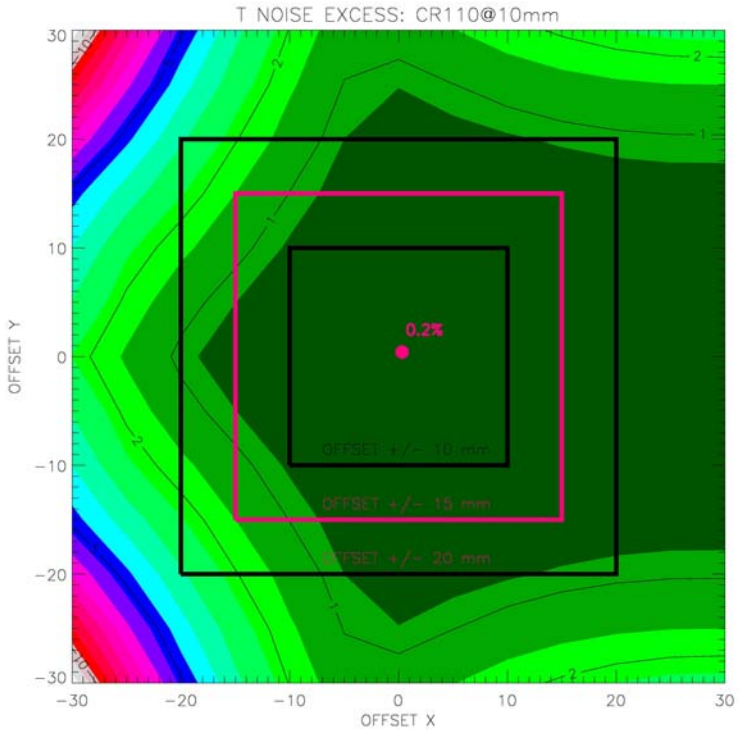

Figure 36 maximum error committed on Noise temperature extimation due to the sky load increased reflectivity , varying with displacement (CR110 layer 10 thick) ; values are in percentage of the nominal noise temperature used here for the test (15K); the three offest regions [X=+/- 10 mm , Y=+/- 10 mm], [X=+/- 15 mm , Y=+/- 15 mm], [X=+/- 20 mm , Y=+/- 20 mm] are displayed

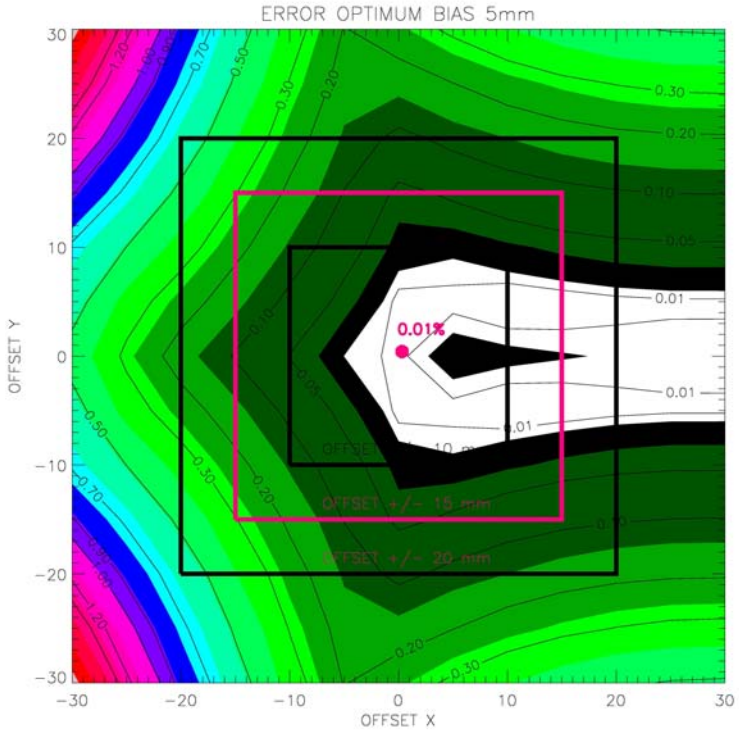

Figure 37 maximum error committed on the optimum bias extimation due to the FPU temperature variation during the test combined with the non ideal emissivity of the load, varying with displacement (CR110 layer 5 thick) ; The three offest regions [X=+/- 10 mm , Y=+/- 10 mm], [X=+/- 15 mm , Y=+/- 15 mm], [X=+/- 20 mm , Y=+/- 20 mm] are displayed

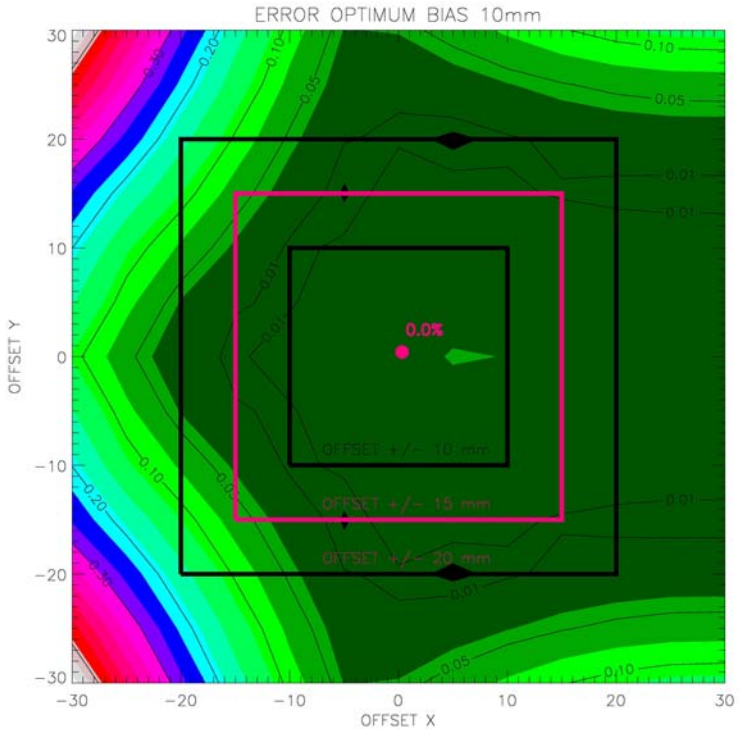

Figure 38 maximum error committed on the optimum bias extimation due to the FPU temperature variation during the test combined with the non ideal emissivity of the load, varying with displacement (CR110 layer 5 thick) . The three offest regions [X=+/- 10 mm , Y=+/- 10 mm], [X=+/- 15 mm , Y=+/- 15 mm], [X=+/- 20 mm , Y=+/- 20 mm] are displayed

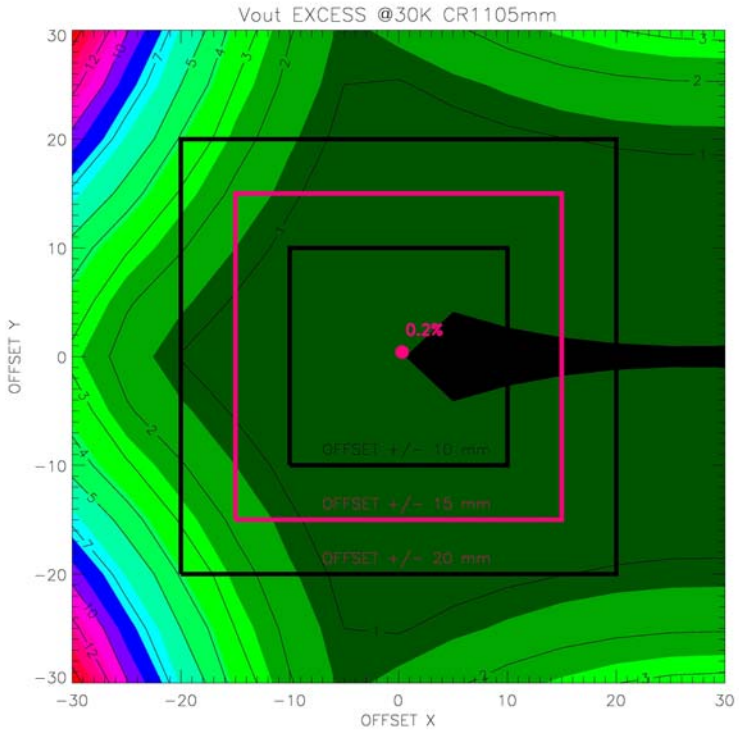

Figure 39 maximum error committed on the scientific output extimation due to the thermal contribution from environment reflected on the non ideal SKL surface (eccosorb flat layer + 3 CFS sources) The CR110 layer is here 5 mm thick . The three offest regions [X=+/- 10 mm , Y=+/- 10 mm], [X=+/- 15 mm , Y=+/- 15 mm], [X=+/- 20 mm , Y=+/- 20 mm] are displayed

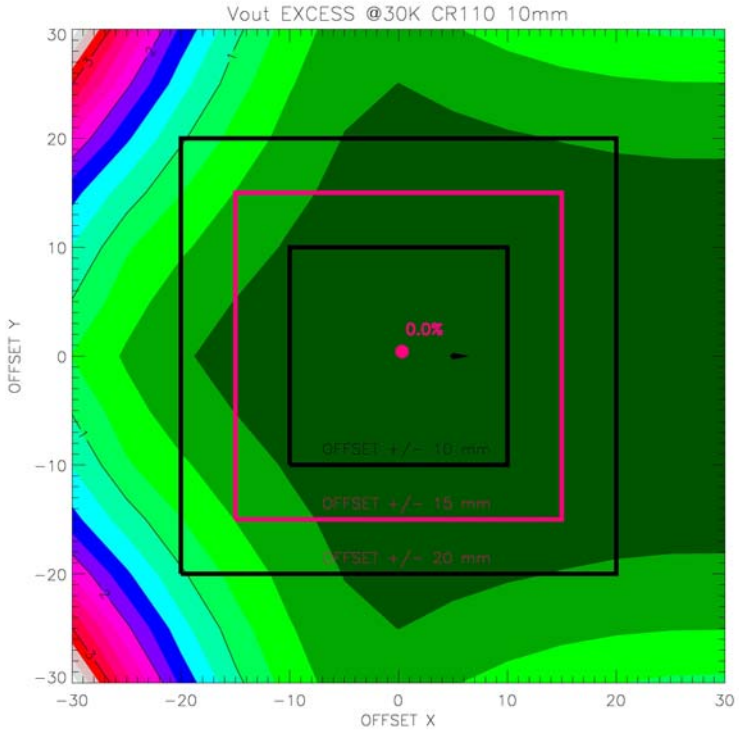

Figure 40 maximum error committed on the scientific output extimation due to the thermal contribution from environment reflected on the non ideal SKL surface (eccosorb flat layer + 3 CFS sources) The CR110 layer is here10 mm thick . The three offest regions [X=+/- 10 mm , Y=+/- 10 mm], [X=+/- 15 mm , Y=+/- 15 mm], [X=+/- 20 mm , Y=+/- 20 mm] are displayed

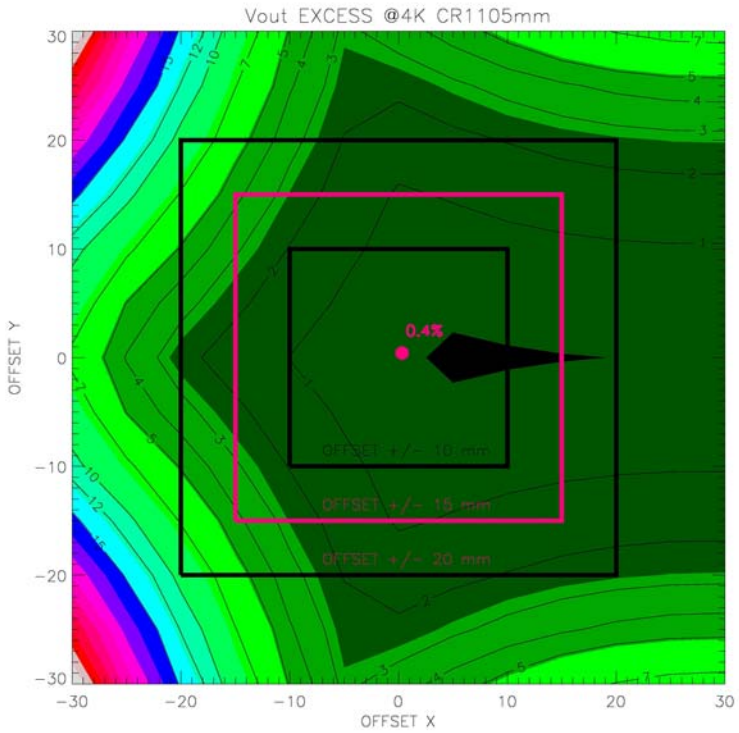

Figure 41 maximum error committed on the scientific output extimation due to the thermal contribution from environment reflected on the non ideal SKL surface (eccosorb flat layer + 3 CFS sources) The CR110 layer is here 5 mm thick .The 4K Reference Load temperature is 4K. The three offest regions [X=+/- 10 mm , Y=+/- 10 mm], [X=+/- 15 mm , Y=+/- 15 mm], [X=+/- 20 mm , Y=+/- 20 mm] are displayed

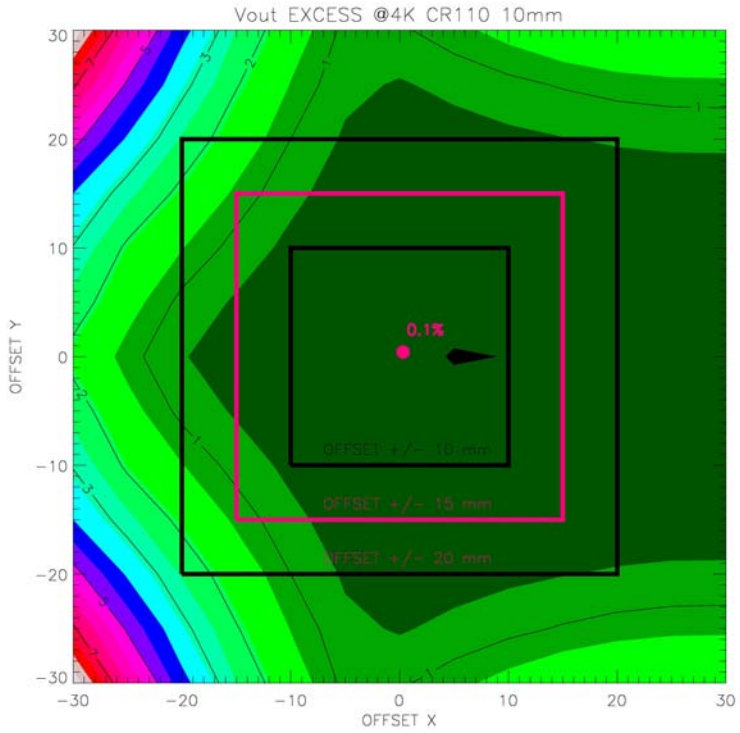

Figure 42 maximum error committed on the scientific output extimation due to the thermal contribution from environment reflected on the non ideal SKL surface (eccosorb flat layer + 3 CFS sources) The CR110 layer is here10 mm thick . The 4K Reference Load temperature is 4K. The three offest regions [X=+/- 10 mm , Y=+/- 10 mm], [X=+/- 15 mm , Y=+/- 15 mm], [X=+/- 20 mm , Y=+/- 20 mm] are displayed

CONCLUSIONS

The Planck Sky load, after the positioning of HFI the three carbon fibre sources , shows a non isotropic behaviour. The position of the sources have been optimized in in the main document, and in the following two ANNEX, in order to minimize the impact on the LFI , saving the functionality of the sources. Since the possibility that the SKL position can not be measured and fixed with a good accuracy , a sensibility analysis has been developed in this document to investigate the possible impact having on the Sky Load performances and , consequently, on the LFI performances. This work should help to understand the maximum non-accuracy acceptable from the LFI instrument.

A new design, using larger sources, has been here considered, basing on the last design provided a few days ago from HFI instrument. The sources, together with the flat absorbing layer masking the metal mounting structures, have been moved rigidly along the Sky Load plane (w.r.t. the 0-RDP) , applying a maximum offset +/30 mm along X and Y by steps of 5mm. This displacement has a strong impact on the Sky Load effective emissivity and reflectivity, depending on the particular position. This change in the SKL properties reflects into a different apparent temperature observed and can bring spurious signals correlated with fluctuations external of the SKL

An attempt to analyse how this changes act on the SKL performances have been done. In particular, for typical electrical values characterising the LFI radiometers, have been calculated:

- Changes in Noise Temperature
- Changes in The scientific output
- Capability to select the optimum bias during tuning operations
- Possible saturation.

Results show that:
The nominal position is actually very close to the best one achievable with these 3 sources.
The effect of the displacement is not symmetrical w.r.t. the X axis, since it is nor the LFI.
The effect of straylight contamination from sources external (from environment) reflects into an extra noise applied on the Noise temperature : this extra signal can also reach considerable values (up to 48% for 30 mm displacement), depending on the position. Accuracy in the positioning within +/- 15 mm seems able to keep the error in the estimation of this parameter below 10% .
The effect of the change in temperature of the HFI FPU required to perform the LFI radiometers tuning procedure can impact , but not strongly, to determine the best bias settings : it can account for 1- 2 LSB maximum , depending on the channel.
The effect on the Scientific bias can be strong (increasing the voltage measured at the DAE), also without changing the overall properties of the LFI radiometers. However, since some channels have already an output very close to the DAE input range limit , when the 4K reference Load stays at 30 K, saturation could be observed for unaccuracy larger than +/- 20 mm.
Moreover, scope of the CSL tests at system level is also to check for the repeatability of settings / outputs measured at Instrument level: especially at low temperature (4K) the percent error becomes high (+/-5%) already for unaccuracy of +/- 15 mm. and larger than 10% for displacement > +/- 15 mm.
The effect of coupling between radiometers can be also strong: an important coupling can induce disturbs from one radiometer to another, masking problems or showing false misfunctioning; a safe condition seems to be unaccuracy < +/- 10 mm, able to keep the correlated signal below 50 mK.
Possible effects induced from thermal fluctuations of the baffle, thermal shield, telescope, are her not considered cause the lack of data available within the time of this analysis. These contributions can introduce spurious signals proportional to the reflectivity of the sky load. At this purpose, all the positions where, from the 'sky load maximum reflectivity analysis', the individual return loss of LFI feeds becomes higher than -20 dB (unaccuracy of +/- 10 mm) , also if only locally, should be avoided. At the same time, every effort to increase the Eccosorb layer thickness up to 10 mm (or to cover the flat surface by pyramids) should be done. It could allow a larger flexibility in positioning.

ANNEX 4 TO : TN PL-LFI-PST-XXX ISSUE 0.3 (Planck cold load performance degradation at LFI frequency caused by HFI carbon fibre noise source, F. Cuttaia, 26-03-07)

F. CUTTAIA, 12-07-07

Scope:

This analysis comes out as answer to action item AI# (Reference: SCI-PT-047553, 20 June 2007)). Its scope is to evaluate the best matching of LFI performances w.r.t possible inaccuracy in SKY LOAD position determination (this analysis expected from CSL) for several frames provided by HFI team. Each frame corresponds to a different positioning of Carbon Fibre Sources (CFS) on the SKY Load surface.

Description

All assumptions made in the main analysis and especially in ANNEX 3 are still true.
Changes are just considered in terms of CFS positioning.
Flat Eccosorb surface baffling the CFS is here supposed, as in the previous analysis, filled as much as possible (meaning not interfering with the FOV of the CFS), by pyramids.
Results, to simplify the reading, will be again provided only in terms of :
Maximum percent error committed in Gain estimation during the Tuning procedure (affecting Calibration analysis)
Maximum percent error committed in Noise Temperature estimation during the Tuning procedure (affecting Calibration analysis)
Maximum percent error committed in Scientific Voltage comparison with results from previous tests (affecting functional analysis)
Maximum error (evaluated in LSB, meaning steps of the tuning sequence) committed when using the optimized bias (gate and drains in the FEM) measured at Instrument level.

Frames analyzed

Following E-mail from Antoine Arondel (20-06-2007) analysis on new three different frames will be here shown:

S#	X	Y
Frame1		
S1	0	20
S2	0	-20
S3	-20	0
Frame2		
S1	0	17.5
S2	0	-17.5
S3	-20	0
Frame3		
S1	5	17.5
S2	5	-17.5
S3	-15	0

Following E-mail from Jean Michel Lamarre (11-07-2007), a last analysis has been performed on a very last frame proposed to match with HFI requirements (and is the favourite one).

S#	X	Y
Frame4		
S1	5	20
S2	5	-20
S3	-15	0

Results:

For each frame many parameters have been characterised

Results will be displayed, per each frame, in the plots below: finally a table summarizing the main results follows. For Frames 1, 2 and 3 just the uncertainty on Noise Temperature and bias settings are reported. For the Frame 4, considered the best choice for HFI, results are fully displayed. Offset regions +/- 10mm, +/- 15mm, +/- 20mm, +/- 30mm are displayed as rectangular contours. The value displayed in the centre refers to the 0-uncertainty position (very close to be the bset positioning for that frame)

Frame 1

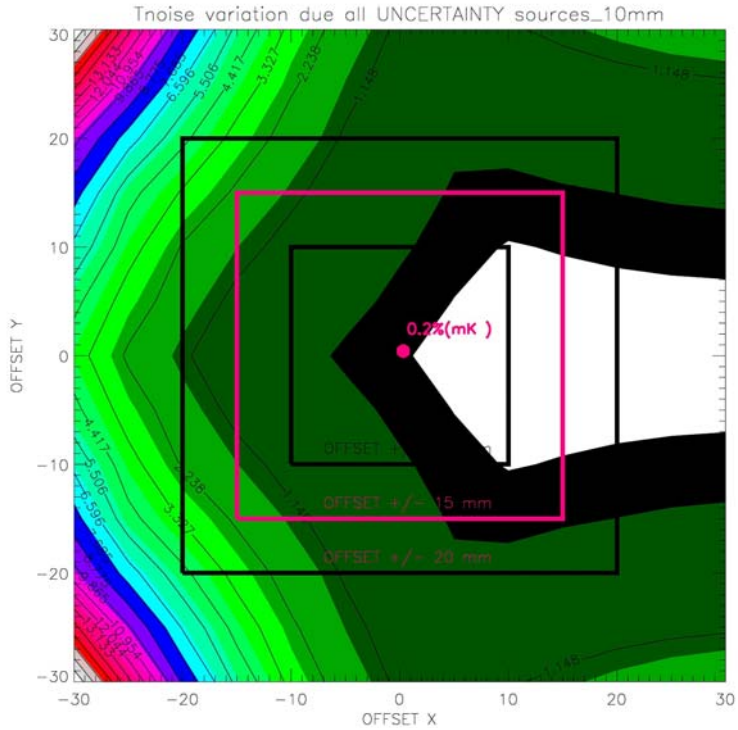

Figure 43 Percent Error on Noise temperature estimation

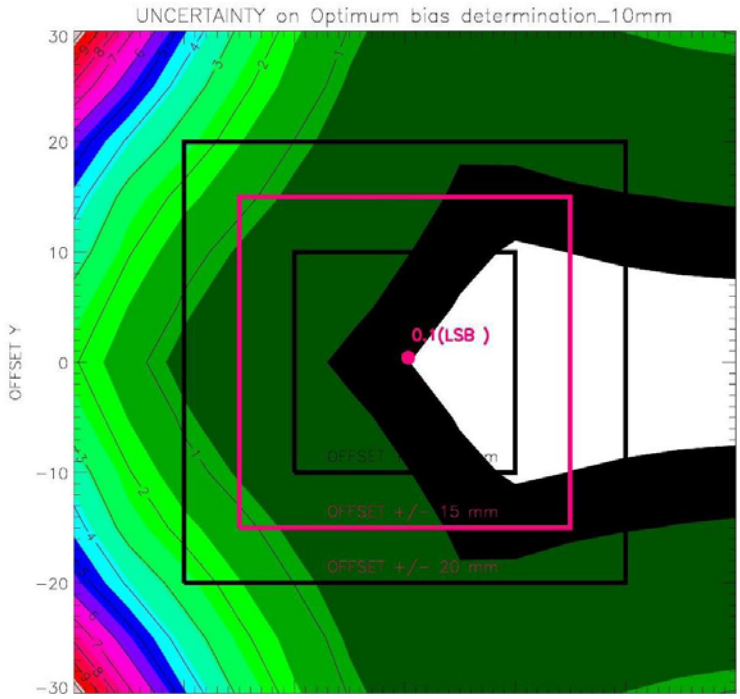

Figure 44 Error on Bias settings determination (given in LSB, meaning one step in bias tuning sequence)

Frame 2

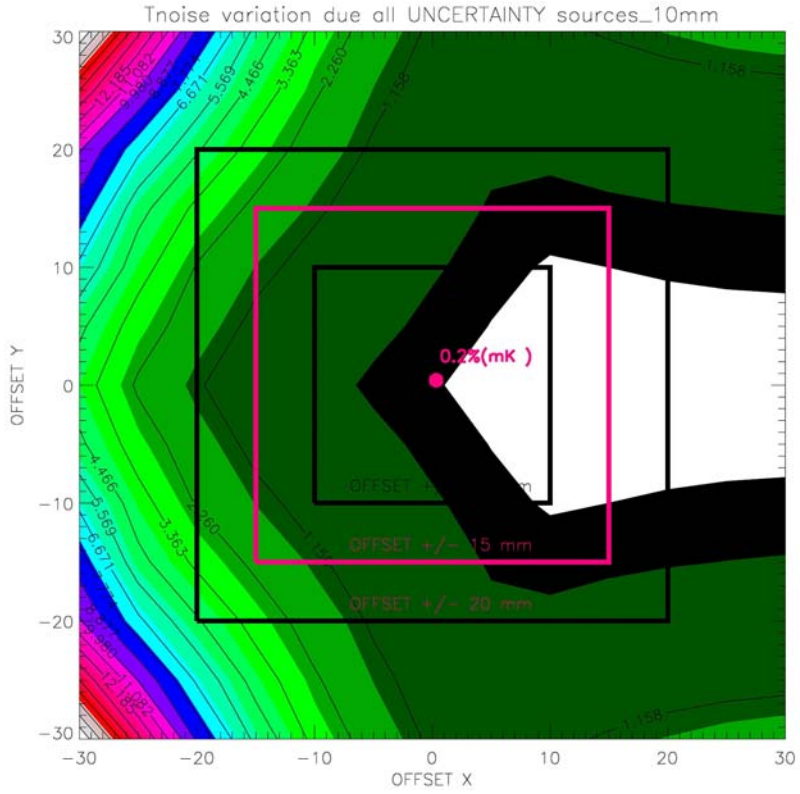

Figure 45 Percent Error on Noise temperature estimation (FRAME 2)

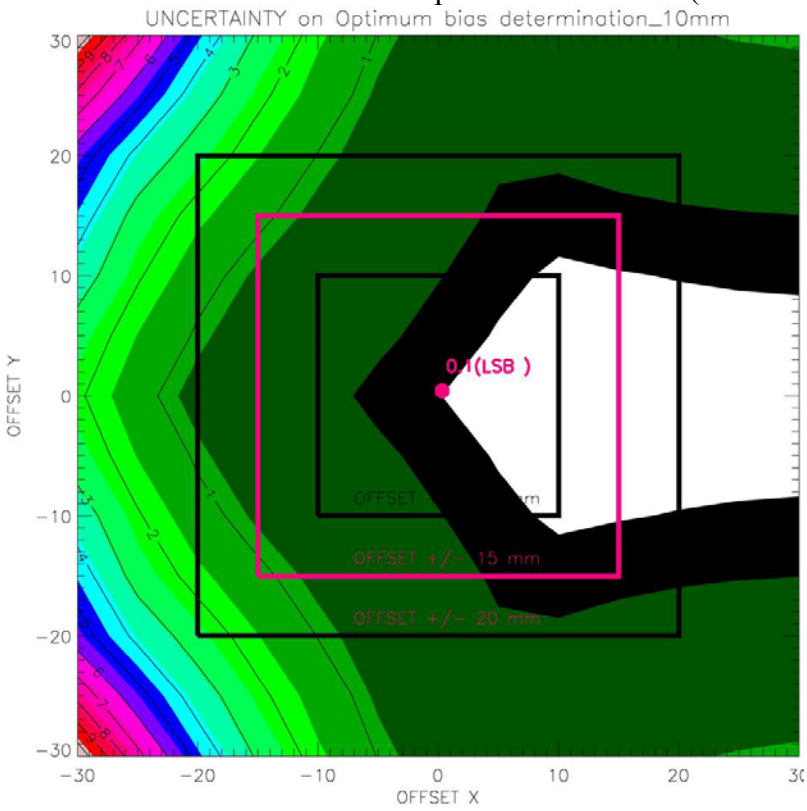

Figure 46 Error on Bias settings determination (given in LSB, meaning one step in bias tuning sequence FRAME2

Frame 3

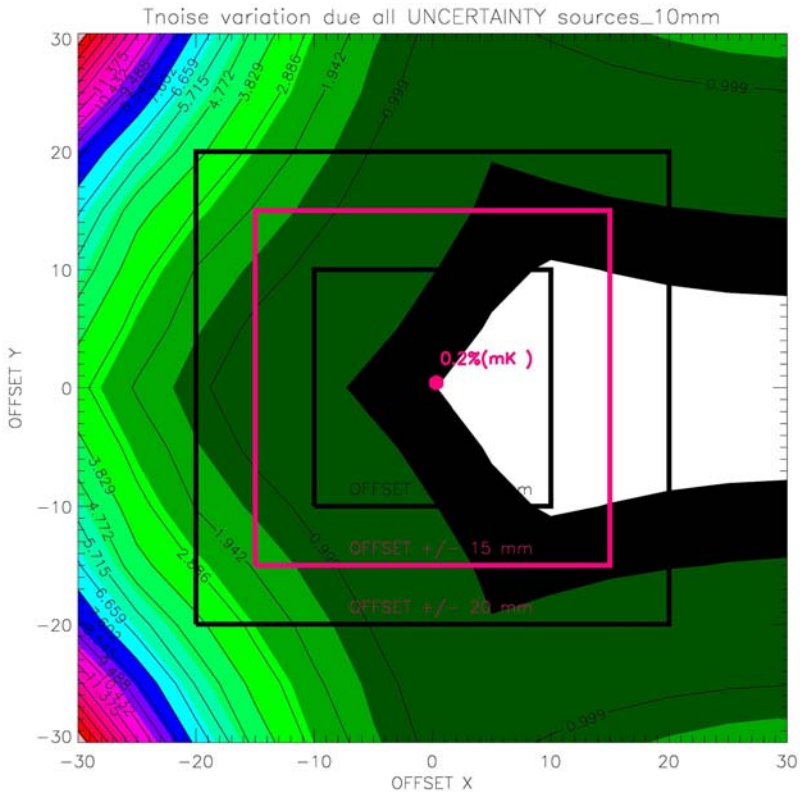

Figure 47 Percent Error on Noise temperature estimation (FRAME 3)

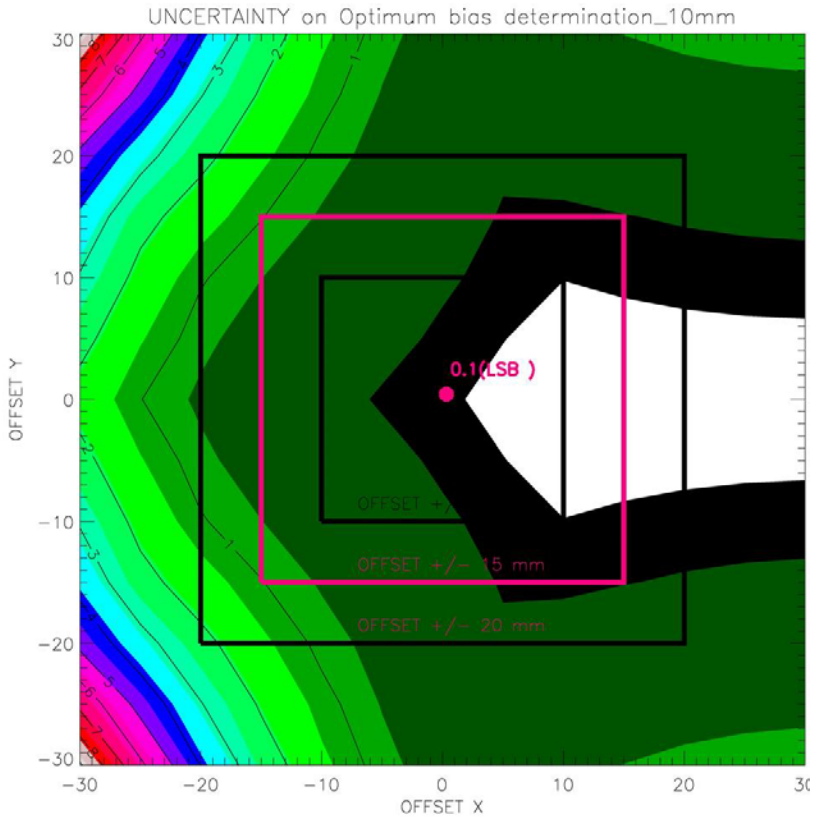

Figure 48 Error on Bias settings determination (given in LSB, meaning one step in bias tuning sequence FRAME3

Frame 4 (HFI best choice)

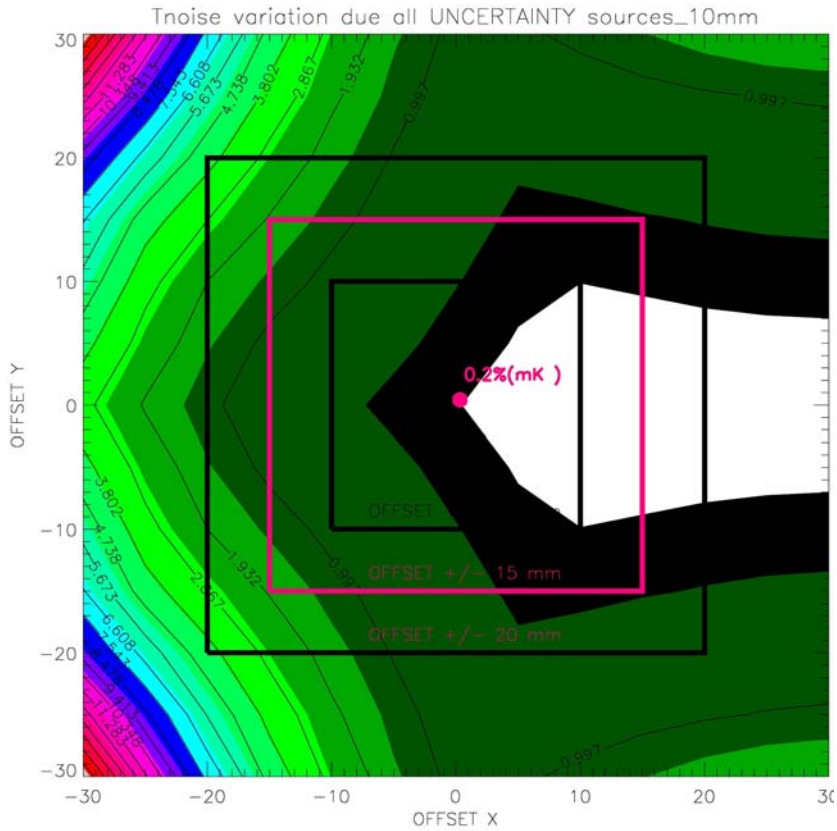

Figure 49 Percent Error on Noise temperature estimation (FRAME 4)

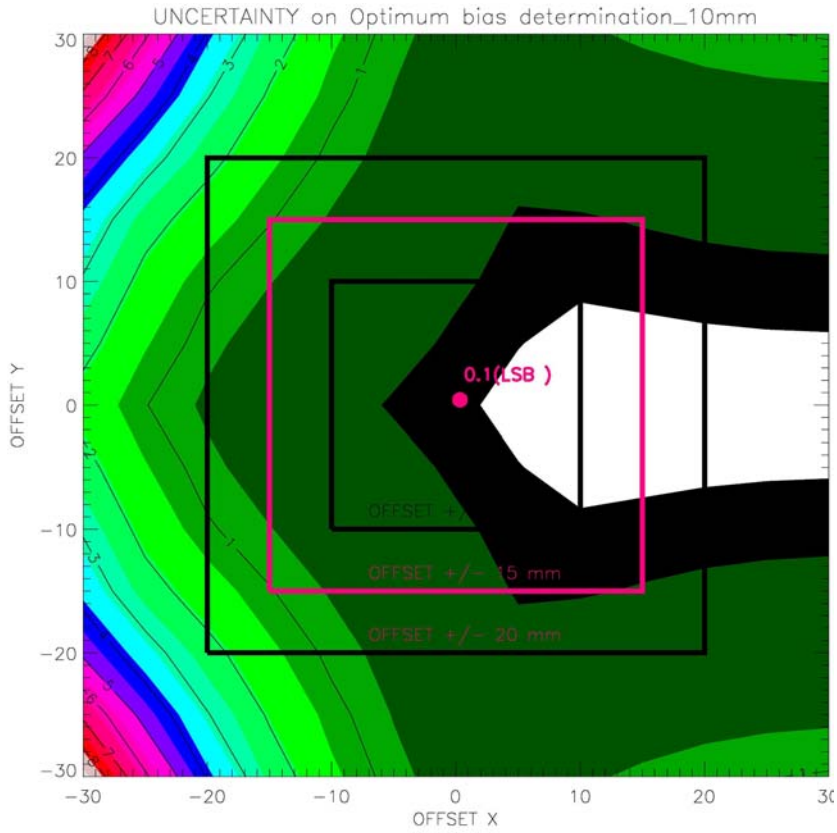

Figure 50 Error on Bias settings determination (in LSB, meaning one step in bias tuning sequence) FRAME4

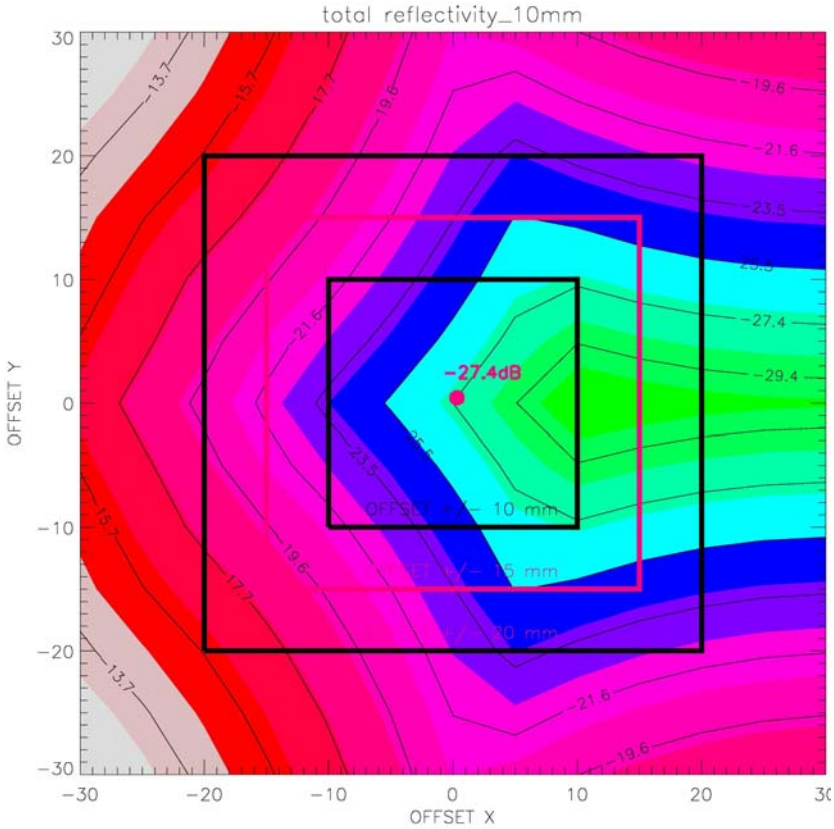

Figure 51 Maximum TOTAL REFLECTIVITY (CFS' + ECCOSORB); in dB - FRAME4

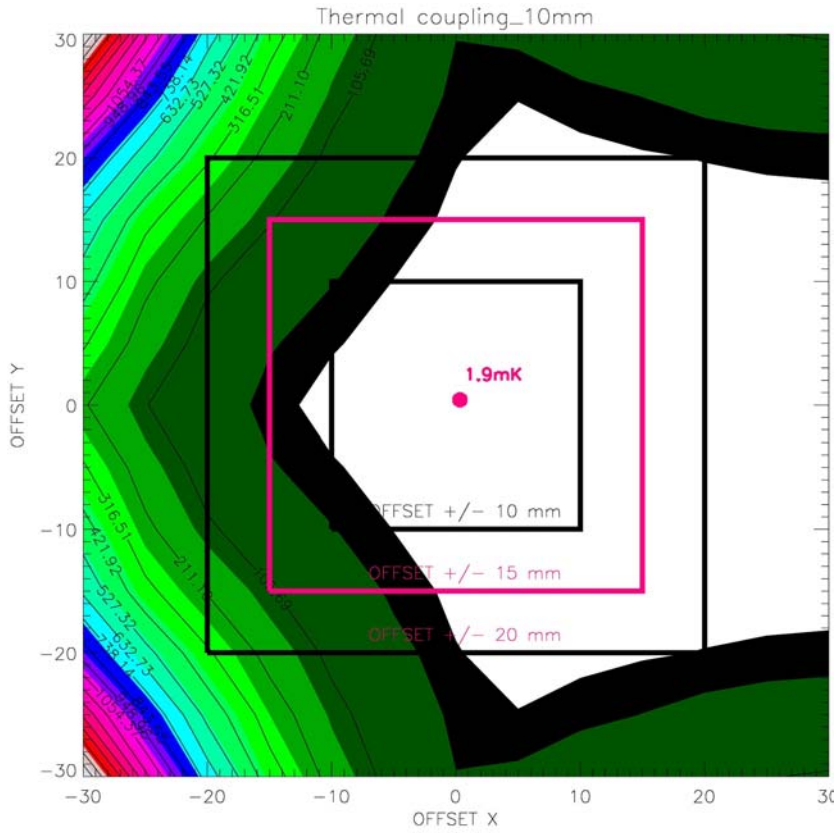

Figure 52 Maximum Thermal Coupling between feeds (mK) - FRAME4

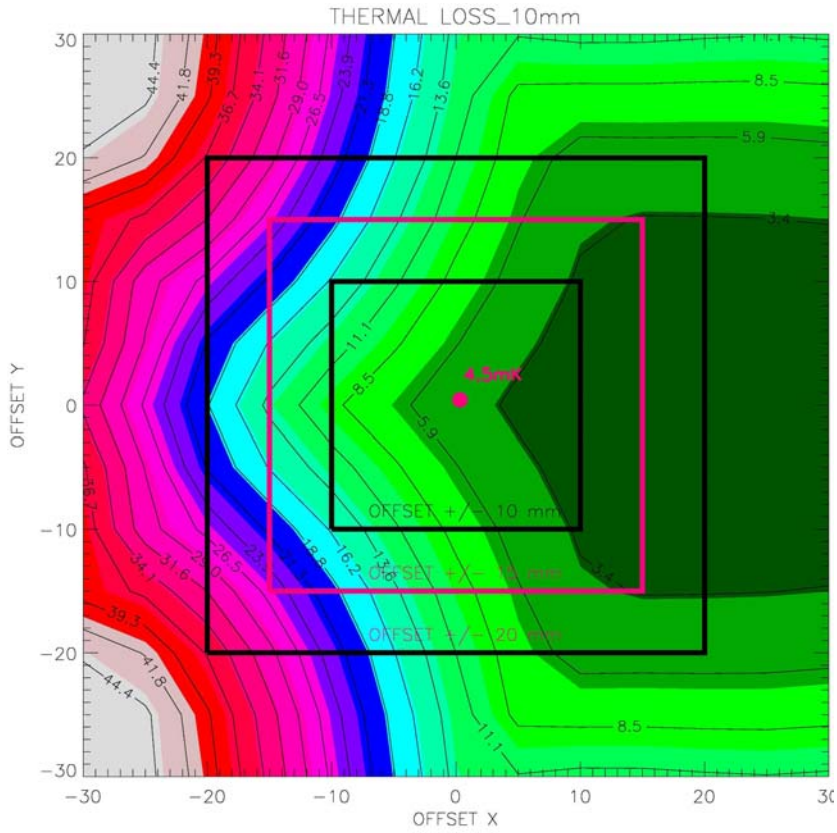

Figure 53 Maximum Thermal Loss (SKL temperature underestimation, in mK) - FRAME4

SUMMARY

Results are summarized in the following tables, displayed in terms of the maximum value subtended by each offset region considered.

S#	OFFSET 10	OFFSET 15	OFFSET 20	OFFSET 30
Tnoise				
Frame1	1%	2.23%	4.41%	18%
Frame2	1%	2.15%	4.48	19%
Frame3	0.85%	1.95%	3.9%	17%
Frame4	0.9%	1.94%	4.2%	17%
Vgate				
Frame1	<1 LSB	1 LSB	<3 LSB	10 LSB
Frame2	<1 LSB	1 LSB	<3 LSB	10 LSB
Frame3	<1 LSB	1 LSB	2 LSB	8 LSB
Frame4	<1 LSB	1 LSB	2 LSB	8 LSB

For the FRAME 4 also other parameters are summarized in the table below

Parameter	NOMINAL	OFFSET 10	OFFSET 15	OFFSET 20	OFFSET 30

MAX Total reflectivity	-27.4 dB	-21.6 dB	-19.6 dB	-15.7 dB	-12 dB
MAX Thermal Coupling	1.9 mK	30 mK	105 mK	320 mK	1600 mK
MAX Thermal Loss	4.5 mK	13.6 mK	26.5 mK	36.7 mK	< 50 mK

CONCLUSIONS

As answer to action item AI#, the three frames analysed provide similar results when the two representative parameters (inaccuracy in Noise temperature and in bias setting determination) are compared.
The LFI best choice is the FRAME 3.
Regarding inaccuracy in positioning , under this frame, the larger value acceptable for LFI is +/- 15 mm.
In add , in the purpose of this Telecom, one more setup was considered, named **FRAME4**. It comes out as best choice for HFI performances.
Results show that, despite results are worse, the examined frame is very close to the FRAME 3 in terms of impact on the LFI.
Under this frame **the maximum inaccuracy in positioning (total displacement of Reference system centred on the SKL w.r.t. the RDP) acceptable for LFI is again +/- 15 mm**. This number comes from maximum error acceptable during the Tuning procedure and the setting / reproducibility of the input bias and scientific output voltage.